НАЦІОНАЛЬНА АКАДЕМІЯ НАУК УКРАЇНИ
ІНСТИТУТ ЗАГАЛЬНОЇ ТА НЕОРГАНІЧНОЇ ХІМІЇ імені В. І. ВЕРНАДСЬКОГО
КИЇВСЬКИЙ НАЦІОНАЛЬНИЙ УНІВЕРСИТЕТ імені ТАРАСА ШЕВЧЕНКА

УКРАЇНСЬКИЙ ХІМІЧНИЙ ЖУРНАЛ

№ 10
Том 90 / Vol. 90
2024
https://ucj.org.ua

UKRAINIAN CHEMISTRY JOURNAL

Зміст

Contents

УДК 546.185 doi: 10.33609/2708-129X.90.10.2024.59-68

ОСОБЛИВОСТІ ЛЕГУВАННЯ КАЛЬЦІЙ-ФОСФАТІВ МІКРОЕЛЕМЕНТАМИ

Н. Ю. Струтинська*, Є. О. Комащенко, М. С. Слободяник

Київський національний університет імені Тараса Шевченка,
вул. Володимирська, 64/13, м. Київ 01601, Україна
**email: n.strutynska@knu.ua*

Досліджено формування кальцій-фосфатів у водному розчині систем Ca^{2+}-Mg^{2+}-Na^{+}-PO_4^{3-}-NO_3^{-} за мольних співвідношень Ca^{2+}: Mg^{2+}: Na^{+}: PO_4^{3-}= (10-x-y/2) : x : y : 6, (x = 0.1, 0.25, 0.5, 0.75; y = 0.25, 0.5, 0.75, 1.0) за температури 25°C із наступним нагріванням до температури 600°C. Встановлено умови формування кальцій-фосфату апатитового типу, що містить мікроелементи магній та натрій (по 0.5 мас %) у системі з мольними співвідношеннями Ca^{2+} : Mg^{2+} : Na^{+} : PO_4^{3-} = (10-x-y/2) : 0.1 : 0.25 : 6 та біфазні кальцій-фосфати (суміші фаз на основі $Ca_{10}(PO_4)_6(OH)_2$ – гексагональна сингонія, просторова група *P6$_3$/m* та β-$Ca_3(PO_4)_2$ – тригональна сингонія, просторова група *R-3c)* – у системах із мольними співвідношеннями Ca^{2+} : Mg^{2+} : Na^{+} : PO_4^{3-}= (10-x-y/2) : x : 0.25 : 6, (x = 0.25, 0.5, 0.75). Встановлено, що вміст фази на основі β-$Ca_3(PO_4)_2$ у складі біфазних кальцій-фосфатів зростає (від 10 мас% до 45мас%) при збільшенні кількості катіонів магнію у вихідному розчині. Для систем із різним вмістом катіонів натрію також встановлено формування біфазних кальцій-фосфатів, однак масове співвідношення фаз на основі $Ca_{10}(PO_4)_6(OH)_2$ та β-$Ca_3(PO_4)_2$ меншою мірою залежить від кількості катіонів натрію у вихідному розчині і становить 10–15 мас % для значень мольних співвідношень Ca^{2+}: Mg^{2+}: Na^{+}: PO_4^{3-}= (10-x-y/2) : 0.25 : y : 6, (y = 0.25, 0.5, 0.75). При спробі одержати кальцій-фосфат апатитового типу, що містив би 0.5 мас % магнію та 2.2 мас % натрію, одержано суміш фази на основі $Ca_{10}(PO_4)_6(OH)_2$ та подвійний ортофосфат $NaCaPO_4$. Оцінено розміри частинок із використанням рівняння Шеррера, що знаходяться в межах значень 30–50 нм. Результати ІЧ-спектроскопії підтверджують присутність ортофосфатного типу аніона та ОН-груп у складі синтезованих фосфатів. Встановлені умови формування кальцій-фосфатів можна надалі використати для розроблення біоматеріалів на основі біфазних кальцій-фосфатів, що містять різні кількості мікроелементів натрію та магнію (від 0.5 до 2 мас %.).

Ключові слова: мікроелемент; магній; натрій; гідроксиапатит; біфазний кальцій-фосфат.

ВСТУП. На сьогодні особливо високою є потреба в матеріалах для відновлення кісткової тканини чи усунення її дефектів. Для цих цілей активно використовують синтетичні матеріали, що дозволяє уникнути низки обмежень при використанні аутотрансплантатів, а також ймовірної передачі захворювання і можливості імунного відторгнення у випадку алотрансплантатів [1]. Серед наявних штучних замінників найбільшу увагу привертають кальцій-фосфати, а саме гідроксиапатит ($Ca_{10}(PO_4)_6(OH)_2$) завдяки його біосумісності, нетоксичності та біоактивності, трикальцій-фосфат (β-$Ca_3(PO_4)_2$), а також їхні суміші – біфазні кальцій-фосфати, що дозволяє покращити механічні властивості та остеоіндуктивну активність матеріалу порівняно з чистими фазами кальцій-фосфатів [2].

Одними з незамінних мікроелементів, що значною мірою присутні в людському організмі та відіграють важливу роль у біопроцесах, є Mg^{2+} та Na^+. Варто відмітити, що легування цими елементами синтетичних матеріалів на основі гідроксиапатиту дозволяє більш точно наблизити хімічний склад неорганічної компоненти природної кістки, а також використати для розширення їхньої функціоналізації у процесах відновлення чи заміщення пошкоджених ділянок кісткової тканини. Введення іонів у катіонну підґратку кальцій-фосфатів дозволяє покращити процеси клітинної адгезії, антимікробні властивості та процеси резорбції [3–4]. Магній важливий в процесах мінералізації кісткової тканини та, своєю чергою, характеризується вагомим впливом на метаболізм кісток, особливо на початкових фазах остеогенезу, а його дефіцит може викликати зниження активності кісткових клітин, уповільнення росту, а також підвищення крихкості кісток [5–8]. Вважливим аспектом у іонному заміщенні іонів Ca^{2+} на Mg^{2+} у кальцій-фосфатах є також вплив на структуру та щільність синтетичних біоматеріалів і співвідношення утворених фаз, причому збільшення катіонів магнію веде до підвищення вмісту β-$Ca_3(PO_4)_2$ та зниження $Ca_{10}(PO_4)_6(OH)_2$ відповідно [9]. Не менш важливу роль у процесах мінералізації відіграють катіони натрію, що також сприяють клітинній адгезії [10].

Метою дослідження було встановити особливості легування кальцій-фосфатів різною кількістю комплексу катіонів натрію та магнію у водних розчинах у межах мольних співвідношень Ca^{2+} : Mg^{2+} : Na^+ : PO_4^{3-}= (10-x-y/2) : x : y : 6, (x = 0.1, 0.25, 0.5, 0.75; y = 0.25, 0.5, 0.75, 1.0) за кімнатної температури з наступним нагріванням до температури 600 °C, а також встановити вплив різних кількостей мікроелементів у вихідному розчині на фазоформування кальцій-фосфатів.

ЕКСПЕРИМЕНТ І ОБГОВОРЕННЯ РЕЗУЛЬТАТІВ. Синтез легованих мікроелементами кальцій-фосфатів здійснено з водних розчинів системи Ca^{2+}-Mg^{2+}-Na^+-PO_4^{3-}-NO_3^- за різних мольних співвідношень Ca^{2+}: Mg^{2+}: Na^+: PO_4^{3-} = (10-x-y/2) : x : y : 6, (x = 0.1, 0.25, 0.5, 0.75; y = 0.25, 0.5, 0.75, 1.0). Як вихідні компоненти використовували: $Ca(NO_3)_2 \cdot 4H_2O$ («ч. д. а»), $Mg(NO_3)_2 \cdot 6H_2O$ (“ч. д. а”), $NaNO_3$ (“ч. д. а”) та $(NH_4)_2HPO_4$ (“ч. д. а”). Розраховані кількості вихідних компонентів розчиняли у дистильованій воді з наступним змішуванням розчинів, що містили катіони натрію, магнію та каль-

цію, з розчином гідрофосфату амонію за кімнатної температури. Гетерофазну систему перемішували 7 хв та додавали 2 мл розчину амонію (25%). Надалі випарювали воду, а твердий залишок після ретельного перетирання у агатовій ступці нагрівали до температури 600 °С з ізотермічним витримуванням 2 години. Муфельну піч SNOL-7.2/1100 з регулятором TermoPro-601 було використано для нагрівання зразків.

Фазовий склад синтезованих зразків досліджували методом рентгенівської дифракції на порошках із використанням порошкового дифрактометра Shimadzu XRD-6000 (метод 2θ безперервного сканування зі швидкістю 1,2°/хв; діапазон 2θ = 5.0–60.0°). Ідентифікацію фаз здійснено шляхом порівняння експериментальних дифрактограм фосфатів із даними з бази ICDD (The International Centre for Diffraction Data). Параметри елементарної комірки розраховано з використанням програми FullProf. Ефективний розмір наночастинок розраховано за формулою Шеррера: $L = k\lambda/(\beta\cos\theta_{hkl})$, де k = 0.9, β – кутове розширення дифракційного максимуму (у радіанах), визначали як ширину максимуму на половині його висоти, θ_{hkl} – кутове положення дифракційного максимуму.

Зразки також досліджено методом ІЧ-спектроскопії з використанням спектрометра PerkinElmer Spectrum BX у діапазоні 400–4000 $см^{-1}$ для порошків, запресованих у таблетки з KBr.

Встановлення особливостей комплексного легування кальцій-фосфатів передбачало реалізацію часткового заміщення атомів кальцію атомами магнію та натрію за принципом ізо- та гетеровалентного заміщення, відповідно: $(x+y/2)Ca^{2+} \rightarrow xMg^{2+} + y/2Na^{+}$ у структурі гідроксиапатиту $Ca_{10}(PO_4)_6(OH)_2$. З цією метою досліджували фазовий склад продуктів взаємодії у системі Ca^{2+}-Mg^{2+}-Na^{+}-PO_4^{3-}-NO_3^{-} за різних мольних співвідношень Ca^{2+}: Mg^{2+}: Na^{+}: PO_4^{3-}= (10-x-y/2) : x : y : 6, (x = 0.1, 0.25, 0.5, 0.75; y = 0.25, 0.5, 0.75, 1.0). За даними порошкової рентгенографії встановлено вплив вмісту легуючих катіонів натрію та магнію у вихідному розчині на фазовий склад продуктів взаємодії (Рис. 1, Рис. 2, Табл. 1). У випадку систем із фіксованим вмістом катіонів натрію в межах співвідношень: Ca^{2+} : Mg^{2+} : Na^{+} : PO_4^{3-}= (9.875-x) : x : 0.25 : 6, (x = 0.1, 0.25, 0.5, 0.75) встановлено формування монофазного зразка складу $Ca_{9.775}Mg_{0.1}Na_{0.25}(PO_4)_6(OH)_2$, що належать до гексагональної сингонії, просторової групи $P6_3/m$ (структурний тип гідроксилапатиту $Ca_{10}(PO_4)_6(OH)_2$ – PDF2 #01-089-6495) лише у випадку низького вмісту катіонів магнію (Рис. 1а).

У міру збільшення вмісту катіонів магнію у вихідному розчині спостерігали формування біфазних кальцій-фосфатів (суміш фаз на основі $Ca_{10}(PO_4)_6(OH)_2$ та β-$Ca_3(PO_4)_2$ – тригональна сингонія, просторова група *R-3c* – структурний тип вітлокіт, PDF2 #00-070-2065). Відмічено зміну масового вмісту основних компонентів у міру підвищення кількості катіонів магнію у вихідному розчині (Табл. 1. Рис. 1 б-г). Встановлено зростання вмісту фази на основі β-$Ca_3(PO_4)_2$ від 10мас% до 45 мас % при підвищенні масового вмісту магнію від 0.5 мас % до 1.2 мас % у складі осадженого кальцій-фосфату.

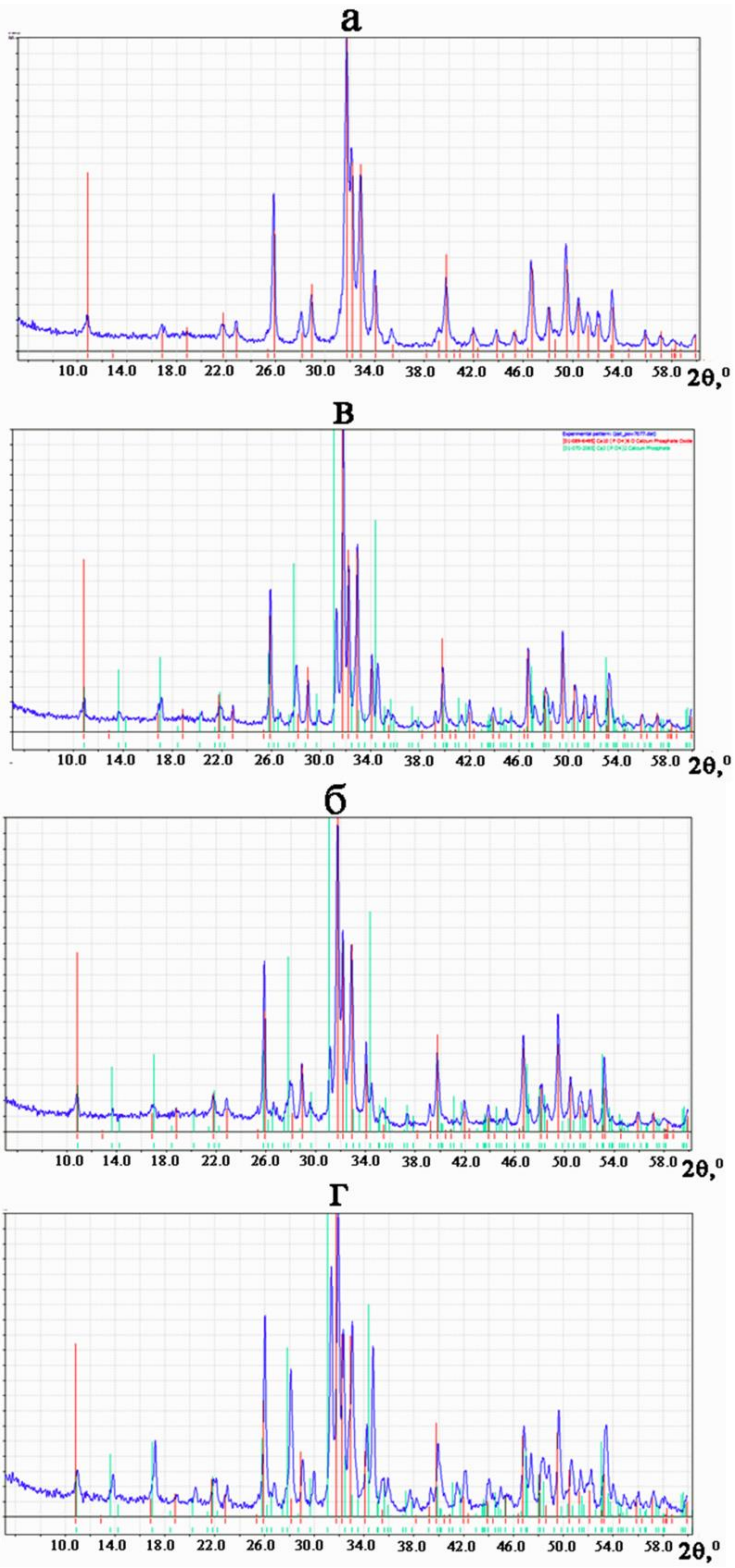

Рис. 1. Порошкові рентгенограми кальцій-фосфатів, синтезованих за мольних співвідношень: Ca^{2+}: Mg^{2+}: Na^{+}: PO_4^{3-} = (9.875-*x*) : *x* : 0.25 :6, (*x* = 0.1 (а), 0.25 (б), 0.5 (в), 0.75 (г)) та нагрітих до температури 600°С. Рефлекси фази $Ca_{10}(PO_4)_6(OH)_2$ (PDF2 # 01-089-6495) позначено червоним кольором, а фази β-$Ca_3(PO_4)_2$ (PDF2 # 01-070-2065) – зеленим кольором.

Fig. 1. XRD patterns for calcium phosphates obtained at molar ratios: Ca^{2+}: Mg^{2+}: Na^{+}: PO_4^{3-}= (9.875-*x*) : *x* : 0.25 :6, (*x* = 0.1 (а), 0.25 (б), 0.5 (в), 0.75 (г)) and heated to temperature 600°C. Reflexes of phase $Ca_{10}(PO_4)_6(OH)_2$ (PDF2 # 01-089-6495) are marked with vertical red lines, while β-$Ca_3(PO_4)_2$ (PDF2 # 01-070-2065) – vertical green lines.

Табл. 1

Фазовий склад продуктів взаємодії у системах із мольними співвідношеннями: Ca^{2+}: Mg^{2+}: Na^{+}: PO_4^{3-}= (10-x-y/2) : x : y : 6, (x =0.1, 0.25, 0.5, 0.75; y = 0.25, 0.5, 0.75, 1.0), відпалених за 600 °С упродовж двох годин

Table 1.

Phase composition of products obtained in systems with molar ratios (10-x-y/2) : x : y : 6, (x = 0.1, 0.25, 0.5, 0.75; y = 0.25, 0.5, 0.75, 1.0) and heated at temperature 600 °C during 2 hours.

Мольні співвідношення			Вміст фаз, мас%		
Ca^{2+}	Mg^{2+}	Na^{+}	$Ca_{10}(PO_4)_6(OH)_2$	β-$Ca_3(PO_4)_2$	Інші фази
9.275	0.1	0,25	100	–	–
9.125	0.25		90	10	–
8.875	0.5		78	22	–
8.625	0.75		55	45	–
9.5	0.25	0.5	87	12	–
9.375		0.75	85	15	–
9.25		1.0	40	–	$NaCaPO_4$

Для систем із варійованим вмістом катіонів натрію також одержано біфазні кальцій-фосфати (суміш фаз на основі $Ca_{10}(PO_4)_6(OH)_2$ та β-$Ca_3(PO_4)_2$), однак вміст останньої у складі зразків змінюється незначно при варіюванні кількості катіонів натрію у вихідному розчині в межах значень мольних співвідношень Ca^{2+}: Mg^{2+}: Na^{+}: PO_4^{3-} = (9.75-y/2) : 0.25 : y : 6, (y = 0.25, 0.5, 0.75) (Рис. 2 а-в). У разі суттєвого підвищення вмісту натрію у вихідному розчині до значення мольного співвідношення Ca^{2+}: Mg^{2+}: Na^{+}: PO_4^{3-} = 9.25 : 0.25 : 1 : 6 формується суміш фаз на основі $Ca_{10}(PO_4)_6(OH)_2$ та подвійного ортофосфату $NaCaPO_4$ - PDF2 #01-076-1456 (Рис. 2 г).

Аналіз та порівняння розрахованих параметрів комірки для синтезованих фаз із відповідними параметрами комірки для β-$Ca_3(PO_4)_2$ (тригональна сингонія, просторова група *R-3c: a* = 10,439(1) Å, *c* = 37,375(2) Å, ICDD № 00-070-2065) та $Ca_{10}(PO_4)_6(OH)_2$ (гексагональна сингонія, просторова група $P6_3/m$: *a* = 9,435(5) Å, *c* = 6,890(1) Å, PDF2 #01-089-6495) (Табл. 2) виявив їхнє незначне зменшення по мірі збільшення кількості магнію у їхньому складі, що підтверджує реалізацію заміщення кальцію (1,0Å) меншим за розміром магнієм (0,72 Å) у обох типах фаз [11].

Розрахунок розмірів частинок монофазних кальцій-фосфатів за формулою Дебая – Шеррера показав їхню нанорозмірність у межах значень 30–50 нм незалежно від складу вихідного розчину (Табл. 2).

Табл. 2

Розраховані параметри елементарних комірок та розміри частинок для обох синтезованих фаз (на основі β-$Ca_3(PO_4)_2$ – тригональна сингонія, просторова група *R-3c* та $Ca_{10}(PO_4)_6(OH)_2$ – гексагональна сингонія, просторова група *P6$_3$/m*) у синтезованих зразках

Table 2.

Calculated lattice parameters and particles size for both type of phases (β-$Ca_3(PO_4)_2$ – trigonal system, space group *R-3c* and $Ca_{10}(PO_4)_6(OH)_2$ – hexagonal system, space group *P6$_3$/m*) in prepared samples.

Мольні співвідношення			Тип фази	Параметри комірки		Розміри частинок нм
Ca^{2+}	Mg^{2+}	Na^+		*a*,*b* Å	*c*, Å	
9.275	0.1	0,25	$Ca_{10}(PO_4)_6(OH)_2$	9.433(9)	6.891(6)	42
9.125	0.25		$Ca_{10}(PO_4)_6(OH)_2$	9.414(5)	6.875(5)	37
			β-$Ca_3(PO_4)_2$	10.377(1)	37.061(2)	48
8.875	0.5		$Ca_{10}(PO_4)_6(OH)_2$	9.412(3)	6.873(8)	29
			β-$Ca_3(PO_4)_2$	10.323(1)	37.058(1)	46
8.625	0.75		$Ca_{10}(PO_4)_6(OH)_2$	9.379(3)	6.872(2)	39
			β-$Ca_3(PO_4)_2$	10.321(3)	37.012(3)	32
9.5	0.25	0.5	$Ca_{10}(PO_4)_6(OH)_2$	9.416(5)	6.878(8)	49
			β-$Ca_3(PO_4)_2$	10.418(4)	37.283(6)	47
9.375		0.75	$Ca_{10}(PO_4)_6(OH)_2$	9.409(3)	6.874(1)	46
			β-$Ca_3(PO_4)_2$	10.429(4)	37.290(6)	38

ІЧ-спектри синтезованих фосфатів наведено на рисунку 3. Загальний вигляд спектрів синтезованих кальцій-фосфатів у відносній інтенсивності та положенні спостережуваних смуг є близьким та вказує на присутність ортофосфатного типу аніона та ОН-групи у їхньому складі. Коливальні моди фосфатних тетраедрів спостерігаємо у частотних діапазонах 550–670 $см^{-1}$ (ν_4) і 1000–1150 $см^{-1}$ (ν_1 і ν_3), а OH^--групи при 3490 $см^{-1}$ (Рис. 3).

Враховуючи результати, представлені у роботі [12], особливостей формування кальцій-фосфатів за мольних співвідношень $Ca^{2+} : Mg^{2+} : PO_4^{3-}$= (10.5-*x*) : *x* : 7 (*x* = 0,2, 0,4, 0,8, 1,0) в умовах осадження з водних розчинів, а саме формування фази типу на основі β-$Ca_3(PO_4)_2$ при заміщенні більше 10% мол атомів Ca на Mg, а при внесенні меншої кількості Mg у вихідний розчин відбувається формування біфазних кальцій-фосфатів зі вмістом фази на основі β-$Ca_3(PO_4)_2$ від 18 до 30 мас %, легованих іонами магнію. Слід відмітити, що у випадку систем, що містили комбінації натрію та магнію, мольне співвідношення $(Ca^{2+} + Mg^{2+})/PO_4^{3-}$ є близьким до відповідного у кальцій-фосфаті апатитового типу, що дозволяє одержувати біфазні кальцій-фосфати з вищим вмістом фази на основі $Ca_{10}(PO_4)_6(OH)_2$.

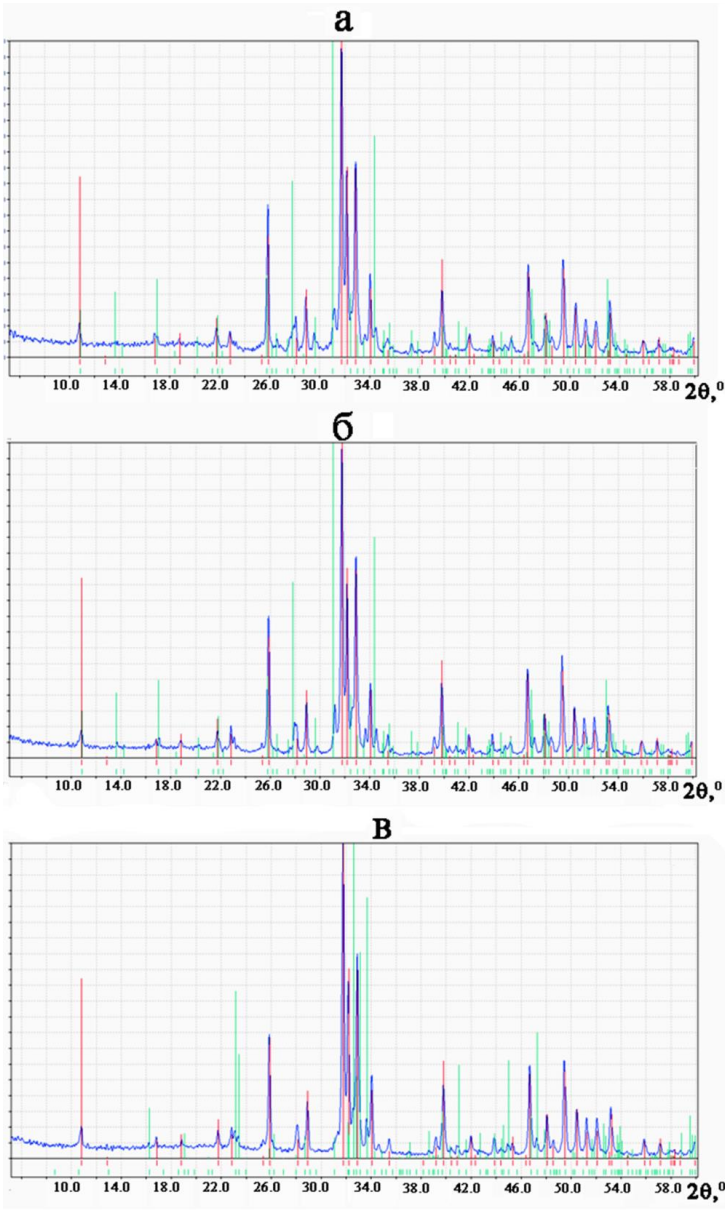

Рис. 2. Порошкові рентгенограми кальцій-фосфатів, синтезованих за мольних співвідношень: Ca^{2+}: Mg^{2+}: Na^{+}: PO_4^{3-}= (9.75-y/2) : 0.25 : y : 6, (y = 0.5 (а), 0.75 (б), 1.0 (в)) та нагрітих до температури 600 °С. Рефлекси фази $Ca_{10}(PO_4)_6(OH)_2$ (PDF2 # 01-089-6495) позначено червоним кольором, а фази β-$Ca_3(PO_4)_2$ (PDF2 # 01-070-2065) на (а-б) і $NaCaPO_4$ (PDF2 #01-076-1456) на (г) – зеленим кольором.

Fig. 2. XRD patterns for calcium phosphates obtained at molar ratios: Ca^{2+}:Mg^{2+}:Na^{+}:PO_4^{3-}= (9.75-y/2) : 0.25 : y :6, (y = 0.5 (а), 0.75 (б), 1.0 (в)) and heated to temperature 600°C. Reflexes of phase $Ca_{10}(PO_4)_6(OH)_2$ (PDF2 # 01-089-6495) are marked with vertical red lines, while β-$Ca_3(PO_4)_2$ (PDF2 # 01-070-2065) – vertical green lines.

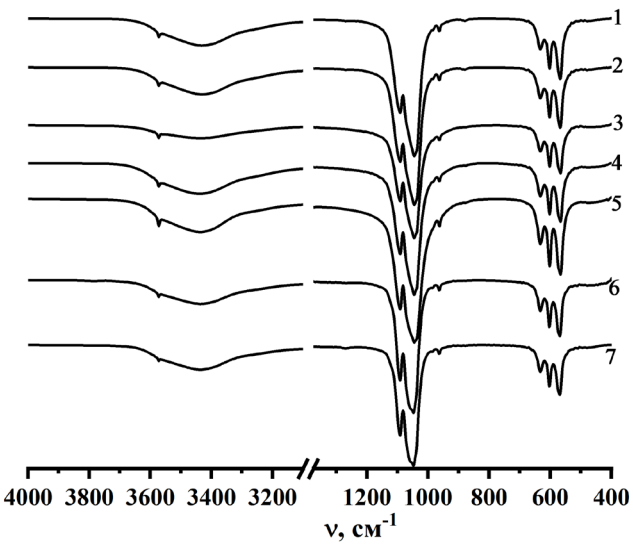

Рис. 3. ІЧ-спектри кальцій-фосфатів, синтезованих за мольних співвідношень: Ca^{2+}: Mg^{2+}: Na^{+}: PO_4^{3-}= (10-x-y/2) : x : y : 6, (y = 0.25: x = 0.1 (крива 1), 0.25 (крива 2), 0.5 (крива 3), 0.75 (крива 4); x = 0.25: y = 0.5 (крива 5), 0.75 (крива 6) та 1,0 (крива 7) нагрітих до температури 600 °С

Fig. 3. FTIR spectra for calcium phosphates obtained at molar ratios: Ca^{2+}:Mg^{2+}:Na^{+}:PO_4^{3-}= (10-x-y/2) : x : y : 6, (y = 0.25: x = 0.1 (curve 1), 0.25 (curve 2), 0.5 (curve 3), 0.75 (curve 4); x = 0.25: y = 0.5 (curve 5), 0.75 (curve 6) and 1,0 (curve 7) and heated to temperature 600 °C.

ВИСНОВКИ. Встановлено умови одержання монофазного кальцій-фосфату апатитового типу, що містить 0.2 мас % магнію та 0.6 мас % натрію, а також біфазних кальцій-фосфатів (суміш фаз на основі β-$Ca_3(PO_4)_2$ та $Ca_{10}(PO_4)_6(OH)_2$), що містять різні кількості мікроелементів: натрій (0.5–2,2 мас %) та магній (0.5–2,0 мас %). Результати ІЧ-спектроскопії підтверджують присутність ортофосфатного типу аніона та ОН-групи. Аналіз розрахованих розмірів частинок кальцій-фосфатів із використанням рівняння Шеррера виявив відсутність впливу складу вихідного розчину на розміри частинок, що знаходяться в межах значень 30–50 нм. Розрахунок параметрів комірок для компонентів біфазних кальцій-фосфатів та їхнє порівняння з відповідними для чистих фаз підтверджує реалізацію легування мікроелементами обох фаз. Одержані результати можна використати у розробках біоактивних кальцій-фосфатів апатитового типу та біфазних кальцій-фосфатів, що містять комплекс мікроелементів для сучасної ортопедії.

Роботу виконано за фінансової підтримки НФДУ (реєстраційний номер №2023.03/0109).

PECULIARITIES OF CALCIUM PHOSPHATES DOPING WITH TRACE ELEMENTS.

N.Yu. Strutynska, Ye.O. Komaschenko, M.S. Slobodyanik

Taras Shevchenko National University of Kyiv, 64/13 Volodymyrska Str., 01601 Kyiv, Ukraine
**email: n.strutynska@knu.ua*

The calcium phosphate formation Ca^{2+}-Mg^{2+}-Na^{+}-PO_4^{3-}-NO_3^{-} at the molar ratios Ca^{2+}: Mg^{2+}: Na^{+}: PO_4^{3-}= (10-x-y/2) : x : y : 6, (x = 0.1, 0.25, 0.5, 0.75; y = 0.25, 0.5, 0.75, 1.0) at temperature 25°C and further heating to 600 °C has been investigated. The conditions for formation of apatite-related calcium phosphate that contains trace elements magnesium and sodium (0.5 wt% of both) in the system with molar ratio Ca^{2+} : Mg^{2+} : Na^{+} : PO_4^{3-} = (10-x-y/2) : 0.1 : 0.25 : 6 as well as biphasic calci-

um phosphates (mixture of phases based on $Ca_{10}(PO_4)_6(OH)_2$ – hexagonal system, space group $P6_3/m$ and β-$Ca_3(PO_4)_2$ – trigonal system, space group *R-3c*) at molar ratio Ca^{2+} : Mg^{2+} : Na^+ : PO_4^{3-}= (10-x-y/2) : x : 0.25 : 6, (x = 0.25, 0.5, 0.75) have been established. It was found, that amount of phase based on β-$Ca_3(PO_4)_2$ in the composition of biphasic calcium phosphates increased (from 10 wt % to 45 wt %) at growing of magnesium quantity in the initial solution. In the case of system with different sodium amount the biphasic calcium phosphates also formed, but the weight ratio of phases based on $Ca_{10}(PO_4)_6(OH)_2$ and β-$Ca_3(PO_4)_2$ less depend on sodium amount in the initial solution and vary in the range 10–15 wt% for values of molar ratio Ca^{2+}: Mg^{2+}: Na^+: PO_4^{3-}= (10-x-y/2) : 0.25 : y : 6, (y = 0.25, 0.5, 0.75). Attempt of preparing of apatite-related calcium phosphate containing 0.5 wt% of magnesium and 2.2 wt% of sodium resulted in formation of mixture of phases based on $Ca_{10}(PO_4)_6(OH)_2$ and double orthophosphate $NaCaPO_4$. According calculation using Sherrera equation the particles size is in the range 30–50 nm. FTIR spectroscopy results confirmed the presence of orthophosphate anions as well as OH-group in the composition of synthesized calcium phosphates. Established conditions of calcium phosphate formation can be used at creation of biomaterials based on biphasic calcium phosphates which contain different amount of trace elements (from 0.5 to 2.2 wtc%).

Key words: trace elements, magnesium, sodium, hydroxyapatite, biphasic calcium phosphates.

ЛІТЕРАТУРА

1. Chen X., Li H., Ma Y., Jiang Y. Calcium Phosphate-Based Nanomaterials: Preparation, Multifunction, and Application for Bone Tissue Engineering. *Molecules.* 2023. **28** (12). 4790 pp. doi: 10.3390/molecules28124790
2. Hou X., Zhang L., Zhou Z., Luo X., Wang T., Zhao X., Lu B., Chen F., Zheng L. Calcium Phosphate-Based Biomaterials for Bone Repair. *Journal of Functional Biomaterials*. 2022. **13** (4). 187 pp. doi: 10.3390/jfb13040187
3. Naqshbandi A., Rahman A. Sodium doped hydroxyapatite: Synthesis, characterization and zeta potential studies. *Materials Letters.* 2022. **312**. 131698 pp. doi: 10.1016/j.matlet.2022.131698
4. Slimen J. B., Mehnaoui M., Jebahi S., Boughzala K., Hidouri M. Thermal and structural properties of sodium, potassium and carbonate doped strontium hydroxyfluorapatite. *Journal of the Indian Chemical Society*. 2022. **99** (6). 100475 pp. doi: 10.1016/j.jics.2022.100475
5. Diba M., Goudouri O.-M., Tapia F., Aldo R. Boccaccini. Magnesium-containing bioactive polycrystalline silicate-based ceramics and glass-ceramics for biomedical applications. *Current Opinion in Solid State and Materials Science*. 2014. **18**. P. 147–167. doi: 10.1016/j.cossms.2014.02.004
6. Lee J., Bae J.S., Kim Y.I., Yoo K.H., Yoon S.Y. Synthesis, Characterization, and Biological Performances of Magnesium-Substituted Dicalcium Phosphate Anhydrous. *Materials (Basel)*. 2024. **17** (18). 4605 pp. doi: 10.3390/ma17184605
7. Lukaviciute L., Ganceviciene R., Tsuru K., Ishikawa K., Yang J.-C., Grigoraviciute I., Kareiva A. Cationic substitution effects in phosphate-based bioceramics – A way towards superior bioproperties. *Ceramics International*. 2024. **50** (19A). P. 34479–34509. doi: 10.1016/j.ceramint.2024.06.398
8. Lu T., Miao Y., Yuan X., Zhang Y, Ye J. Adjusting physicochemical and cytological properties of biphasic calcium phosphate by magnesium substitution: An in vitro study. *Ceramics International*. 2023. **49** (10). P. 15588–15598. doi: 10.1016/j.ceramint.2023.01.148

9. Qi C., Zhu Y.-J., Chen F., Wu J. Porous microspheres of magnesium whitlockite and amorphous calcium magnesium phosphate: microwave-assisted rapid synthesis using creatine phosphate, and application in drug delivery. *J. Mater. Chem.* B. 2015. **3.** P. 7775–7786. doi: 10.1039/C5TB01106J
10. Li H., Zhao X., Cao S., Li K., Chen M., Xu Z., Lu J., Zhang L. Na-doped hydroxyapatite coating on carbon/carbon composites: Preparation, in vitro bioactivity and biocompatibility, *Applied Surface Science*. 2012. **263.** P. 163–173. doi: 10.1016/j.apsusc.2012.09.022
11. Shannon R. D. Revised Effective Ionic Radii and Systematic Studies of Interatomic Distances in Halides and Chalcogenides. *Acta Crystallogr*. 1976. A32. P. 751–767. doi: 10.1107/S0567739476001551
12. Струтинська Н. Ю., Тітов Ю. О., Слободяник М. С. Синтез магнійвмісних кальцій фосфатів методами хімічного осадження з водних розчинів та твердофазної взаємодії. *Питання хімії та хімічної технології*, 2023. 6. С. 196–202. doi: 10.32434/0321-4095-2023-151-6-196-202

REFERENCES

1. Chen X., Li H., Ma Y., Jiang Y. Calcium Phosphate-Based Nanomaterials: Preparation, Multifunction, and Application for Bone Tissue Engineering. *Molecules.* 2023. **28** (12): 4790. doi: 10.3390/molecules28124790
2. Hou X., Zhang L., Zhou Z., Luo X., Wang T., Zhao X., Lu B., Chen F., Zheng L. Calcium Phosphate-Based Biomaterials for Bone Repair. *Journal of Functional Biomaterials*. 2022. **13** (4): 187. doi: 10.3390/jfb13040187
3. Naqshbandi A., Rahman A. Sodium doped hydroxyapatite: Synthesis, characterization and zeta potential studies. *Materials Letters.* 2022. **312**: 131698. doi: 10.1016/j.matlet.2022.131698
4. Slimen J. B., Mehnaoui M., Jebahi S., Boughzala K., Hidouri M. Thermal and structural properties of sodium, potassium and carbonate doped strontium hydroxyfluorapatite. *Journal of the Indian Chemical Society*. 2022. **99** (6): 100475. doi: 10.1016/j.jics.2022.100475
5. Diba M., Goudouri O.-M., Tapia F., Boccaccini A. R. Magnesium-containing bioactive polycrystalline silicate-based ceramics and glass-ceramics for biomedical applications. *Current Opinion in Solid State and Materials Science*. 2014. **18**: 147–167. doi: 10.1016/j.cossms.2014.02.004
6. Lee J., Bae J.S., Kim Y.I., Yoo K.H., Yoon S.Y. Synthesis, Characterization, and Biological Performances of Magnesium-Substituted Dicalcium Phosphate Anhydrous. *Materials (Basel)*. 2024. **17** (18): 4605. doi: 10.3390/ma17184605
7. Lukaviciute L., Ganceviciene R., Tsuru K., Ishikawa K., Yang J.-C., Grigoraviciute I., Kareiva A. Cationic substitution effects in phosphate-based bioceramics – A way towards superior bioproperties. *Ceramics International*. 2024. **50** (19A): 34479–34509. doi: 10.1016/j.ceramint.2024.06.398
8. Lu T., Miao Y., Yuan X., Zhang Y, Ye J. Adjusting physicochemical and cytological properties of biphasic calcium phosphate by magnesium substitution: An in vitro study. *Ceramics International*. 2023. **49** (10): 15588–15598. doi: 10.1016/j.ceramint.2023.01.148
9. Qi C., Zhu Y.-J., Chen F., Wu J. Porous microspheres of magnesium whitlockite and amorphous calcium magnesium phosphate: microwave-assisted rapid synthesis using creatine phosphate, and application in drug delivery. *J. Mater. Chem. B*. 2015. **3**: 7775–7786. doi: 10.1039/C5TB01106J
10. Li H., Zhao X., Cao S., Li K., Chen M., Xu Z., Lu J., Zhang L. Na-doped hydroxyapatite coating on carbon/carbon composites: Preparation, in vitro bioactivity and biocompatibility, *Applied Surface Science*. 2012. 263:163–173.
11. Shannon R. D. Revised Effective Ionic Radii and Systematic Studies of Interatomic Distances in Halides and Chalcogenides. *Acta Crystallogr*. 1976. **A32**: 751–767. doi: 10.1107/S0567739476001551
12. Strutynska N.Yu., Titov Y.O., Slobodyanik M.S. Synthesis of magnesium-containing calcium phosphates by methods of chemical precipitation in aqueous solutions and solid-state interaction. *Voprosy khimii i khimicheskoi tekhnologii.* 2023. **6**: 196–202. (in Ukrainian) doi: 10.32434/0321-4095-2023-151-6-196-202

Стаття надійшла 12.10.2024.

UDC 546.650+547.1'13+541.64+543.426 doi: 10.33609/2708-129X.90.10.2024.69-87

COMPARATIVE CHARACTERISTICS OF SPECTRAL-LUMINESCENCE PROPERTIES OF Yb(III) COMPLEXES WITH UNSATURATED β-DIKETONES.

N.B. Ivakha[1,2]*, O.S. Berezhnytska[1,2]

1 *V.I.Vernadsky Institute of General and Inorganic Chemistry of the NAS of Ukraine, 32/34 Acad. Palladin Avenue, 03142 Kyiv, Ukraine;*
2 *National Technical University of Ukraine «Igor Sikorsky Kyiv Polytechnic Institute», 37 Beresteiskyi Ave., 03056 Kyiv, Ukraine*
e-mail: ivakhanadiia@gmail.com

The study presents a comparative analysis of the spectral-luminescent properties of synthesized β-diketonate coordination complexes of ytterbium with the following ligands: 2,7-dimethyl-oct-1-en-3,5-dione, 2,6-dimethyl-hept-1-en-3,5-dione, 2-methyl-5-phenylpent-1-en-3,5-dione, 2-methyl-5-biphenylpent-1-en-3,5-dione. In addition, research was conducted on polymeric compounds based on these complexes and their phenanthroline mixed-ligand derivatives.

Using a range of physicochemical analysis methods, it was established that the structure of the elementary unit during polymerization, as well as the coordination sphere of the complexes during the formation of mixed-ligand compounds, does not undergo significant changes compared to the initial β-diketonate molecules. Thermal analysis revealed a significant increase in the decomposition onset temperature of mixed-ligand and metallopolymeric compounds compared to their monomeric counterparts. Luminescence spectroscopy demonstrated that the studied samples exhibit luminescence in the infrared (IR) range.

A comparative analysis of the integral luminescence intensities of ytterbium complexes identified key factors influencing the emission characteristics. Primarily, the synthesis of mixed-ligand complexes with phenanthroline mitigates the negative effects of one of the most well-known quenching factors: OH-oscillators of water molecules, which complement the coordination sphere of monomeric ytterbium complexes. Furthermore, the synthesis of polymeric compounds based on β-diketonate complexes positively affects the luminescence, potentially due to a reduction in concentration quenching, as in polymers, the emitting centers are uniformly distributed along the macromolecular chain. Besides directly enhancing luminescent properties, this approach aims to address the practical application of the synthesized compounds since polymers are significantly easier to process and can form film materials.

Based on the conducted research, the following luminescence intensity dependencies were established: dmod>dmhpd>mbphpd>mphpd, as well as monomer-polymer-MLC-MLC polymer. As seen from the presented data, the best emission characteristics are exhibited by ytterbium mixed-ligand mono- and polycomplexes with β-diketones containing alkyl substituents.

Keywords: ytterbium, complex, luminescence, β-diketones, polymers.

INTRODUCTION. The luminescence of ytterbium(III) coordination compounds is a subject of intensive research due to their unique spectroscopic properties and potential applications across various fields. A key feature of the Yb^{3+} ion is its ability to emit in the near-infrared (NIR) range [1], making it highly appealing for investigation. For example, Yb-containing compounds can be used as luminescent markers in immunofluorescence analysis [2–5], as well as in laser systems, electroluminescent devices, optoelectronics, and communication technologies [6, 7].

Ytterbium complexes with organic ligands, particularly β-diketones, are actively studied due to their ability to provide high luminescence efficiency and resistance to external influences. The ligand used for energy transfer determines the luminescence process's efficiency. β-Diketones, which have a high absorbance in the UV spectral range, serve as effective sensitizers for luminescence due to their ability to efficiently transfer absorbed energy to lanthanide ions [8, 9]. The luminescence intensity of lanthanide ions, including Yb^{3+}, in β-diketonate complexes is influenced by two primary factors: energy transfer from the triplet state of the ligand (T_1) to the resonant level of the Ln(III) ion and deactivation processes of the excited levels of the Ln(III) ion. The efficiency of energy transfer from the ligand to the metal is determined by the energy gap (ΔE) between the triplet and resonant levels, with the optimal ΔE value depending on the type of ligand and Ln(III) ion [9]. Experimentally, the T_1 energy levels of ligands are determined from molecular phosphorescence spectra of their complexes with rare-earth metals that have an empty (Y, La) or fully filled (Lu) 4f subshell or with gadolinium, as the resonant $6P_7/_2$ level of the Gd(III) ion lies above the triplet levels of most organic ligands [10].

The energy of triplet states in β-diketonates of Ln(III) depends on the nature of the radicals attached to the chelating [OCCCO] fragment of the ligand and generally decreases in the following substituent series: aliphatic > fluorinated > aromatic [11]. The energy of the triplet level also decreases with the elongation of the aliphatic chain of the fluorinated substituent. For instance, using fluorinated β-diketonates of Yb^{3+} can affect luminescence intensity, reducing it with the increasing chain length of fluorinated compounds [12, 13]. In β-diketonates containing aromatic substituents, a decrease in T_1 energy levels is observed with the increasing size of the conjugated radical system, e.g., phenyl > biphenyl > naphthyl ≈ phenanthryl > anthracenyl. Furthermore, the branching of the alkyl radical chain reduces the spectroscopic properties of the complexes due to increased steric hindrance during coordination.

Most β-diketones form hexacoordinated complexes [Ln(β-dik)$_3$] with lanthanide ions, where the coordination sphere of Ln(III) is completed by solvent molecules, particularly water. However, as shown in many studies, water is a primary quencher of luminescence due to the vibrational oscillations of O–H groups, which facilitate non-radiative energy transfer. Replacing water with organic ligands free of such quenchers (e.g., phenanthroline or its derivatives) significantly enhances the quantum yield of luminescence. The additional ligand may also participate in the energy transfer process to the Ln(III) ion, further increasing luminescence intensity [14-16]. The degree of luminescence quenching by water molecules is inversely proportional to the energy

gap ΔEg between the emitting and ground states. For Yb(III), this gap is relatively large (~10,000 cm^{-1}), enabling the synthesis of ytterbium compounds with sufficiently high quantum yields. Among β-diketonate lanthanide compounds emitting in the IR region, Yb(III) compounds exhibit higher quantum efficiency and longer luminescence lifetimes, with emission wavelengths of 980–1000 nm. This is particularly advantageous for applications in bio-objects, as they are transparent in this range [17–19].

Ytterbium(III) is a unique ion among lanthanides, as it has only one emission band corresponding to the $^2F_5/_2 \rightarrow {}^2F_7/_2$ transition. Optimizing Yb^{3+} luminescence requires selecting appropriate ligands that act as "antennas," absorbing light more efficiently than the lanthanide ion and transferring this energy to the excited state of Yb^{3+}, thereby enhancing luminescence intensity.

However, monomeric lanthanide complexes have several drawbacks, including insufficient thermal stability, a tendency to aggregate, and difficulties in obtaining film materials, limiting their use as precursors for luminescent materials. One approach to overcoming these challenges is incorporating polymer matrices such as polymethyl methacrylate (PMMA), polyvinylcarbazole (PVK), or polystyrene (PS) to create stable materials with high luminescence yields [20–22]. Lanthanide ion-based polymer compositions, prepared by dispersing lanthanide salts or β-diketonate complexes into polymer matrices, have been thoroughly studied. Ytterbium polymer complexes are typically formed by incorporating ytterbium coordination compounds into a polymer matrix, which acts as a stabilizing environment to enhance luminescence stability and efficiency. Polymers not only provide a protective coating but also influence the coordination environment of the ion, reducing the impact of luminescence-quenching factors such as water or ligand vibrations. However, these products often lack uniform metal distribution within the polymer matrix, resulting in unpredictable properties. Polymer compounds based on monomeric complexes are promising in terms of stability and enhanced luminescence intensity. Lanthanide complexes with unsaturated β-diketones containing a metal-chelating ring and a double bond represent a readily available and promising class of compounds for synthesizing polymeric metal complexes. These compounds enable one-stage synthesis of macromolecular metal chelates and uniform metal distribution throughout the polymer, which generally exhibits isotropic properties.

Despite the evident potential of such compounds as polymerization monomers, research on lanthanide β-diketonates with unsaturated substituents remains limited. Combining polymers with coordination complexes reduces the impact of external factors such as moisture or temperature on luminescent properties. This paves the way for stable materials for optical communication and biosensors operating under challenging conditions.

Since the 2010s, researchers at the Department of Heterophase Synthesis of Inorganic Compounds and Materials, Vernadsky Institute of General and Inorganic Chemistry, NAS of Ukraine, have investigated the polymerization of unsaturated diketonate lanthanide complexes [23–25]. Radical polymerization has been used to obtain metallopolymers based on mono- and mixed-ligand β-diketonate complexes of Ln(III) with 2,7-dimethyl-oct-1-en-3,5-dione, 2,6-dimethyl-hept-1-en-3,5-dione,

2-methyl-5-phenylpent-1-en-3,5-dione, 2-methyl-5-biphenylpent-1-en-3,5-dione, and their mixed-ligand derivatives with phenanthroline.

Currently, key challenges in this field include identifying optimal ligands to enhance luminescence efficiency and refining methodologies for controlling the coordination environment of ytterbium ions. Despite significant progress in understanding luminescence mechanisms, future research should focus on developing new ligand types that minimize quenching processes. Systematizing previously obtained data, including those by the authors of this article, is essential for these advancements.

This work summarizes the results of research on ytterbium metal complexes and their polymers with unsaturated β-diketones containing alkyl and aromatic substituents and compares the spectral-luminescent characteristics of the compounds depending on the nature of the substituents.

EXPERIMENT AND DISCUSSION OF RESULTS. The study focused on mono-, mixed-ligand, and polymer coordination compounds of ytterbium (III) with unsaturated β-diketones. The synthesis of the initial β-diketones was carried out via Claisen condensation according to the methodology described in [26–27] (Fig. 1).

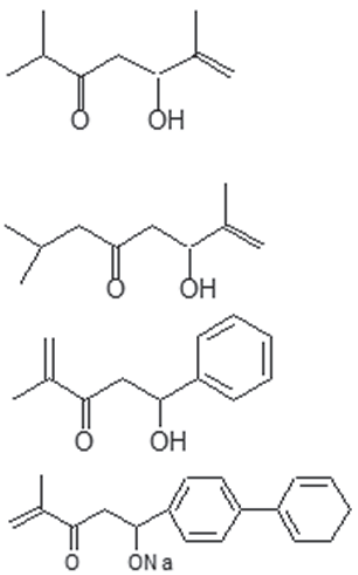

2,6-Dimethyl-hept-1-en-3,5-dione (Hdmhpd)

2,7-Dimethyl-oct-1-en-3,5-dione (Hdmod)

2-Methyl-5-phenylpent-1-en-3,5-dione (Hmphpd)

2-Methyl-5-biphenylpent-1-en-3,5-dione (Hmbphpd)

Fig. 1 – Structural formulas of β-diketonate ligands.

The synthesis of Yb(III) complexes with β-diketones was conducted in aqueous-alcohol solutions by reacting ytterbium chloride ($YbCl_3 \cdot 6H_2O$) with the sodium salt of the respective ligand at a molar ratio of 1:3.5 (pH 8–8.5) at room temperature. The synthesis of mixed-ligand complexes, where phenanthroline was used as the second ligand, was performed in alcoholic solutions with a $Yb(\beta\text{-dik})_3 \cdot Phen$ ratio of 1:1 following the method described in [23].

Polymer β-Diketonates of Yb (III) were

obtained through the homopolymerization of the synthesized monomeric complexes via a radical mechanism [24]. The polymerization was carried out at 80 °C, with azobisisobutyronitrile (AIBN) chosen as the initiator for the radical polymerization, as the polymerization mechanism for β-diketonates of lanthanides is identical to that of vinylmonomers.

All synthesized compounds were investigated using IR spectroscopy, DRS, thermogravimetry, and luminescence analysis.

IR spectra were recorded using a Specord M80 spectrometer in the range of 400–4000 cm^{-1} in KBr pellets.

Diffuse reflectance spectra in the range of 300 – 1100 nm were registered using a UV-VIS-IR Shimadzu UV-3600 spectrophotometer.

The hydratecomposition of the synthesized compounds and their thermal stability were determined using DTA. Thermograms were recorded using a Q–1500°D derivatograph system from F. Paulik, J. Paulik, L. Erdey, in the temperature range of 20–500 °C at a heating rate of 5 °C/min in a platinum crucible with a carrier (anhydrous Al_2O_3) under a static air atmosphere.

The excitation and emission spectra of solid complexes were recorded using a Fluorolog FL 3-22 spectrofluorimeter, Horiba Jobin Yvon (Xe lamp 450 W), with a light filter OS 11, followed by corrections accounting for the emission distribution of the xenon lamp and the sensitivity of the photomultiplier tube (PMT). For the IR region, InGaAs photoresistors (DSS-IGA020L, Electro-Optical Systems, Inc, USA, cooled to liquid nitrogen temperatures) were used as radiation receivers.

The coordination mode of β-diketonates with the Yb(III) ion was determined by IR spectroscopy, which, in cases where direct X-ray structural analysis is not possible, allows the structural identification of β-diketonate complexes. Fig. 2 shows a typical IR spectrum of Yb(III) coordination compounds with β-diketonate ligands containing unsaturated substituents in the α-position, and Table 1 summarizes the main vibrational frequencies and their assignments for all studied ytterbium-containing β-diketonates.

The main characteristic vibration bands of complex β-diketonate compounds are located in the region of 1500–1700 cm^{-1}, which correspond to stretching vibrations of carbonyl groups and multiple CC bonds of the dicarbonyl fragment [28, 29].

Since there is a delocalization of electron density in the diketonate fragment, the stretching vibration bands occupy an intermediate position between the stretching vibrations of single C-O and C-C and double C=O and C=C bonds. Thus, the band with a higher frequency (~1580–1610 cm^{-1}) corresponds to the symmetric stretching vibration of the bond (C⁻⁻⁻O), and with a lower frequency (~1540–1580 cm^{-1}) to the asymmetric stretching vibration of the bond (C⁻⁻⁻C). It should be noted that for monomeric and polymeric complexes with mbphpd and Phen, the splitting of the ν_s(C⁻⁻⁻O) band into 2 components is observed, which may be due to the structural inequivalence of some chelate rings. For most polymeric compounds, the ν(C=C) band appears in the region of ~1650–1660 cm^{-1} as a shoulder, indicating the presence of terminal unsaturated groups, and in the case of the $[Yb(mphpd)_3Phen]_n$ complex, the average intensity of this band may indicate an incomplete polymerization process and the formation of a certain number of oligomeric products.

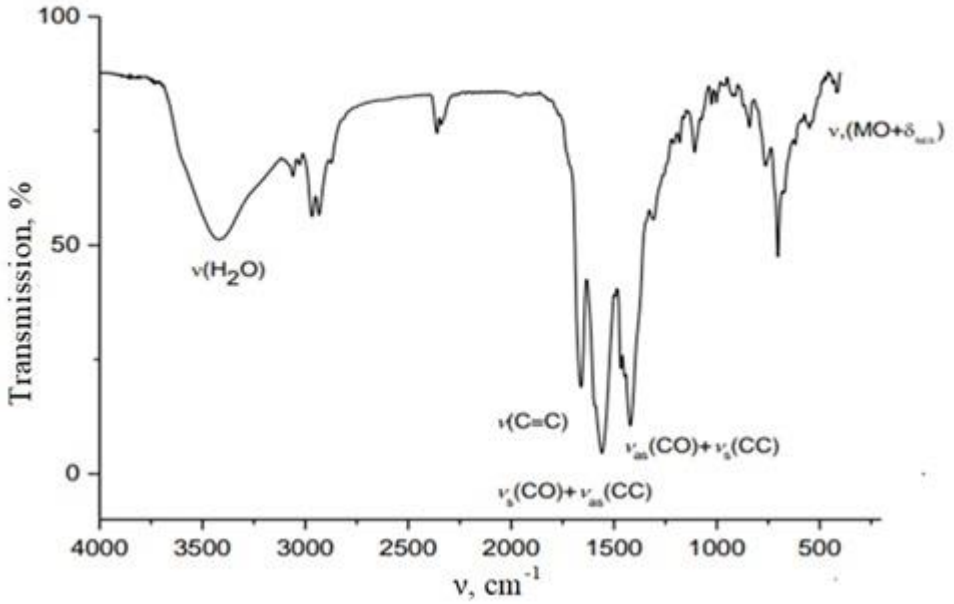

Fig. 2. – IR spectrum of the complex $Yb(mphpd)_3 \cdot 2H_2O$.

Table 1.

Assignment of vibration bands in the IR spectra of Yb(III) β-diketonate (cm^{-1})

Complex	$\nu(Yb–O)+\delta_{hel.\ ring}$	ν (Yb-N)	$\nu_{as}(C{=}{-}{=}C)$	$\nu_s(C{=}{-}{=}O)$	$\nu_s(C{=}C)$
$Yb(mphpd)_3 \cdot 3H_2O$	421, 453, 490, 505, 545	-	1580	1596	1655
$Yb(mphpd)_3 \cdot Phen$	405, 464, 487, 504, 545	467	1582	1601	1655
$Yb(mbphpd)_3 \cdot 2H_2O$	411, 429, 450	-	1560	1586	1653
$Yb(mbphpd)_3 \cdot Phen$	410, 428, 451	474	1558	1575, 1607	1653
$Yb(dmhpd)_3 \cdot 2H_2O$	408,430, 478, 501, 526	-	1555	1555	1640, 1660
$Yb(dmhpd)_3 \cdot Phen$	420, 435, 481, 495, 507	477	1552	1590	1630
$Yb(dmod)_3 \cdot 2H_2O$	456, 470, 489, 520	-	1542, 1560	1590	1680
$Yb(dmod)_3 \cdot Phen$	450, 468, 470, 515	480	1547	1592	1650
$[Yb(mphpd)_3]_n$	421, 453, 490, 505, 545	-	1560	1590	1651sh.
$[Yb(mphpd)_3 \cdot Phen]_n$	410, 420, 435, 495, 507	481	1565	1585	1650
$[Yb(mbphpd)_3]_n$	406, 427, 455	-	1559	1581, 1599	1652sh.
$[Yb(mbphpd)_3 \cdot Phen]_n$	409, 432, 461	481	1561	1580, 1607	1651sh.
$[Yb(dmhpd)_3]_n$	419, 426, 484, 511	-	1537	1578	1659sh.
$[Yb(dmhpd)_3 \cdot Phen]_n$	417, 429, 475, 515	468	1535	1577	1653sh.
$[Yb(dmod)_3]_n$	421, 435, 481, 511	-	1542	1581	1661sh.
$[Yb(dmod)_3 \cdot Phen]_n$	419, 439, 474, 518	465	1544	1584	1663sh.

In the low-frequency region of the spectra (400–600 cm^{-1}) a set of bands appears, which corresponds to a combination of stretching vibrations of the Yb-O bond and deformation vibrations of the chelate ring. At the same time, the frequencies of the δ_{ring} and ν(Yb–O) differ slightly for different complexes, since the structure of the [OCCCO] fragment of the ligands practically does not depend on the type of substituents in them, which may indicate a close coordination environment of Yb(III) in all the studied compounds. For complexes with phenanthroline in the IR spectra in the range of 465–480 cm^{-1}, bands corresponding to the stretching vibration of Yb-N are additionally observed. Their presence confirms the formation of mixed-ligand complexes. The position of the ν vibration of the Yb-O bonds in the IR spectra of polymer and monomer complexes is almost the same, and the slight shift of the band data to the low-frequency region (up to 20 cm^{-1}) for polymer complexes is probably due to the deformation of the coordination site. That is, during polymerization, the immediate environment of the lanthanide ion practically does not change in comparison with metal complexes.

In the region of 3200–3600 cm^{-1} for all monomer complexes, there is a broad vibration band of the O-H groups, which is associated with the addition of water molecules to the coordination sphere of ytterbium(III) complexes. In the case of phenanthroline complexes, this band is not observed in the IR spectra, which indicates the displacement of water molecules from the inner coordination sphere due to the coordination of the Phen molecule to the central ion. In the case of polymer complexes, the ν(O–H) band has a low intensity in the given spectral range. This can be explained by the presence of a small amount of occluded water in the structure of metal polymers.

The similarity of the IR spectra of metal chelate monomers, mixed ligand and polycomplexes suggests the proximity of the ligand environment of metal ions in these compounds.

Based on the analysis of the IR spectra, it can be unequivocally stated that in the complexes $Yb(\beta\text{-dik})_3 \cdot 2H_2O$ the metal ion coordinates the β-diketonate ligands bidentately-cyclically with a delocalized system of π-bonds in the chelate ring. In this case, six-membered metallocycles are formed (Fig. 3).

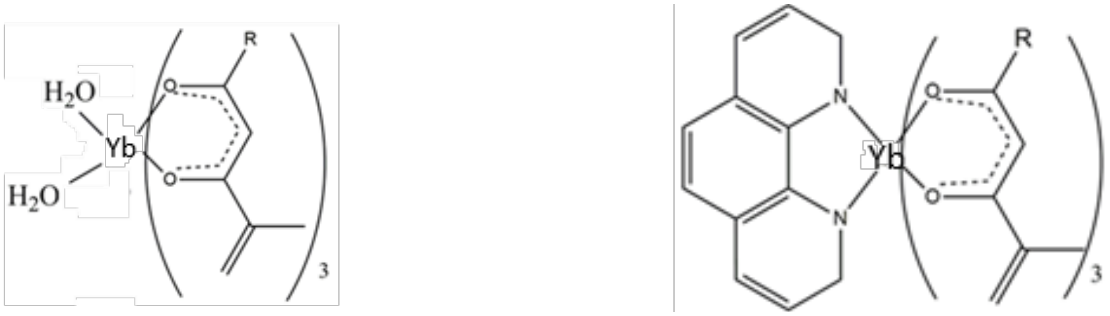

a b

Fig. 3 – Schematic structure of Yb(III) complexes: $Yb(\beta\text{-dik})_3$ (a), $Yb(\beta\text{-dik})_3Phen$ (b).

From the point of view of the possible practical application of the synthesized coordination compounds of ytterbium (III), an important stage of the study is the thermal analysis, in particular the determination of the thermal stability of the synthesized compounds. The thermal stability of Yb(III) complexes with unsaturated β-diketonesis analyzed in sufficient detail in [23, 24]. The generalization of the results of thermal studies of Yb(III) β-diketonates shows that the thermal decomposition of all compounds proceeds in the same way:

- dehydration of monomeric complexes $Yb(\beta\text{-dik})_3$, regardless of the β-diketone, occurs in the temperature range of 120–127 °C and is accompanied by endoeffects, which corresponds to the elimination of two coordinated water molecules;
- for mixed-ligand compounds, the absence of this thermal effect indicates the replacement of water molecules by a phenanthroline molecule. The elimination of a phenanthroline molecule begins at about 170 °C;
- in the case of polymer complexes at a temperature of ~ 130 °C, a slight endoeffect is observed, which may indicate the elimination of water remaining in the voids of the polymer matrix during polymerization of the monomer;
- at a temperature of > 180 °C, polymerization of complexes occurs without an initiator;
- in the temperature range of 250–450 °C, oxidative thermal destruction of all complexes is accompanied by a number of exoeffects, which is due to the decomposition of organic fragments of the molecule, and the final decomposition products are non-stoichiometric ytterbium(III) oxides;
- the thermal stability of the studied compounds increases in the following order: monocomplexes>mixed-ligand complexes>metalpolymers>mixed-ligand metalpolymers.

The temperature at the onset of degradation varies from 250 °C (for monomers) to 375 °C (for polymers). This effect may be due to the denser, ordered packing of polycomplexes with a complex, possibly branched, system of bonds.

The geometry evaluation, coordination number, and determination of the symmetry of the nearest coordination environment around the Yb(III) ion were carried out based on the analysis of the position and intensity of the f-f transition bands in the diffuse reflectance (DR) spectra of the studied compounds.

In Fig. 4, as an example, the DR spectra of Yb(III) complexes with 2,7-dimethyl-octen-1-dione-3,5 are shown, while Table 2 lists the characteristics of the $^2F_{7/2} \rightarrow {}^2F_{5/2}$ transition for all synthesized complexes. In the DR spectra of all complexes, one $^2F_{7/2} \rightarrow {}^2F_{5/2}$ transition characteristic of the Yb(III) ion is observed, with a maximum in the range of 970–980 nm. At the same time, the overall appearance of the spectra for both monomeric and polymeric complexes is similar, indicating that polymerization does not affect the geometry and structure of the coordination polyhedron of the lanthanide. The slight difference in λ_{max} values is due to the geometric structure of the substituents in the β-diketonate ligands, which have different λ_{max} values for allowed π–π^* transitions in the near ultraviolet region (200–400 nm). For example, replacing a biphenyl substituent with an alkyl substituent causes a significant shift in the absorption maximum and broadening of spectral lines, which is due to different energy characteristics of the of the ligands being studied [10, 24].

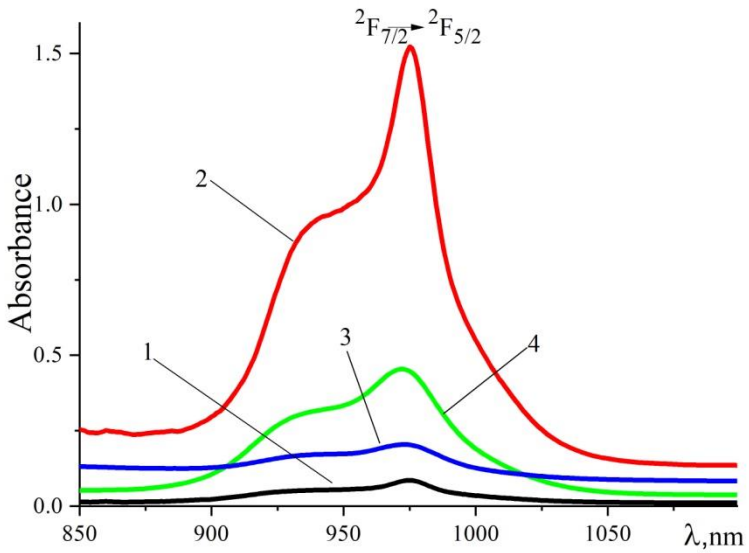

Fig. 4 – Diffuse reflection spectra of complexes$Yb(dmod)_3 \cdot 2H_2O$ (1), $Yb(dmod)_3 \cdot Phen$ (2), $[Yb(dmod)_3]_n$ (3), $[Yb(dmod)_3 \cdot Phen]_n$ (4) [24].

Table 2

Position of the maxima of the $^2F_{7/2} \rightarrow {}^2F_{5/2}$ transitions in the DRS of Yb(III) complexes with unsaturated β-diketones

Complex	λ_{max}, nm	β	δ	$b^{1/2}$
$Yb(mphpd)_3 \cdot 3H_2O$	975	0,9945	0,5530	0,05244
$Yb(mphpd)_3 \cdot Phen$	978	0,9968	0,3210	0,04000
$Yb(mbphpd)_3 \cdot 2H_2O$	974	0,9957	0,4319	0,04637
$Yb(mbphpd)_3 \cdot Phen$	976	0,9941	0,5935	0,05431
$Yb(dmhpd)_3 \cdot 2H_2O$	973	0,998	0,2004	0,03162
$Yb(dmhpd)_3 \cdot Phen$	974	0,998	0,2004	0,03162
$Yb(dmod)_3 \cdot 2H_2O$	975	0,9951	0,4924	0,04950
$Yb(dmod)_3 \cdot Phen$	975.5	0,9969	0,3110	0,03937
$[Yb(mphpd)_3]_n$	971	0,9978	0,2205	0,03317
$[Yb(mphpd)_3 \cdot Phen]_n$	973	0,9962	0,3814	0,04359
$[Yb(dmhpd)_3]_n$	972	0,998	0,2004	0,03162
$[Yb(dmhpd)_3 \cdot Phen]_n$	973.5	0,997	0,3009	0,03873
$[Yb(dmod)_3]_n$	973	0,9978	0,2205	0,03317
$[Yb(dmod)_3 \cdot Phen]_n$	972	0,9947	0,5328	0,05148

It should be noted that for mixed-ligand phenanthroline complexes, regardless of the ligand, there is a slight (~30 cm^{-1}) bathochromic shift of the band maximum and a significant increase in absorption intensity. Probably, the N,N-donor ligand makes the structure of the complexes more rigid due to the axial distortion of the f-metal coordination site during the coordination of the Phen molecule with two nitrogen heteroatoms, providing effective shielding of the Yb^{3+} nucleus from external quenching compared to the original complexes without Phen.

However, in general, the shape and position of the $^2F_{7/2} \rightarrow {}^2F_{5/2}$ transition band for all ytterbium compounds are almost the same, which indicates a similar coordination environment of Yb(III) in all synthesized samples. At the same time, the absorption maxima for monocomplexes are close to λ_{max} of the aquated Yb_{aq3+} ion (973 nm), which indicates a close symmetry of the nearest coordination environment of the ytterbium ion in complexes and inorganic salts [30]. Thus, it can be assumed that the synthesized Yb(III) β-diketonates are characterized by C_{4v} symmetry, the lanthanide coordination number = 8, to which the coordination polyhedron corresponds is a deformed square antiprism.

For all synthesized compounds, the covalent bond parameters were calculated: the nepheloxetic parameter (β), the covalent parameter ($b_{1/2}$) and the Sinha parameter (δ) (Table 2). As can be seen from the data in Table 2, for all complexes the values of β are close to 1, which may indicate a high ionicity of the Yb–O bond [31]. The parameters $b_{1/2}$ and δ characterize the degree of covalent bond of the lanthanide with the donor ligand molecules. The largest values of $b_{1/2}$ are found in monomeric complexes, which also correspond to the largest values of δ, which indicates a smaller contribution of the covalent component to the Yb–O bond. During polymerization of the complexes, the values of $b_{1/2}$ decrease by almost 1.5 times, which indicates an increase in the covalent bond when transitioning from mononuclear to polymeric complexes. This is also confirmed by the values of the parameter δ: $\delta_{[Yb(\beta\text{-dik})3]n} < \delta_{Yb(\beta\text{-dik})3}$. The lowest values of covalence parameters are found in ligands with alkyl substituents (2,7-dimethyl-oct-1-en-3,5-dione, 2,6-dimethyl-hept-1-en-3,5-dione), which are structurally less bulky than β-diketones with phenyl substituents (2-methyl-5-phenylpent-1-en-3,5-dione, 2-methyl-5-biphenylpent-1-en-3,5-dione). Therefore, dmhpd/dmod easily "fit" to the central atom, while bulky mphpd/mbphpd molecules do not create additional shielding of the emitting centers and can form a more ionic bond with the central atom. Thus, a decrease in the parameter $b_{1/2}$ in the order mphpd> mbphpd>dmod>dmhpd indicates a decrease in the covalent contribution to the metal-ligand bond. It is clear that in the case of polymers, the contribution of the covalent componentis greater, which is due to the insignificant deformation of the coordination site due to the polymerization processes, while the structure and symmetry of the complexes do not under go major changes. Due to the weakening of the ionicity of the bond with increasing covalency, the intensity of the radiation can increase due to the decrease in the shielding of the emitting ion. However, this is not the only factor affecting the intensity of luminescence.

For all obtained Yb(III) complexes, a characteristic 4f-luminescence is observed in the near-IR region of the spectrum ($\lambda_{lum.}$ = 980–1015 nm, transition $^2F_{5/2} \rightarrow {}^2F_{7/2}$).

An important condition for observing intense luminescence is the optimal energy gap between the triplet level of the ligand (E_T) and the resonance level of the lanthanide. To experimentally determine the energy of the triplet levels of β-diketones, the fluorescence spectra of Gd(III) complexes were studied, which were synthesized by a similar method as the Yb(III) complexes (Fig. 5, Table 3) [10].

Table 3.

Calculated energies of the triplet levels of the ligands.

Ligand	E_T (cm^{-1})	$\Delta E_T - E_{Yd(2F5/2),}$($cm^{-1}$)
dmhpd	19570	9370
$[dmhpd]_n$	19230	9030
dmod	19350	9150
$[dmod]_n$	18900	8700
mphpd	19490	9290
$[mphpd]_n$	20600	10400
mbhppd	21000	10800
$[mbhppd]_n$	20750	10550

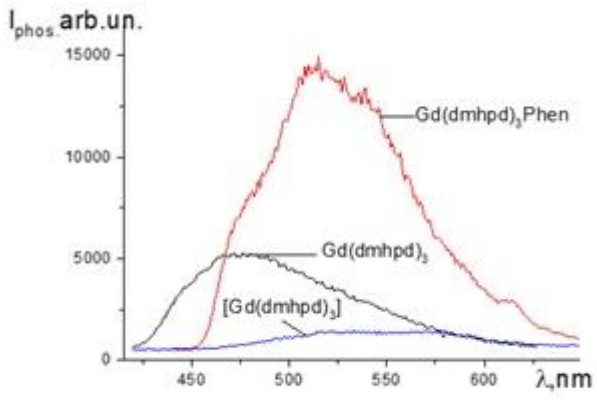

Fig. 5 – Phosphorescence spectra of some gadolinium complexes, T=77 K.

The calculated values of the triplet energy levels of the ligands and the width of the energy gap between the E_T of the ligands and the resonance $^2F_{5/2}$ level of Yb(III) (10330 cm^{-1}) show that in all cases, intramolecular energy transfer to the metal ion is fundamentally possible, which indicates the ability of the complexes to exhibit effective 4f-luminescence.

Fig. 6 (a, b, c) presents the excitation and luminescence spectra of ytterbium compounds with the studied β-diketones. The excitation spectra of the complexes (Fig. 6, a) are similar for all compounds regardless of the ligands and represent broad structured bands in the region of 230–410 nm, corresponding to the π-π* transitions of the β-diketonate fragment. The partial overlap of the ligand absorption spectra and the excitation spectra of the complexes indicates the sensitization of 4f-luminescence due to intramolecular energy transfer from the β-diketonate fragment to the ytterbium ion. Compared with the absorption of the organic ligand, the bands of the f-f transitions of Yb(III) are quite weak, which confirms the predominant sensitization due to the excitation of the ligand compared to the direct excitation of the lanthanide ion.

In the luminescence spectra of Yb(III) β-diketonates, the most intense is one band, which corresponds to the transition from the excited level $^2F_{5/2} \rightarrow {}^2F_{7/2}$ in the region λ_{max}= 978–985 nm. Table 5 shows the position of this band for all synthesized ytterbium complexes, and also the calculated integral intensities of luminescence of the samples. In addition to the narrow peak, a broad band at λ≈1000nm is observed in the spectra, which corresponds to optical transitions of an electron between the Stark sublevels of the ion and depends on the symmetry of the crystal field of the ligand. The difference in the shape of the spectral lines and the integrated intensity for different ligands can be due to both the different

structure of the ligands and the screening of the emitting centers by phenyl substituents of aromatic β-diketones or phenanthroline. Thus, the maximum relative emission intensity is observed for complexes with dmod, which is up to ≈ 6 (for monomers) and ≈ 1.5 (for polymers) times higher than the relative intensity for complexes with other β-diketones, which can be explained by the positive effect of the additional methylene group of the hydrocarbon radical in dmod, which in a certain way weakens the bond of the Yb(III) ion with the ligand due to there distribution of the electron density in the molecule, and, presumably, contributes to a more efficient transfer of energy from the ligand to the metal.

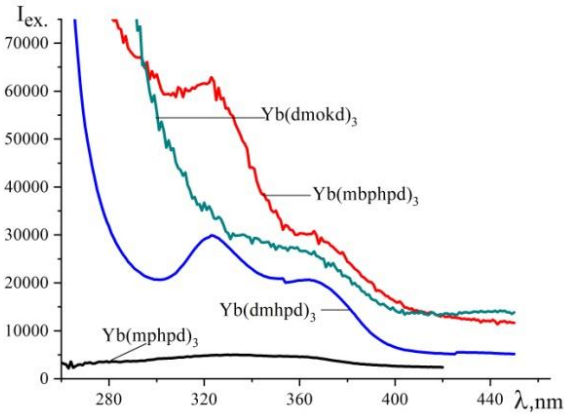

a

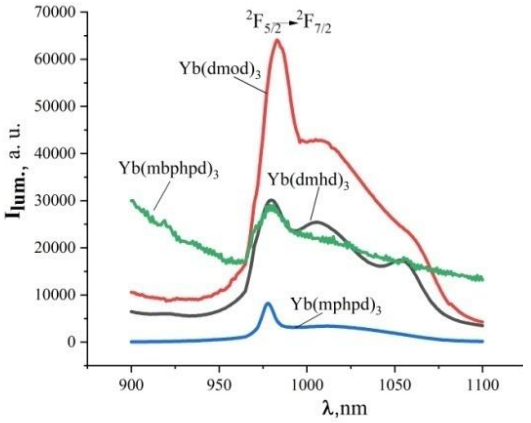

b

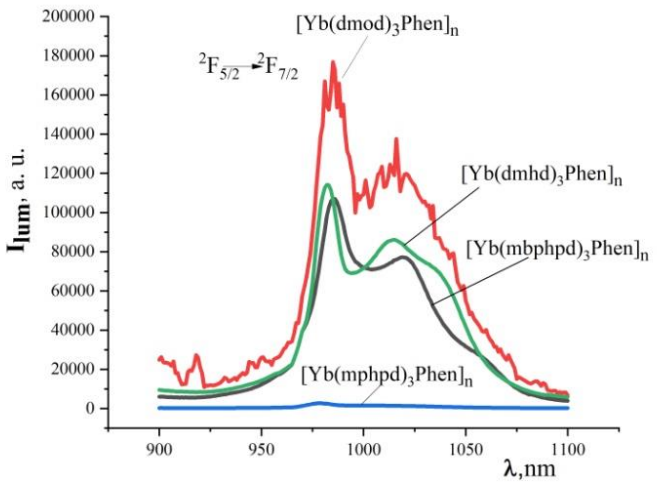

c

Fig. 6 – Excitation (a) and luminescence (b, c) spectra of Yb(III) β-diketonates (λ_{em}.=365 nm, T=293K).

The minimum value of I_{lum} is exhibited by complexes based on methacroylacetophenone (Table 4), which maybe due to the structural features of the methacroylacetophenone molecule, namely, the screening of the emitting centers of the ytterbium ion by the aromatic-ring. The higher integral intensity of complexes based on mbphpd compared to mphpd could be explained by an antenna effect or stacking-stacking interactions in the biphenyl substituent.

Table 4.

Characteristics of luminescence spectra of complexes with unsaturated diketones.

Complex	λ_{lum}, nm	$I_{lum.}$ 10^{-4},a.u.	Complex	λ_{lum}, nm	$I_{lum.}$ 10^{-4},a.u.
$Yb(mphpd)_3 \cdot 3H_2O$	978	309580.54	$Yb(dmhpd)_3 \cdot 2H_2O$	980, 1005, 2054	1758376.24
$Yb(mphpd)_3 \cdot Phen$	978	1758712.35	$Yb(dmhpd)_3 \cdot Phen$	984	5416980.82
$[Yb(mphpd)_3]_n$	978	477261.68	$[Yb(dmhpd)_3]_n$	982	2076017.15
$[Yb(mphpd)_3 \cdot Phen]_n$	979, 1001, 1037	114618.03	$[Yb(dmhpd)_3 \cdot Phen]_n$	985,1020	5927269.72
$Yb(mbphpd)_3 \cdot 2H_2O$	980	514338.36	$Yb(dmod)_3 \cdot 2H_2O$	983	3348353.14
$Yb(mbphpd)_3 \cdot Phen$	982	5446747.50	$Yb(dmod)_3 \cdot Phen$	982	6284268.62
$[Yb(mbphpd)_3]_n$	981	529824.78	$[Yb(dmod)_3]_n$	985	2693542.02
$[Yb(mbphpd)_3 \cdot Phen]_n$	982, 1014, 1038	6367072.55	$[Yb(dmod)_3 \cdot Phen]_n$	981, 985, 987, 990	9429427.30

For the all studied complexes, the integral luminescence intensity of metallo polymers exceeds the luminescence of their monomeric analogues, which is due to the presence of a larger number of emitting centers in $[Yb(\beta\text{-}dik)_3]_n$ (Fig. 5, b, c). In addition, the higher luminescence intensity of polymeric metal complexes enhanced with monomeric ones may be due to an increase in the molecular weight of the metallopolymer, which, in turn, contributes to a decrease in exchange interactions between lanthanide ions, and, consequently, to a decrease in energy loss, and also contributes to a more efficient transfer of energy from the molecular levels of the polymer to the resonance level of Yb(III).

The highest luminescence intensity is observed in the mixed ligand complexes, regardless of the β-diketonate ligand. Thus, for monomeric dimethyloctene and dimethylheptene complexes I_{lum}. increases by 2 and 3 times, respectively, and for complexes with mphpd and mbphpd $I_{lum.}$ increases by 6 and 10 times, respectively. The tendency to increase the intensity of luminescence is also preserved for polymeric mixed-ligand compounds, with this value of $I_{lum.}$ individual monoligand polymers increases by up to 1.5 times. The exception is the complex with methacroylacetophenone, the luminescence of which decreases upon formation of a mixed-ligand polymer complex. The obtained data can be explained by two reasons, one of which is possibly due to the removal of OH oscillators from the inner sphere of the complexes, which quench the luminescence of the compounds [32]. On the

other hand, due to the additional coordination of the REE ion of the neutral phenanthroline ligand, intramolecular energy transfer occurs from Phen to β-dik, after E_T(β-dic)<E_T(Phen) (E_T(Phen) = 21480 cm^{-1}), which only leads to an additional antenna effect.

As can be seen from Fig. 5c, for the homopolymer $[Yb(dmod)_3 \cdot Phen]_n$, a broadening and splitting of the $^2F_{5/2} \rightarrow {}^2F_{7/2}$ transition line into 4 components at 981, 985, 987, and 990 nm is observed. Such splitting indicates the presence of several emitting centers. This may be due to the formation of complexes with different degrees of polymerization. It is known that compounds with long alkyl substituents polymerize with a low degree of conversion, which is due to the transfer of the chain to the monomer, therefore, during polymerization, several polymer compounds of different molecular weights and, accordingly, different optical properties can be formed.

Summarizing the data of the luminescent properties of Yb(III) complexes with unsaturated β-diketones, we can draw the following conclusions (Fig. 7):

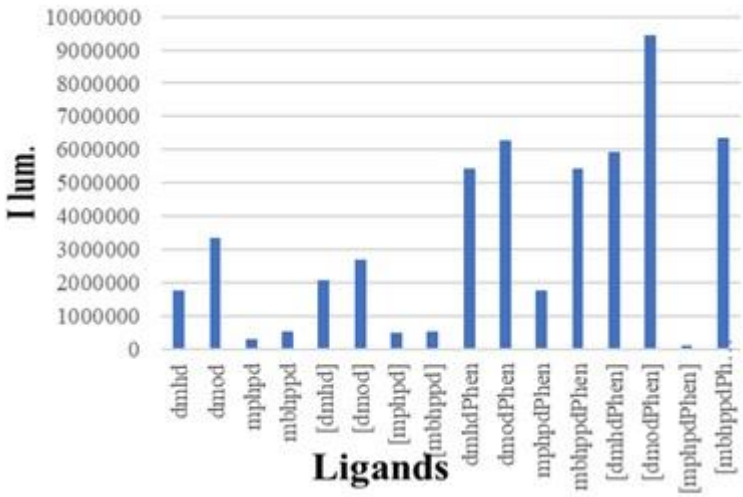

Fig. 7 – Diagram of the change of integral intensity of luminescence inYb(III) β-diketonates depending on the nature of the substituents in the ligands molecules.

• the intensity and efficiency of luminescence directly depend of the nature of the substituents in the ligand molecules (aliphatic substituents in the α-position contribute to more efficient emission in the near-IR range than aryl ones) and increase in the order dmod> dmhpd>mbphpd>mphpd;

• the luminescence intensity of Yb(III) complexes with phenanthroline for all synthesized compounds is higher than for monoligand complexes, which is due to the leveling of the gassing action of water molecules and additional energy transfer and luminescence sensitization;

• the luminescence intensity of metallopolymers is higher than that of monomeric complexes. Not a very significant difference in the integral intensity of luminescence between monomeric and polymeric samples maybe due to the complex structure of ytterbium (III)

β-diketonate complexes, which prevents the production of polymers with high molecular weight;

• the change in the luminescent properties of Yb(III) β-diketonates occurs in the following series: $Yb(\beta\text{-dik})_3 \cdot 2H_2O < [Yb(\beta\text{-dik})_3]_n < Yb(\beta\text{-dik})_3 \cdot Phen < [Yb(\beta\text{-dik})_3 \cdot Phen]_n$, β-dik: mphpd<mbphpd<dmhpd<dmod.

According to the obtained data for the studied Yb(III) complexes with unsaturated β-diketones, the following excitation and energy transfer scheme can be proposed (Fig. 8)

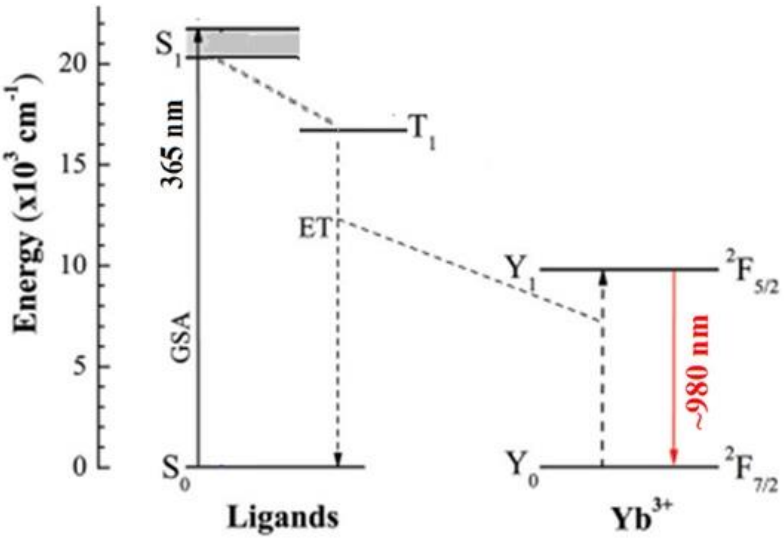

Fig. 8 – Scheme of energy transfer from an organic ligand to the Yb(III) (GSA – ground state absorption).

As calculated above, there is a significant energy gap between the triplet state of the ligand and the excited state of the ytterbium (III) ion. In addition, for Yb^{3+} ions, the $^2F_{5/2}$ fluorescence level lies ~10,000 cm^{-1} above the $^2F_{7/2}$ ground state, which in this case allows us to speak about vibronic interaction or the mechanism of internal electrontransfer from the ligand to the metal [33]. We propose that the energy transfer from the ligand triplet state to the excited level of Yb^{3+}, facilitated by vibronic coupling, accounts for the population of the Yb^{3+} excited state, which can then relax radiatively to the ground state by emitting photons at approximately 980 nm. This indicates an effective antenna effect, since the excitation energy photogenerated inorganic ligands is quickly transferred to the Yb^{3+} nucleus. The type of β-diketone mainly affects the intensity of absorption and emission.

CONCLUSIONS. Monomeric, mixed-ligand and polymeric complexes of ytterbium (III) with β-diketonate ligands with alkyl and aryl substituents were synthesized and studied. It was established that the Yb(III) ion forms triscomplexes with β-diketonate ligands of the general formula $Yb(\beta\text{-dik})_3 \cdot 2H_2O$, the coordination sphere in monoligand complexes is supplemented by 2 water molecules, the coordination number of the lanthanide = 8,

the coordination polyhedron is a square antiprism. Yb(III) β-diketonates easily attach a donor ligand (phenanthroline), which displaces H_2O molecules (OH-oscillators) due to the formation of stronger bonds with the central ion. Replacing water molecules with a phenanthroline molecule does not affect the structure of the coordination polyhedron, but causes only its slight deformation, which is reflected in the covalence parameters (increasing the covalence of the bond). The polymerization process also does not significantly affect the structure of the elementary unit, there is only a slight distortion of the coordination polyhedron. The thermal stability of the synthesized complexes increases from monoligand monomeric compounds to mixed-ligand polymers, which can be explained by the formation of compounds with a more rigid structure and a system of branched chemical bonds.

The study of luminescent characteristics showed that the integral intensity of luminescence varies in the series: dmod>dmhpd>mbphpd>mphpd and monomer-polymer-MLC-MLC polymer. The best luminescent characteristics are possessed by the ytterbium complex based on dmod. A significant increase in the luminescent properties of the synthesized complexes occurs when obtaining mixed ligand complexes with phenanthroline, which is primarily associated with solving the problem of the quenching effect of water molecules. Also, a noticeable increase in I_{lum} occurs when synthesizing MLC polymers. The preparation of such compounds is of practical importance, since it is easy to obtain film materials from polymer samples. Thus, the conducted studies of Yb(III) β-diketonate complexes may hold promise for practical applications as precursors of luminescent materials.

The work was financially supported by the National Academy of Sciences of Ukraine within the framework of the state budget topic 322E «Creation of new hybrid, composite and polymeric materials doped with coordination compounds of 3d- and 4f-metals based on β-diketonate and carboxylate acyclic ligands» (state registration number 0122U001299).

ПОРІВНЯЛЬНА ХАРАКТЕРИСТИКА СПЕКТРАЛЬНО-ЛЮМІНЕСЦЕНТНИХ ВЛАСТИВОСТЕЙ КОМПЛЕКСІВ Yb(III) З НЕНАСИЧЕНИМИ β-ДИКЕТОНАМИ

Н. Б. Іваха[1,2]*, О. С. Бережницька[1,2]

[1]Інститут загальної та неорганічної хімії ім. В. І. Вернадського НАН України, просп. Академіка Палладіна, 32/34, Київ 03142, Україна;
[2]Національний технічний університет України «Київський політехнічний інститут імені Ігоря Сікорського», просп. Берестейський, 37, Київ 03056, Україна
e-mail: ivakhanadiia@gmail.com

У роботі проведено порівняльний аналіз спектрально-люмінесцентних властивостей синтезованих координаційних β-дикетонатних комплексів ітербію з такими лігандами: 2,7-диметил-октен-1-діоном-3,5, 2,6-диметил-гептен-1-діоном-3,5, 2-метил-5-фенілпентен-1-3,5-діоном, 2-метил-5-бі-фенілпентен-1-3,5-діоном. Крім цього проведено дослідження полімерних сполук на основі представлених комплексів та їхніх

фенантролінових змішанолігандних похідних.

За допомогою низки фізико-хімічних методів аналізу встановлено, що будова елементарної ланки при полімеризації, а також координаційна сфера комплексів при утворенні змішанолігандних сполук не зазнає суттєвих змін порівняно з вихідними молекулами β-дикетонатів. Термічний аналіз показав значне підвищення температури початку розкладання змішанолігандних і металополімерних сполук відносно їхніх мономерних аналогів. Методом люмінесцентної спектроскопії встановлено, що досліджувані зразки проявляють люмінесценцію в ІЧ-діапазоні.

Порівняльний аналіз інтегральних інтенсивностей люмінесценції ітербієвих комплексів дозволив виявити ключові фактори впливу на емісійні характеристики. Насамперед це одержання змішанолігандних комплексів із фенантроліном, що дозволяє нівелювати негативний вплив одного з найбільш відомих чинників гасійної дії: ОН-осциляторів молекул води, яка доповнює координаційну сферу мономерних ітербієвих комплексів. Крім цього позитивно позначається на I_{lum}синтез полімерних сполук на основі β-дикетонатних комплексів, що може бути зумовлено зменшенням впливу концентраційного гасіння, оскільки у полімерах випромінювальні центри рівномірно розподілені по ланцюгу макромолекули.Такий підхід, окрім прямого позитивного впливу на люмінесцентні властивості, має на меті вирішення питання прикладного застосування синтезованих сполук, оскільки полімери значно легше піддаються переробленню та можуть утворювати плівкові матеріали.

Загалом на основі проведених досліджень можна сформувати такі залежності інтенсивності люмінесценції: dmod> dmhpd>mbphpd>mphpd та мономер-полімер-ЗЛК-ЗЛК-полімер. Як видно з цих даних, найкращими емісійними характеристиками володіють ітербієві змішанолігандні моно- та полікомплекси з β-дикетонами з алкільними замісниками.

Ключові слова: ітербій, комплекс, люмінесценція, β-дикетони, полімери.

REFERENCES

1. Nehra K., Dalal A., Hooda A., Bhagwan S., Saini R. K., Mari B., Kumar S., Singh D. Lanthanides β-diketonate complexes as energy-efficient emissive materials: A review. *Journal of Molecular Structure*. 2022. **1249:** 131531. https://doi.org/10.1016/j.molstruc.2021.131531.
2. Ning Y., Zhu M., Zhang J.-L. Near-infrared (NIR) lanthanide molecular probes for bioimaging and biosensing. *Coord. Chem. Rev.* 2019. **399**. https://doi.org/10.1016/j.ccr.2019.213028.
3. Cao J., Zhang R., Chen L., Wang D., Wang W., Tan E., Meng X., Xiu H., Wang L., Yang X., Yang Z., Yang Q., Zhao L. Design strategies and applications of responsive metal-based luminescence probes in the bioanalysis. *TrAC Trends in Analytical Chemistry*. 2023. **168**: 117338. https://doi.org/10.1016/j.trac.2023.117338.
4. Cheng P. Chapter 8 - Lanthanides in biosensing. In: Cheng P., editor. *Lanthanides*. Elsevier. 2023. 409–540. https://doi.org/10.1016/B978-0-12-822250-8.00008-4.
5. Cheng P. Chapter 9 - Lanthanides in bioimaging. In: Cheng P., editor. *Lanthanides*. Elsevier. 2023. 541–647. https://doi.org/10.1016/B978-0-12-822250-8.00009-6.

6. Dalal A., Nehra K., Hooda A., Singh D., Kumar P., Kumar S., Malik R. S., Rathi B. Luminous lanthanide diketonates: Review on synthesis and optoelectronic characterizations. *Inorganica Chimica Acta*. 2023. **550:**121406. https://doi.org/10.1016/j.ica.2023.121406.
7. Sun Z., Sun L. Chapter 337 – Rare-earth upconversion luminescence and its applications: from molecular to nano and micro scales. In: Bünzli J.-C. G., Kauzlarich S. M., editors. *Handbook on the Physics and Chemistry of Rare Earths*. 2024. **65**. 1–33. https://doi.org/10.1016/bs.hpcre.2024.03.001.
8. Balmus D. Novel stable ytterbium acetylacetonate–quinaldinate complexes as single-molecule magnets and surprisingly efficient luminophores. *Dalton Transactions***.** 2023. https://doi.org/10.1039/D3DT03253A
9. Fan, W.; Wang, H.; Huang, X.; Shi, T.; Du, J.; Xu, H. B. Energy transfer process, luminescence optimizing and various applications of lanthanide complexes. *Chem. Synth.* 2024, **4**, 12. http://dx.doi.org/10.20517/cs.2023.35
10. Berezhnytska O., Horbenko A., Savchenko I., Rohovtsov O., Rusakova N., Trunova O. Investigation of coordination compounds of Gadolinium (III) with β-diketones. *Chem. Chem. Technol.* 2023. **17**(4): 748–757. https://doi.org/10.23939/chcht17.04.748
11. Su L., Liu X., Niua Q., Li G. Photoresponsive lanthanide luminescent materials *J. Mater. Chem. C***.** 2024. **12**: 10759–10774. https://doi.org/10.1039/D4TC01353K
12. Ahmed Z., Mahiya K., Iftikhar K. Synthesis, crystal structure, NMR and near infra-red luminescence studies of nine-coordinate Nd and Yb complexes based on fluorinated β-diketone and a tridentate antenna chromophore, 2, 4, 6-Tris-(2-pyridyl)-s-triazine. *Inorganica Chimica Acta*. 2022. 541: 121086. https://doi.org/10.1016/j.ica.2022.121086.
13. Bhat, S. A., Hasan, N., Zargar, R. A., Wankar, S., Rawat, J. Evidencingthe NIR luminescence and longer lifetime from ytterbium complex constructed from perfluorinated β-diketone and heteroatom based ancillary ligand. *Journal of Molecular Structure*. 2024. **1299**: 137016. https://doi.org/10.1016/j.molstruc.2023.137016
14. Hasegawa M., Ohmagari H., Tanaka H., Machid K. Luminescence of lanthanide complexes: From fundamental to prospective approaches related to water- and molecular-stimuli. *Journal of Photochemistry and Photobiology C: Photochemistry Reviews*. 2022. **50:** (100484). doi.org/10.1016/j.jphotochemrev.2022.100484
15. Brito-Santos G., Gil-Hernández B., Martín I. R., Guerrero-Lemus R., Sanchiz J. Visible and NIR emitting Yb (III) and Er (III) complexes sensitized by β-diketonates and phenanthroline derivatives. *RSC advances*. 2020. **10**(46): 27815–27823. https://doi.org/10.1039/D0RA05539E
16. Santos H. P., Gomes E. S., dos Santos M. V., D'Oliveira K. A., Cuin A., Martins J. S., Quirino W. G., Marques L. F. Synthesis, structures and spectroscopy of three new lanthanide β-diketonate complexes with 4,4′-dimethyl-2,2′-bipyridine. Near-infrared electroluminescence of ytterbium(III) complex in OLED. *Inorganica Chimica Acta*. 2019. **484**: 60–68. https://doi.org/10.1016/j.ica.2018.09.030.
17. Ning Y., Tang J., Liu Y., Jing J., Sun Y., Zhang J. Highly luminescent, biocompatible ytterbium(III) complexes as near-infrared fluorophores for living cell imaging. *Chem. Sci***.** 2018. **9:** 3742–3753. https://doi.org/10.1039/C8SC00259B
18. Staszak K., Wieszczycka K., Marturano V., Tylkowski B. Lanthanides complexes – Chiral sensing of biomolecules. *Coordination Chemistry Reviews*. 2019. **397:** 76–90. https://doi.org/10.1016/j.ccr.2019.06.017.
19. Dasari S., Singh S., Kumar P., Sivakumar S., Patra A. K. (). Near-infrared excited cooperative up conversion in luminescent Ytterbium (III) bioprobes as light-responsive the ranosticagents. *European Journal of Medicinal Chemistry*. 2019. **163**: 546–559.

https://doi.org/10.1016/j.ejmech.2018.12.010,
20. Fan S., Yao X., Li J., Li W., Li G. Near-infrared luminescent materials: From β-diketonate ytterbium complexes to β-diketonate-ytterbium-complex@PMMA thin film. *Journal of Luminescence*. 2018. **203**. 473–480. https://doi.org/10.1016/j.jlumin.2018.07.003.
21. Yang D., Li H., Li H. Recent advances in the luminescent polymers containing lanthanide complexes. *Coord. Chem. Rev*. 2024. **514:** 215875. https://doi.org/10.1016/j.ccr.2024.215875
22. Zhang Z., Yu C., Liu L., Li H., He Y., Lü X., ... & Jones R.A. Efficient near-infrared (NIR) luminescent PMMA-supported hybrid materials doped with tris-β-diketonate Ln^{3+} complex (Ln= Nd or Yb). *Journal of Photochemistry and Photobiology A: Chemistry*. **2016**. 314: 104–113. https://doi.org/10.1016/j.jphotochem.2015.08.022
23. Ivakha N., Berezhnytska O., Rohovtsov O., Rusakova N., Trunova O. Mono- andmixed-ligand complexes of Yb(III) with new β-diketones. *Ukrainian Chemistry Journal*. 2021. **87**(2): 65–76. https://doi.org/10.33609/2708-129X.87.02.2021.65-76
24. Ivakha N., Berezhnytska O., Rohovtsov O., Trunova O., Smola S. Investigation of new polymer complexes based on Yb (III) β-diketonates. *Ukrainian Chemistry Journal*. 2022. **88**(5): 3–14. https://doi.org/10.33609/2708-129X.88.05.2022.3-14
25. Berezhnytska O., Savchenko I., Ivakha N., Trunova O., Rusakova N., Smola S., Rogovtsov O. Synthesis, characterization, and luminescent properties of polymer complexes of Nd (III) with β-dicarbonyl ligands. *Nanoscale Research Letters*. 2017. **12**: 1–8. https://doi.org/10.1186/s11671-017-2074-0
26. Savchenko I., Berezhnytska O., Fedorov Ya., Smola S., Trunova O. Luminescent properties of new polymer metal complexes based β-diketones and REE. *Molecular Crystals and Liquid Crystals,* 2018. **673**(1): 48–60. https://doi.org/10.1080/15421406.2019.1578493
27. Ivakha N.B., Berezhnytska O.S., Rohovtsov O.O., Trunova O.K. Complexes of Nd(III) and Er(III) with novel unsutaratedβ-diketones. *Ukr. Chem. J*. 2019. **85** (6): 87–96. [in Ukrainian] https://doi.org/10.33609/0041-6045.85.6.2019.87-96
28. Nakamoto K. *Infrared and Raman Spectra of Inorganic and Coordination Compounds*, 2009, Sixth Edition, Part B, Wiley, Hoboken, New Jersey.
29. Larkin P. *Infrared and Raman spectroscopy: principles and spectral interpretation*. 2017 Elsevier. Amsterdam.
30. Kofod N., Nawrocki P., Platas-Iglesias C., &Sørensen T. J. Electronic structure of ytterbium (III) solvates – a combined spectroscopic and theoretical study. *Inorganic chemistry*. 2021. **60**(10): 7453–7464. https://doi.org/10.1021/acs.inorgchem.1c00743
31. Yatsimirskii K.B., Davidenko N.K. Absorption spectra and structure of lanthanide coordination compounds in solution. *Coordination Chemistry Reviews*. 1979. **27**(3): 223–273. https://doi.org/10.1016/S0010-8545(00)82068-8
32. daSilva P.S.P., Martín-Ramos P., Silva M.R., Lavín V., Chamorro-Posada P., Martín-Gil J. X-ray analysis, molecular modeling and NIR-luminescence of erbium (III) 2, 4-octanedionate complexes with N,N-donors. *Polyhedron*. 2014. **81**: 485–492. https://doi.org/10.1016/j.poly.2014.07.006
33. Martín-Ramos P., da Silva P. S. P., Lavín V., Martín I. R., Lahoz F., Chamorro-Posada P., ... & Martin-Gil J. Structure and NIR-luminescence of ytterbium (III) beta-diketonate complexes with 5-nitro-1, 10-phenanthroline ancillary ligand: assessment of chain length and fluorination impact. *Dalton Transactions*. 2013. **42**(37): 13516–13526. https://doi.org/10.1039/C3DT51376A

Стаття надійшла 27.05.2024.

UDC 546.26-162: 541.13:549.21 doi: 10.33609/2708-129X.90.10.2024.88-134

HAMARI'S CONTRIBUTION TO THE ASYMMETRIC SYNTHESIS OF TAILOR-MADE AMINO ACIDS.

Jianlin Han[1]*, Hong Liu[2], Jiang Wang[2]*, Alicja Wzorek[3], Alexander E. Sorochinsky[4]*, Karel D. Klika[5], Taizo Ono[6], Hiroki Moriwaki[7]*, Tatsunori Sato[7], Kunisuke Izawa[7], Hiroyuki Konno[8]*, Vadim A. Soloshonok[9,10]*

[1]Jiangsu Co-Innovation Center of Efficient Processing and Utilization of Forest Resources, College of Chemical Engineering, Nanjing Forestry University, Nanjing 210037, China;
[2] State Key Laboratory of Drug Research, Shanghai Institute of Materia Medica, Chinese Academy of Sciences, Shanghai 201203, China;
[3] Institute of Chemistry, Jan Kochanowski University in Kielce, Uniwersytecka 7, 25–406 Kielce, Poland;
[4] V.P. Kukhar Institute of Bioorganic Chemistry and Petrochemistry, The National Academy of Sciences of Ukraine, Kyiv 02094, Ukraine;
[5] Molecular Structure Analysis, German Cancer Research Center (DKFZ), Im Neuenheimer Feld 280, 69120 Heidelberg, Germany;
[6] National Institute of Advanced Industrial Science and Technology, 463–8560, Nagoya, Japan.
[7] Hamari Chemical Ltd., Osaka, Japan;
[8] Department of Chemistry and Biological Engineering, Graduate School of Science and Engineering, Yamagata University, 992–8510 Yonezawa, Yamagata, Japan;
[9] Department of Organic Chemistry I, Faculty of Chemistry, University of the Basque Country UPV/EHU, Paseo Manuel Lardizábal 3, 20018 San Sebastián, Spain;
[10] IKERBASQUE, Basque Foundation for Science, María Díaz de Haro 3, Plaza Bizkaia, 48013 Bilbao, Spain
email: vadimsoloshonok@gmail.com

This article reviews the development of the asymmetric synthesis of tailor-made amino acids conducted at Hamari Chemicals during the 10-year period 2013–2022.The discussion is based on strategies such as direct chiral modification of unprotected amino acids via intermediate formation of Ni(II) complexes and elaboration of chiral nucleophilic or electrophilic glycine equivalents. The former approach includes, for example, second-order asymmetric transformation, dynamic kinetic resolution, and inversion of chirality while the latter approach involves construction of the desired amino acid architecture using, for example, alkylation, aldol, Mannich, or Michael addition reactions as well as multistep procedures. Operational convenience, scalability, and practicality of the developed methods are emphasized.

Keywords: tailor-made amino acids; drug design and development; second-order asymmetric transformation; dynamic kinetic resolution; inversion of chirality.

INTRODUCTION. Amino acids (AAs) are a fundamental class of compounds that are intrinsically linked to the origin and evolution of all recognized life forms. Since their structural elucidation in the early 19th Century, AAs have maintained a crucial role in advancing various fields of health sciences and technology [1]. A myriad of AAs have been obtained from natural sources [2–16] while synthetic variants have been engineered in research laboratories [17–33]. To manage the extensive structural diversity of AAs, workers have used several classifications. These include distinctions such as proteinogenic vs. non-proteinogenic, genetically coded vs. non-coded, natural vs. synthetic, common vs. uncommon, and usual vs. unusual. These terms are frequently used in the literature [34] and while these definitions provide some sense of structural identity, they can be somewhat ambiguous and perplexing. In this article, we have chosen to use the term 'tailor-made AAs', a definition proposed by Hruby et al. [35]. This term emphasizes the intended purpose of the AAs rather than their assumed origin or perceived distinction.

Beyond fundamental scientific investigation, the primary objective of medicinal chemistry research in the realm of tailor-made AAs is to engineer more selective and efficacious pharmaceuticals. From a structural perspective, AAs exemplify a form of molecular dichotomy, facilitating the step-by-step synthesis of polymers with unique, non-repeating sequences of monomers. These polymers, known as peptides for short length chains and proteins for longer chains, perform numerous vital roles in living organisms, including catalysis (enzymes), signaling (hormones), and mechano-structural functions [36–38]. In the context of contemporary drug discovery paradigms, tailor-made AAs are essential components with their derivatives increasingly appearing in newly marketed pharmaceuticals [39–45]. In fact, over 30% of small molecule drugs contain residues of tailor-made AAs or their derivatives, such as amino-alcohols and di-amines [46–60].

The asymmetric synthesis of AAs is a well-established field that provides a plethora of varied methodologies [17–33]. However, the challenges of cost-effectiveness, operational ease, and environmental impact continue to evolve necessitating corresponding advancements in synthetic techniques. A review of the literature reveals that the synthesis of both general and tailor-made AAs via Ni(II) complex intermediates, as shown in Scheme 1, has emerged as the most prevalent and methodologically superior approach [61–65].

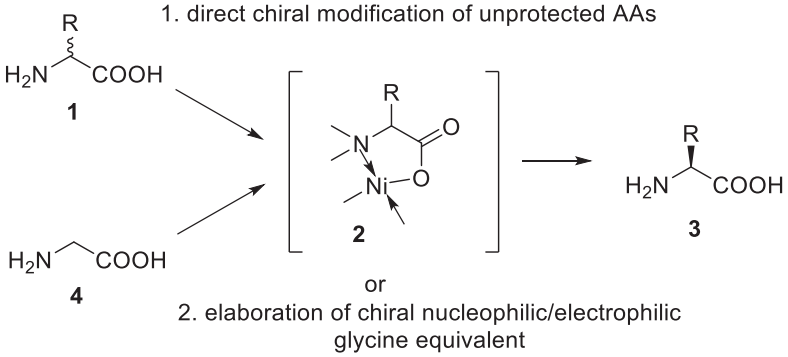

Scheme 1. General concept of the preparation of tailor-made AAs in enantiomerically pure form via intermediate Ni(II) complex formation.

A particularly attractive feature of this methodology is its practicality for the large-scale preparations of pharmacologically important AAs. At the outset, we envisioned two general strategic approaches: 1. direct chiral modification of unprotected AAs by way of means such as second-order asymmetric transformation (SOAT), dynamic kinetic resolution (DKR), or inversion of chirality; and 2. elaboration of chiral nucleophilic/electrophilic glycine equivalents, which involves constructing the desired AA architecture starting from glycine using, for example, alkylation, aldol, Mannich, or Michael addition reactions as well as multistep procedures. Both approaches have their advantages and shortcomings which will be noted in the following sections for the particular subsets of the strategies described herein.

Chiral tridentate ligands.

Hamari ligand.

From the standpoint of recyclability, having a recoverable source of asymmetric information of "indestructible" chirality is of great interest. Among obvious candidates possessing stable chirality, we considered (3*Z*,5*Z*)-2,7-dihydro-1*H*-azepine-derived axially chiral tridentate ligand – the Hamari ligand – **13** (Scheme 2) [66] as a potential system.

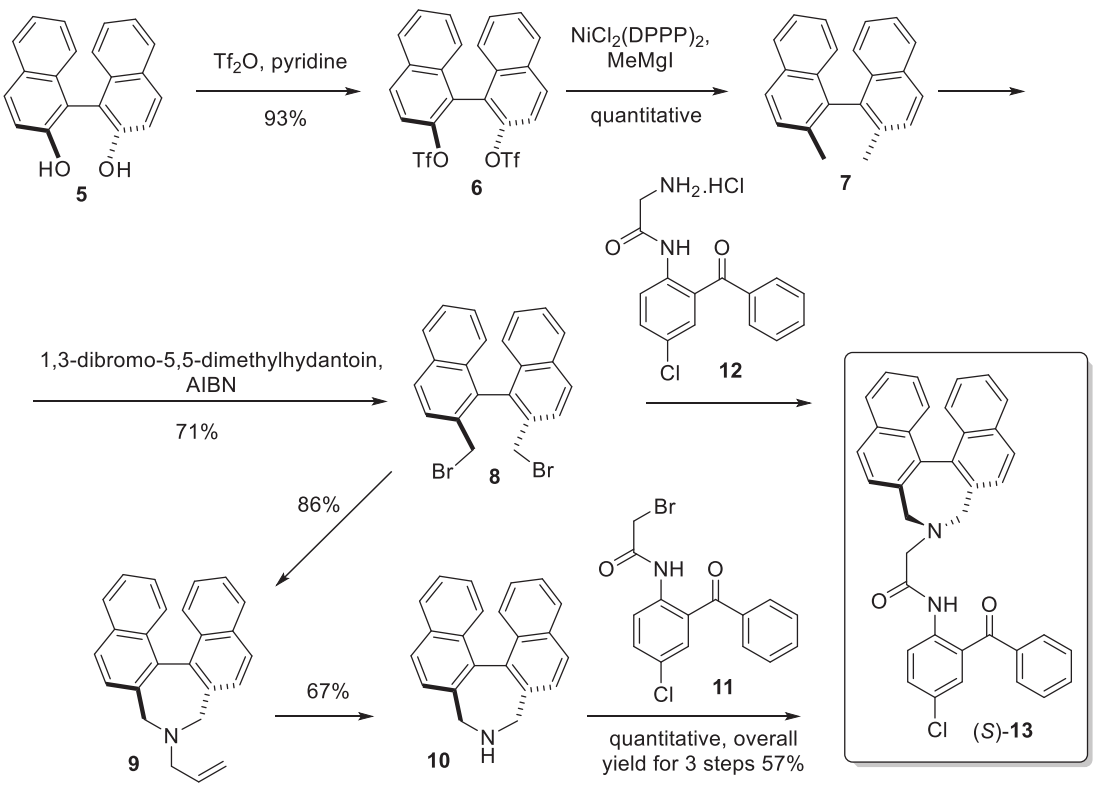

Scheme 2. Synthesis of Hamari ligand **13.**

ISSN 2708-129X. Укр. хім. журн., 2024

Commercially available enantiomerically pure binaphthol **5** was converted to dimethyl compound **7** via intermediate ditriflate **6** using Kumada coupling of **6** with a Grignard reagent. Subsequent bromination of **7** with 1,3-dibromo-5,5-dimethylhydantoin in ethyl acetate afforded dibromide **8**. This procedure reliably afforded key compound **8** in 71% yield.

Taking advantage of the previously developed strategy of modular approach to the design of chiral tridentate ligands [67–69], we envisioned the use of modules **11** and **12** for assembly of Hamari ligand **13**. Formation of the requisite azepine **9** by dialkylationof allyl amine [70] with dibromide **8** and subsequent removal of the allyl group to provide secondary amine **10** was accomplished in moderate yield. Alkylation of **10** with aminobenzophenone module **11** proceeded quantitatively affording Hamari ligand **13** after three steps in atotal yield of 57%. The procedure was found to have some disadvantages, though, notably being a multistep reaction sequence and the necessity for silica gel column purification, thus rendering this approach less attractive for large-scale manufacturing.The alternative solution, with application of module **12**, turned out to be significantly more attractive. The procedure was carefully optimized and was able to be reproduced on a 500 g scale.

Soloshonok–Liu ligand.

The proline-derived ligand **14** (Scheme 3) – the Soloshonok–Liu ligand – bearing three chlorine atoms in strategic positions was developed in a collaboration between the laboratories of Prof.s Soloshonok and Liu in 2014 [71,72]. It's phenomenal success for the asymmetric synthesis of tailor-made AAs can be attributed to its very high stereochemical preference. The strategic positioning of the three chlorine atoms in **14** were rationally deduced based on critical analysis of numerous crystallographic structures of the corresponding Ni(II) complexes of various types of AAs [73]. In particular, the aromatic stacking, parallel-displaced type of interactions between the *o*-aminobenzophenone and the Pro-*N*-benzyl rings was found to be of primary importance in shaping the spatial arrangements of the corresponding Ni(II) complexes. The influence of these aromatic interactions is very sensitive to the position and nature of the substituents, thereby determining the degree of parallel orientation of the interacting aromatic rings [73]. A large-scale synthesis of ligand **14** has been developed by Hamari [74].

The challenges of selectively alkylating a zwitterionic substance, such as proline **15**, are 3-fold: first, selective alkylation on nitrogen; second, forming the zwitterionic product under appropriate pH conditions; and third, separating and isolating the product from the large amount of potassium chloride formed in the reaction. A thorough examination of various conditions allowed us to determine that isopropanol using 85% potassium hydroxide pellets as the baseis an ideal system for the N-benzylation of proline **15** with benzyl chloride **16**. Upon completion of the alkylation reaction, the addition of concentrated HCl causes precipitation of KCl from the solution, simplifying the isolation and purification of the product **17** in greater than 90% yield. Similar to the previous step, the zwitterionic nature of **17** significantly complicates the activation of the carboxylic acid and subsequent amide formation. Furthermore, aromatic amine **18** is considerably electron deficient and requires a highly activated electrophile to effect reaction.

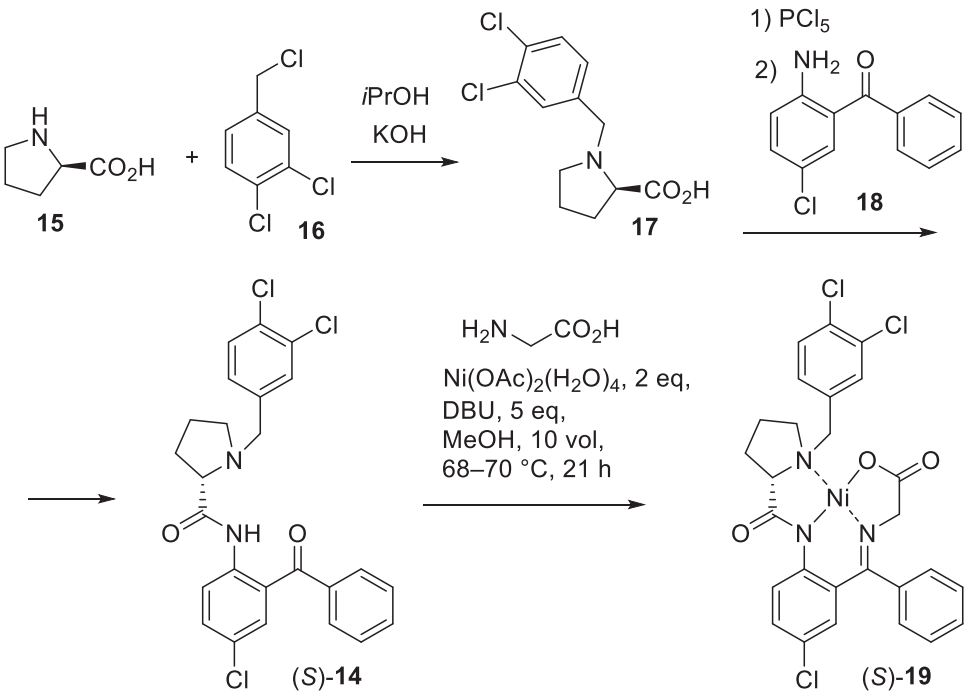

Scheme 3. Synthesis of the Soloshonok–Liu ligand **14.**

Previously, we reported [75,76] the use of methanesulfonyl chloride and 1-methylimidazole/DMAP to form the acid chloride/mixed anhydride, but the process proved to be problematic upon scaling up the reaction. Even though proline has a low intrinsic tendency for epimerization [77], we focused on finding asingle reagent that would serve to activate the carboxylic acidwithout the addition of base. After an extensive search for reaction conditions utilizing thionyl chloride orphosphorus (V) chloride, we settled on the latter reagent as it gave more consistent and reproducible results. Initial experiment susing dichloromethane as the solvent showed that wecould indeed prepare the desired product **14** using one equivalent of PCl_5 without the addition of base. Once again, this process allowed isolation of ligand **14** via simple filtration in over 80% yield. Our next goal was to establish a method for the satisfactory preparation of Ni(II) complex **19** on an industrial scale. The major finding of our work was the application of the relatively strong, but hindered, base 1,8-diazabicyclo-[5.4.0]-undec-7-ene (DBU) which met two important criteria, viz. chiral integrity of the product and simplicity of isolation. In particular, upon completion of the reaction, the addition of aqueous acetic acid simultaneously neutralizes the reaction mixture and causes precipitation of the enantiomerically pure product **19** in near-quantitative yield and in high purity. This procedure offered a practical advancement of the synthesis of Ni(II) complexes (*S*)- and (*R*)-**19** from bench scale to multikilogram scale [78].

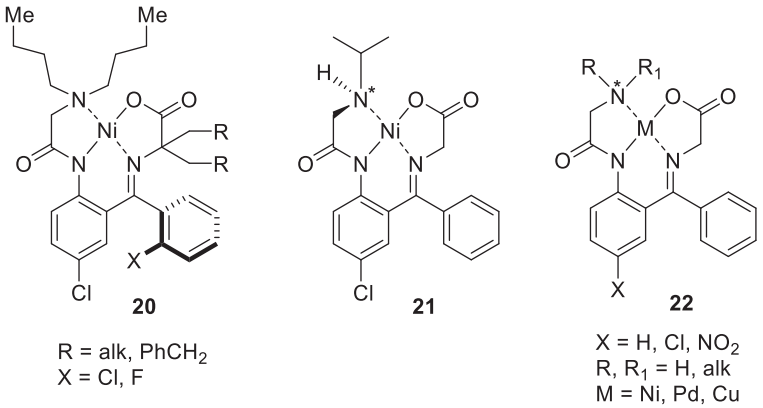

Fig. 1. Structures of novel axial chiral and N chiral (*) metal (II) complexes.

Our work on chiral HPLC resolution and the kinetics of racemization of various novel Ni(II) complexes was conducted in collaboration with the group of Prof. Christian Roussel. In particular, we successfully developed innovative structural models of Ni(II) complexes of type **20** (Figure 1) to probe and quantify the rotational barriers about the Ar–C_q bond of the benzophenone moiety. We demonstrated that axially chiral *ortho*-fluoro derivatives **20** are configurationally unstable due to relatively unhindered rotation about the Ar–$C_q$bond. By contrast, the configuration of the *ortho*-chloro-substituted analogs **20** are effectively indefinitely stable under ambient conditions ($t_{½}$ from 4 to 216 centuries) [79]. In another study, we described the design of a model Ni(II) complex of a glycine Schiff base possessing a nitrogen stereogenic center **21**. Measurement of its configurational stability using HPLC revealed that the configurational stability of the Ni(II)-coordinated nitrogen depends heavily on the solvent, ranging from very unstable in polar solvents with $t_{½}$s < 5 minutes to highly stable in apolar solvents with $t_{½}$s of the order of a century [80]. We also investigated configurational stability of a series of N chiral complexes **22** as a function of the substituents as well as the nature of coordinating metal(II). In general, electron-withdrawing substituents led to decreased configurational stability. With respect to the coordinating metal, the configurational stability was found to increase from Cu to Ni with Pd complexes the most stable with $t_{½}$s of 1.25 minutes, 7 hours, and 10 hours, respectively [81]. The data is of great of theoretical and synthetic value suggesting avenues for the rational design of a new generation of complexes for the asymmetric synthesis of tailor-made α-AAs [82].

Direct chiral modification of unprotected AAs. SOAT.

SOAT is defined as a crystallization-induced asymmetric transformation during which the racemic mixture is converted into a pure, less-soluble diastereomer [83–89]. This approach has tremendous practical appeal for large-scale synthesis as the target product can be isolated and purified simply by filtration. However, the major challenge associated with SOAT is that diastereomers usually do not show such dramatically distinct differences in properties such as crystallinity and solubility and

furthermore, which, for organic compounds at least, are rather unpredictable.

Rimantadine (**24**) (Scheme 4) was approved for medical use in 1993 as an orally administered antiviral drug. It is the most clinically advanced compound among adamantane-based chemotherapeutics developed for viral infections including influenza A, herpes simplex, hepatitis C, and HIV [90–92]. It is relatively inexpensive and readily commercially available as a racemate as well as in both enantiomeric forms [93–96].

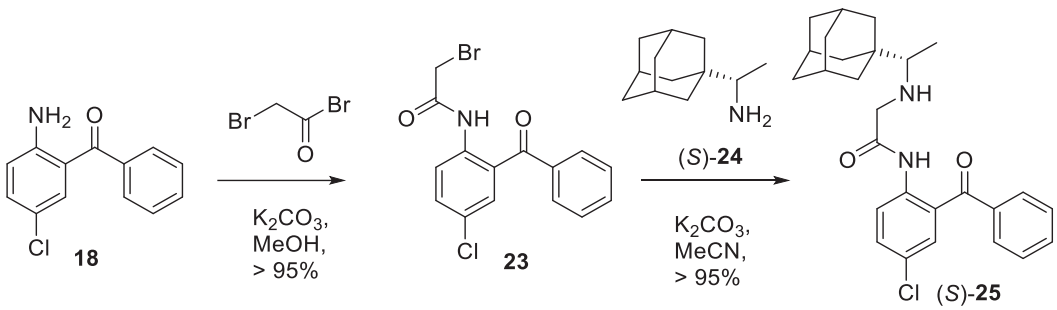

Scheme 4. Synthesis and application of adamantyl-containing ligand **25** for the preparation of enantiomerically pure, tailor-made-AAs via SOAT.

The therapeutic success of Rimantadine (**24**) is attributed to the presence of the adamantyl moiety – dubbed a "lipophilic bullet" – providing its derivatives with exceptional lipophilicity allowing them to penetrate lipophilic domains, including the blood–brainbarrier [97]. Taking into account the unique lipophilicity of adamantane, we assumed that this group can be used to modify the physicochemical properties of the corresponding Ni(II) complexes to conduct SOAT-controlled preparation of diastereomerically pure products. Drawing on previous experience with various N–H type ligands [98,99], we designed and prepared adamant ly-containing ligand **25** as presented in Scheme 4 [100]. Amide bond formation between benzophenone **18** and bromoacetyl bromide was accomplished cleanly in acetonitrile in the presence of K_2CO_3 to obtain **23** in quantitative yield. The subsequent alkylation of (*S*)-**24** with **23** was conducted using K_2CO_3 giving rise to ligand (*S*)-**25** in > 95% yield.

As presented in Scheme 5, the reactions of Rimantadine ligand (*S*)-**25** and racemic AA **26** were conducted in methanol using 1.1 equivalents of both **26** and $Ni(NO_3)_2{\cdot}6H_2O$ and 4 equivalents of K_2CO_3. After heating the reaction mixture for about 2 hours at 70 °C, all four possible diastereomers **27**–**30** were observed in the reaction mixture. However, diastereomer ($S_C R_N R_C$)-**30** was formed in noticeable excess (~9:1:1:1). An important feature of this method is that under the basic conditions, all diastereomers **27**–**30** are interconvertible by the step-wise inversion of the two labile stereogenic centers. Therefore, under SOAT conditions, one of the diastereomers can potentially arise as the predominant entity. Depending on the nature of AA **26**, the precipitation of the major diastereomer can occur either spontaneously or it can be initiated by a gradual addition of water. After precipitation, the diastereomerically pure product is usually obtained simply by filtration in 60–90% yield [100].

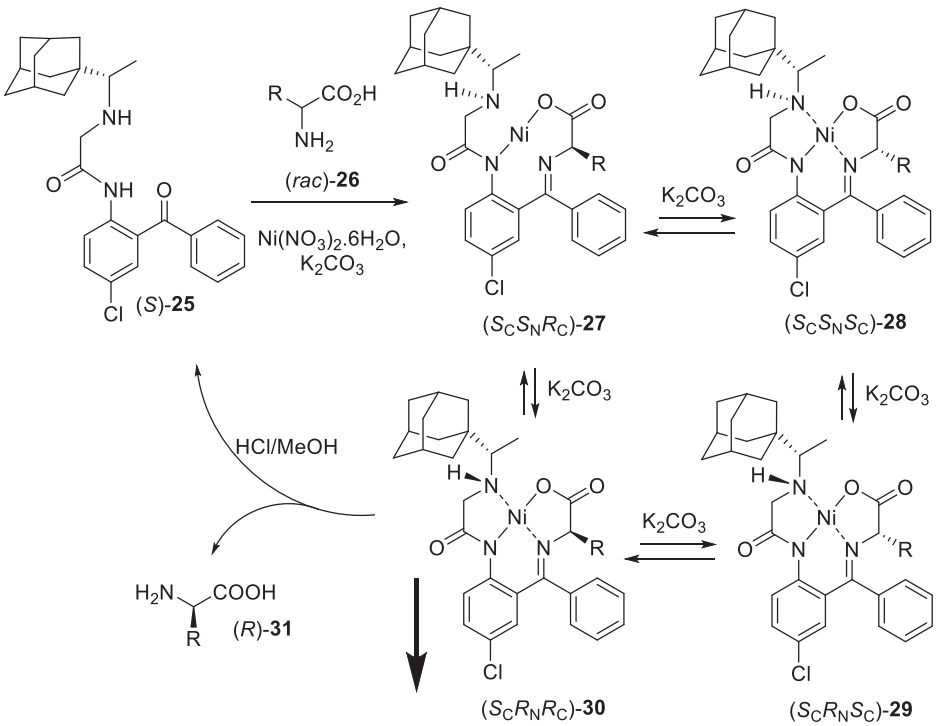

Scheme 5. SOAT approach for the preparation of enantiomerically pure tailor-made AAs.

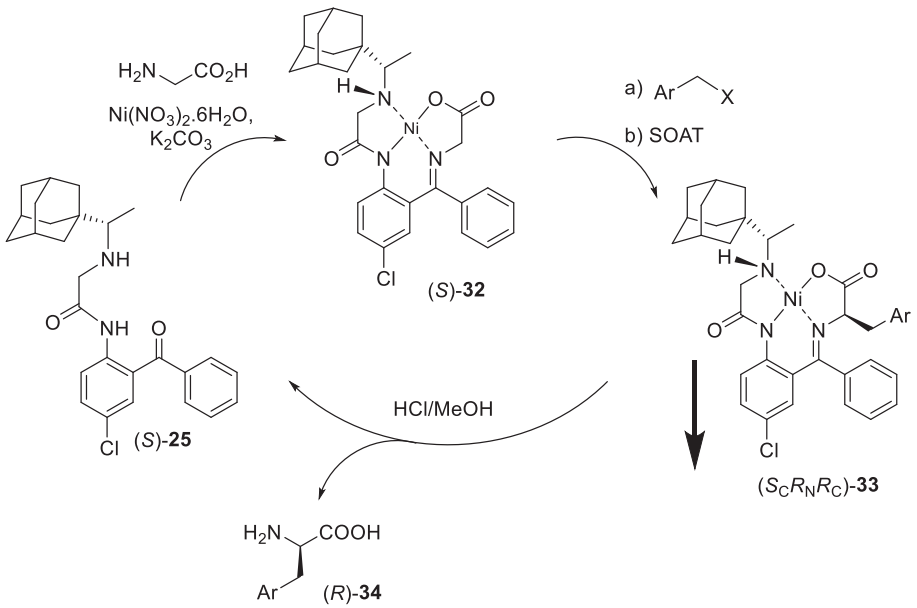

Scheme 6.Tandem alkylation–SOAT protocol for the preparation of phenylalanine-type tailor-made α-AAs.

Our next goal in the area of SOAT was the development of an advanced general process for the preparation of tailor-made *α*-AAs via tandem alkylation–SOAT. As presented in Scheme 6, Rimantadine-containing ligand **25** was reacted with glycine and a Ni(II) salt to assemble complex **32**. For the first step of the alkylation of **32**, very mild phase-transfer conditions were used [101] allowing the introduction of a side chain to the target *α*-AA. The second step utilized SOAT methodology affording nearly complete precipitation of the corresponding (S_C,R_N,R_C)-configured diastereomer **33**. Disassembly of **33** provided the target AA **34** as well as recovery of the starting Rimantadine ligand **25** for reuse [102]. Due to the very mild conditions of the first step, this approach is limited to the preparation of aromatic AAs, such as phenylalanine and its various derivatives. Nevertheless, this method is exceptionally practical and of high synthetic value.

DKR

Another approach for the direct chiral modification of unprotected AAs is DKR [103–115]. Like SOAT, DKR requires efficient, unimpeded interconverison of diastereomeric species in the reaction mixture. However, in contrast to SOAT, DKR is based on the thermodynamic stability of products. Our research in DKR began with the design of ligands **35** (Scheme 7) derived from phenylethylamine, one of the most inexpensive and readily available chiral compounds [116–118].

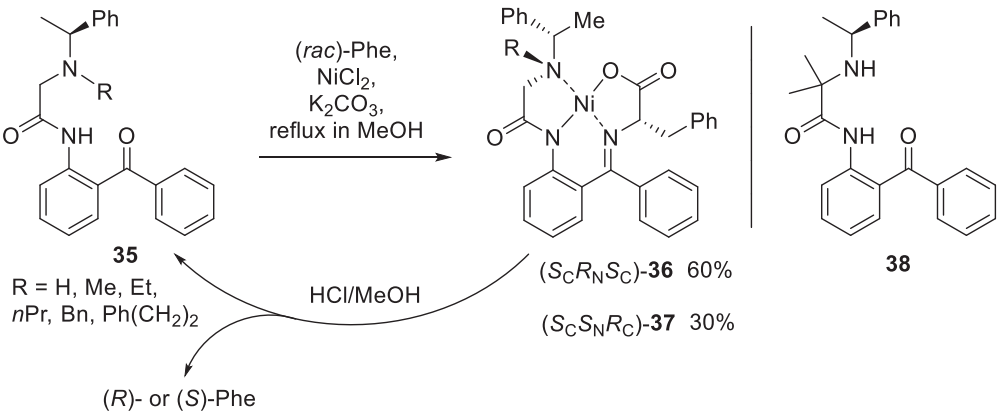

Scheme 7. Phenylethylamine-derived ligands for the DKR of unprotected tailor-made AAs.

As presented in Scheme 7, the reaction of ligand **35** with *rac*-phenylalanine, Ni(II), and base resulted in almost quantitative formation of diastereomers **36** and **37** in a ratio of about 2 to 1. Compounds **36** and **37** can be isolated by precipitation from the reaction mixture and are separableby column chromatography. Then either **36** or **37** can be disassembled to yield the enantiomerically pure AA as well allowing for the recovery of ligand **35**. Additionally, the undesired diastereomer can be treated in a methanol solution with base to convert it to the desired diastereomer, e.g. **36** into **37** or vice versa, followed by the chromatographic separation. The process can be repeated until all of the product is converted into the desired diastere-

omer to yield the desired (*S*)- or (*R*)-AA. Diastereoselectivity in this method can be improved by adding some structural rigidity to the ligand design. For example, ligand **38** was successfully used for the DKR of various AAs [119], including fluorinated tailor-made derivatives [120].

The conceptual breakthrough inthe DKR of unprotected AAs was made with the design of Soloshonok–Liu ligand **14** (Scheme 3). As shown in Scheme 8, ligand **14** reacts with various AAs under very mild conditions to produce the corresponding Ni(II) complexes **39** with diastereoselectivity>97:3 [121–125].

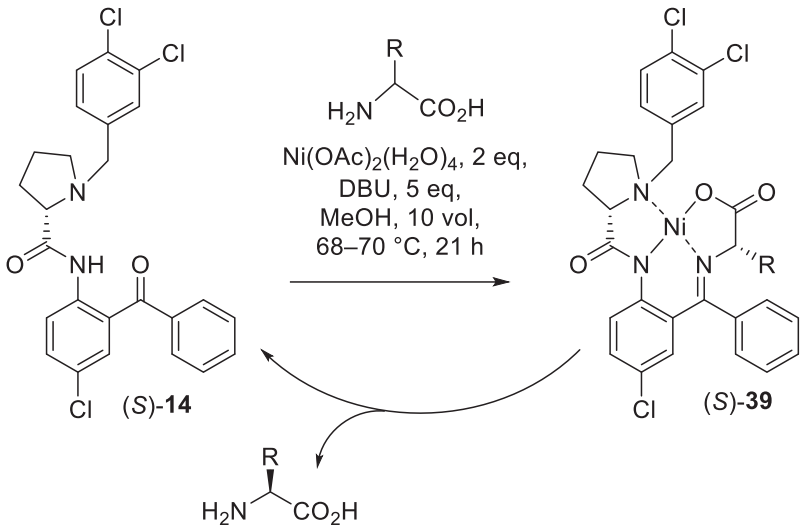

Scheme 8. DKR of unprotected tailor-made AAs using Soloshonok–Liu ligand 14.

Precipitation of the major product from the reaction mixture affords virtually diastereomerically pure **39** which can be disassembled under standard acidic conditions to release the target AA along with recovery of the chiral ligand **14**. The process is very clean as virtually no byproducts are formed allowing the isolation of complex **39** in yields >90%. DKR can be applied to a great variety of tailor-made AAs differing of structural types. The limitations, however, include AAs containing *ω* functional groups such as aliphatic CO_2H, NH_2, SH, or OH.

Similar results for the DKR of unprotected AAs were also obtained using the Hamari ligand **13**. As shown in Scheme 9, ligand **13** readily reacted with racemic AAs forming complex **39** as the major diastereomer (>95:5) [126,127].

The stereochemical outcome of DKR and reaction limitations for ligands **13** and **14** are very similar rendering these two chiral ligands of high synthetic value for the preparation of enantiomerically pure tailor-made AAs on a large scale. It should be noted that proline-derived ligand **14** is significantly less expensive in comparison to **13**. On the other hand, the chirality of ligand **13** is resistant under the applied conditions and therefore its recycling is amenable without requiring additional purification.

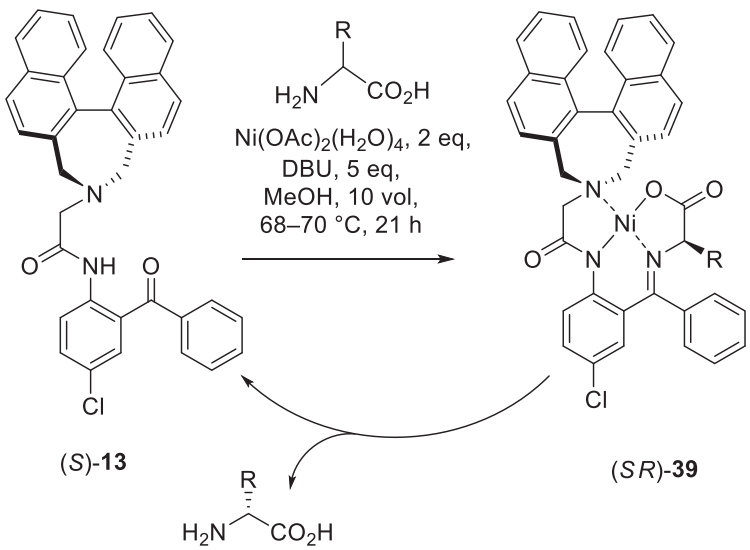

Scheme 9. DKR of unprotected tailor-made AAs using Hamari ligand 13.

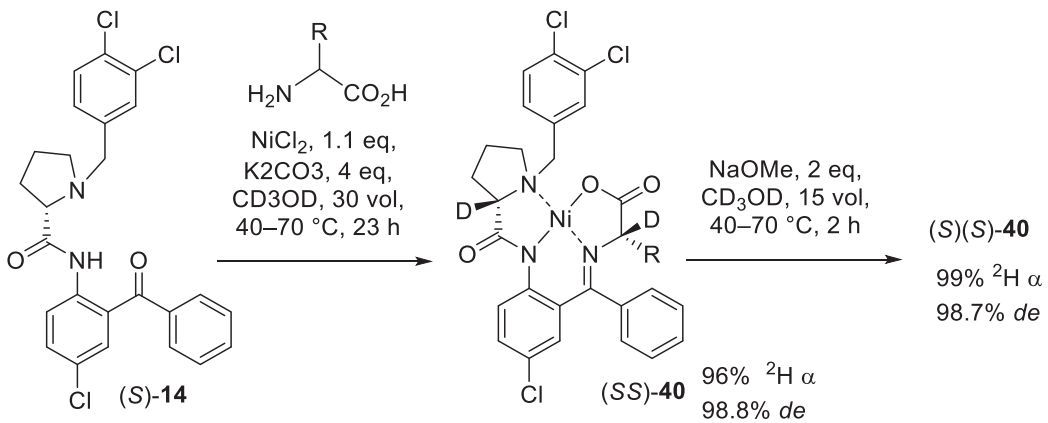

Scheme 10. Synthesis of tailor-made *α*-deutereo-AAs via DKR.

DKR has an additional synthetic advantage for the preparation of *α*-deutereo-AAs [128] as a special class of isotopically labeled compounds. Though the market for *α*-deutereo-AAs is relatively small, they have numerous applications in the mechanistic studies of various enzymes and biochemical processes [129–138]. Furthermore, tailor-made *α*-deutereo-AAs play an indispensable role in the emerging area of clinical functional metabolomics for obtaining essential data on *in vivo* AA metabolism and protein turnover [139–140]. While the asymmetric synthesis of *α*-deutereo-AAs has received due attention [141–151], optimal solutions with regards to the problems of selectivity, level of deuterium incorporation, and enantiomeric purity of the target AA shave not yet been found. In this respect, the protocol developed by us represents the most advanced procedure reported to date. As presented in

Scheme 10, conducting DKR under the standard conditions in deuterated methanol affords product **40** in quantitative yield with 98.8% diastereomeric excess (*de*) and 96% deuterium incorporation at the *α* position. For most applications of *α*-deutereo-AA this is an acceptable level and thus complex **40** can be disassembled under the usual acidic conditions to produce the target *α*-deutereo-AA. However, if a very high level of deuterium incorporation is required, for example for mechanistic kinetic studies, an additional exposure of **40** to deuterated methanol in the presence of a stronger base can be performed to produce **40** of ~99% deuterium incorporation at the *α* position.

Elaboration of chiral nucleophilic or electrophilic glycine equivalents.

Alkylation.

The alkylation of chiral glycine equivalents is one of the most widely used approaches for the asymmetric synthesis of tailor-made AAs [152–154]. Both the Hamari ligand **13** and the Soloshonok–Liu ligand **14** have been successfully used in our laboratories for the large-scale preparation of tailor-made AAs. As already pointed out above, one of the most rapidly growing areas inmodern drug design is the application of fluorinated residues as bioisosteres of naturally occurring molecular entities. Based on considerations of the biologically relevant size, as cumulatively defined by van der Waals (vdW) volume, A values, Taft Es values, and biphenyl rotational interference values [155–159], a trifluoromethyl group has often been considered to be isosteric with an isopropyl substituent. Although – CF_3 and – *i*Pr groups are clearly of different shape, they are sterically much closer than to –Me, –Et, and –*t*Bu groups. As shown in Figure 2, the differences projected by several biphenyl rotational interference values are relatively modest, suggesting steric mimicry between these two groups and thereby fueling interest in the synthesis of trifluoromethyl containing *α*- and *β*-AAs [160]. Thus, 2-amino-4,4,4-trifluorobutanoic acid (**41**) can be used as a substitute for leucine (**42**) in the de novo design of biologically active peptides and peptidomimetics [161–171].

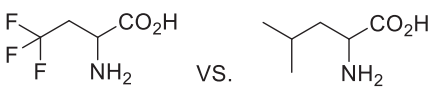

41 **42**

	–CF_3	–*i*Pr	–CH_3	–C_2H_5	–*t*Bu
vdW volume (Å^3)	39.8	56.2	21.6	38.9	–
Taft Es value	−2.40	−1.71	−1.24	−1.31	−2.70
A value (kcal/mol)	2.1	2.15	1.7	1.7	> 4.5
BRIV* (kcal/mol)	12.1	12.6	9.7	–	18.3
BRBV** (Δ*Grot*, kcal/mol)	10.5	11.1	7.4	8.7	15.4

*Biphenyl rotational interference value
**Experimental biphenyl rotational *B* value

Fig. 2. Bioisosteric relationships between –CF_3 and –*i*Pr groups in the context of using 2-amino-4,4,4-trifluorobutanoic acid (**41**) as a substitute for leucine (**42**) in drug design.

Responding to the high interest in trifluoro-AA **41**, we selected this molecule as one of our research targets. As shown in Scheme 11, chiral glycine equivalent **19** was alkylated with CF_3CH_2I to produce the target complex (*S*2*S*)-**43** as the major diastereomer with 97% *de* [172,173]. Of note, usually the alkylation of glycine Schiff base complexes derived from ligands of type **14** is performed in the presence of a large excess of a base, usually 5–10 equivalents [174–177]. Consequently, it was an

important finding that for large-scale synthesis, the optimized conditions only required a quite small excess of base (5 mol%). The same stoichiometry was found to be optimal for the alkylating reagent. Thus, only a 5 mol% excess of the trifluoroethyl iodide was sufficient for optimal yields and stereochemical outcome. Similar to trifluoro-AA **41**, we prepared (*S*)-2-amino-6,6,6-trifluorohexanoic acid **44** [178,179] and *α*-(octyl)glycine **45** [180].

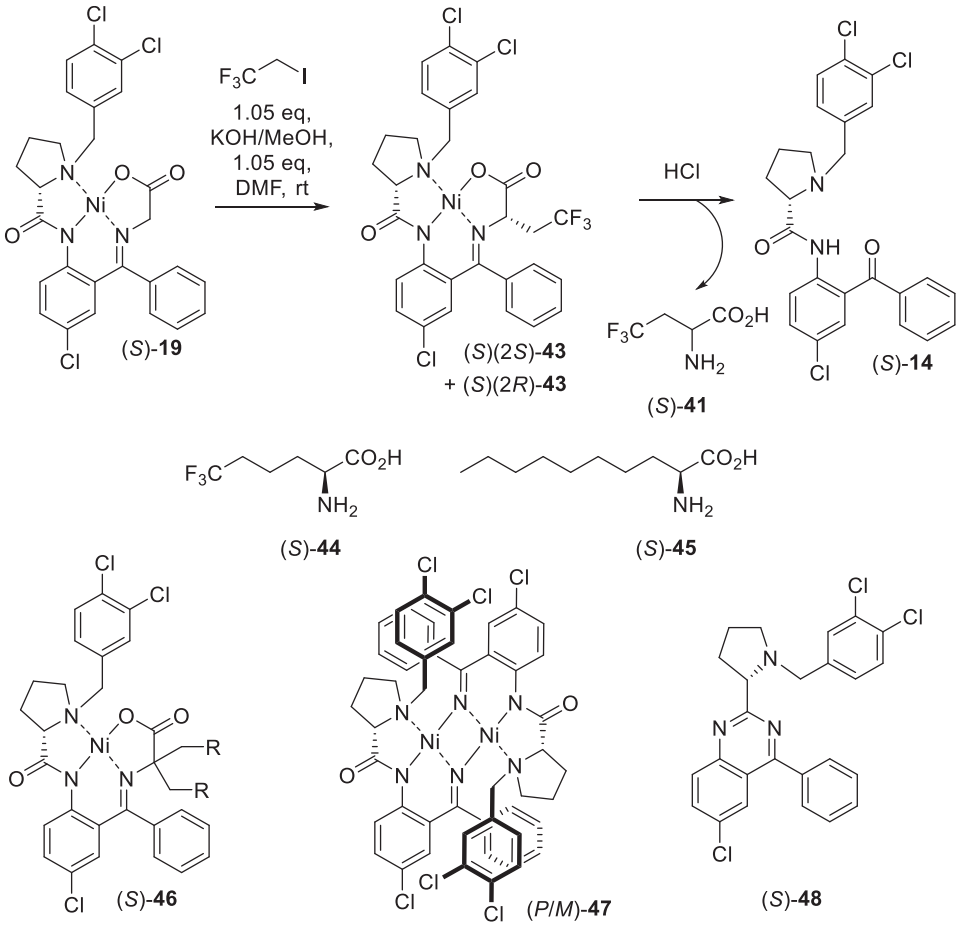

Scheme 11. Asymmetric synthesis of tailor-made AA via alkylation of a glycine complex.

Close attention to all aspects of the reaction process and thorough examination of the chemical entities in the reaction mixture allowed us to isolate not only the usual dialkylation products **46**, but also the previously undetermined byproducts **47** and **48**. Characterizing these byproducts was instrumental in gaining a more complete understanding of the reaction chemistry and in formulating more conducive reaction conditions [181,182].

The installation of sterically constrained tailor-made*α*-AAs into strategic positions of peptide chains brings about noticeable conformational restrictions of the corresponding *φ*,

ψ, and χ angles in the folded biologically active three-dimensional structure [183–190]. In this regard, the synthesis and applications of α,α-disubstituted AAs have received widespread consideration [191,192]. Among the highly interesting targets is α-(methyl)cysteine (**51**) (Scheme 12), a quite rare, naturally occurring quaternary AA isolated from blue-green algae [193,194]. In particular, several natural products that contain anα-(methyl)cysteine (**51**) fragment, such as mirabzoles [195, 196], tantazoles [197], and thiangazoles [198, 199], were found to possess promising antitumor and anti-HIV-1 activities which provide considerable motivationfor the development of asymmetric synthesis and in-depth biological-investigation of α-(methyl)cysteine (**51**).

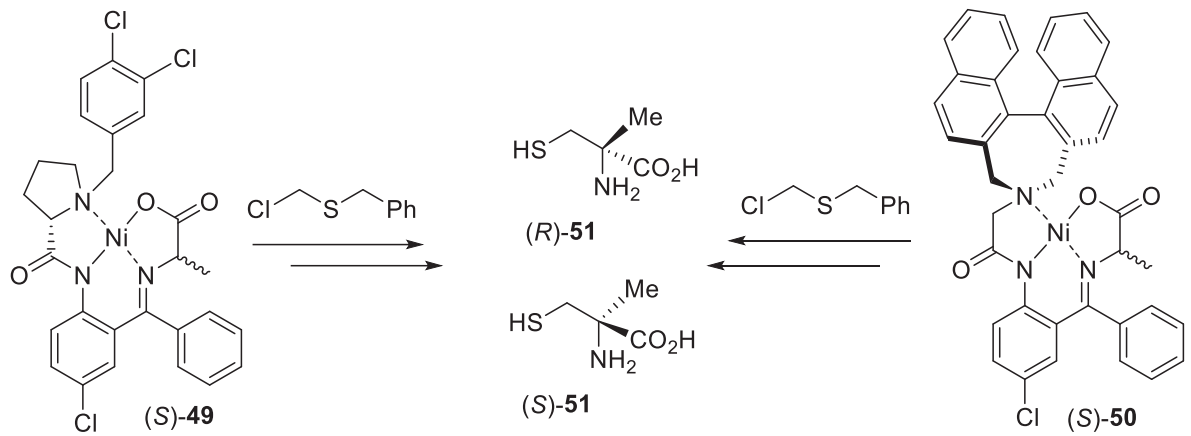

Scheme 12. Asymmetric synthesis of α-(methyl)cysteine (**51**).

As presented in Scheme 12, the synthesis of **51** was accomplished by the alkylation of alanine complexes **49** and **50** derived from Hamari **13** and Soloshonok–Liu **14** ligands, respectively [200]. It should be noted that the alanine residue in complexes **49** and **50** can be racemic as the reaction proceeds via formation of the achiral intermediate enolate. Proline derived complex **49** exhibited better stereochemical preference allowing the preparation of the major diastereomer in 77% yield with 80% *de*. The major product can be purified by column chromatography and disassembled to provide the target AA **51**. Both enantiomers of **51** were prepared with the same stereochemical outcome.

Another interesting example of tailor-made AAs is 7-azatryptophan **52**. AA **52** has been widely used as a biological fluorescent probe [201–204], an antiplasmodial compound [205], and an inhibitorof checkpoint kinase 1 [206–208]. Although there have been several reports on the synthesis of azatryptophanes [209–215], the synthesis of 7-azatryptophan **52** has remained less developed, in particular, by asymmetric synthesis. We demonstrated that the synthesis of AA **52** can be effectively realized via alkylation of a glycine complex (Scheme 13).

As shown in Scheme 13, N-protected chloride **53** reacted with glycine complex **19** in the presence of a strong base in DMSO affording

alkylated product **54** as a single diastereomer in 74% yield. Disassembly of **54** under acidic conditions took place with simultaneous removal of the Boc protecting groupproviding the target AA **52** in 95% yield [216]. It should be noted that chiral ligand **14** was also collected with 97% recovery for re-use.

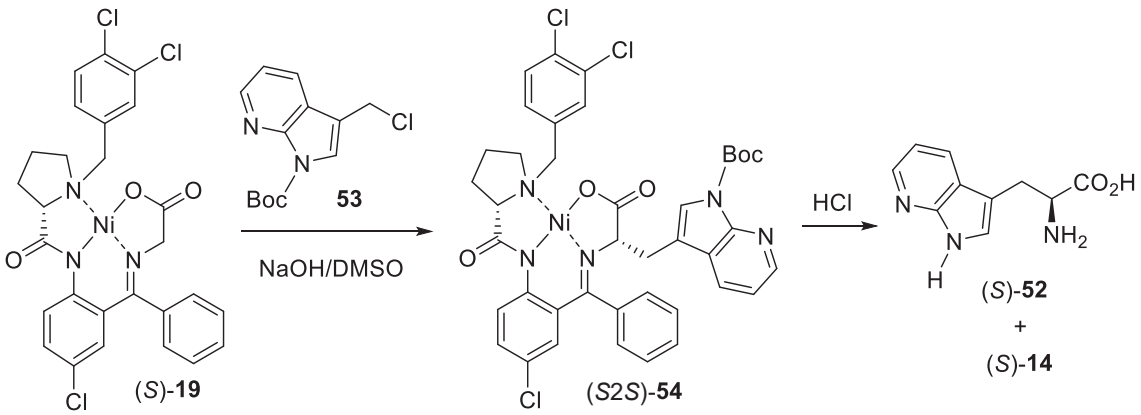

Scheme 13. Asymmetric synthesis of 7-azatryptophan via alkylation of glycine–Ni(II)complex.

Scheme 14 illustrates various AAs synthesized using Hamari ligand **13**. The glycine-derived complex **55** can be prepared quantitatively by treating ligand **13** with glycine and a source of Ni(II), e.g. $NiCl_2$, in methanol in the presence of base. Any alkylating reagent compatible with the reaction conditions can be used to alkylate the glycine moiety in **55**. For instance, mono-, di-, or polysubstituted benzyl chlorides/bromides provide excellent alkylations. The substituents on the phenyl ring only have a negligible effect on the stereochemical outcome. Similarly, variously substituted naphthyl derivatives and some heterocyclic derivatives also produce excellent results. Although inactivated alkyl halides react more slowly, they still achieve the same high stereochemical outcome, typically around 95% *de*, with chemical yields exceeding 90%. The alkylation products **56** can be conveniently disassembled to yield the corresponding AA and chiral ligand **13** which can be easily recovered with uncompromised enantiomeric purity [217].

Chiral glycine alkylation methodology can also be used for the synthesis of bis-AA (Scheme 15) [218, 219]. This particular class of tailor-made AAs is frequently found in naturally occurring peptides. For example, bis-AAs play an important role in the structure of the peptidoglycan cell walls of fungi and bacteria and can act ascross linking elements to allow for efficient control of thepeptide secondary structure. Representative examples of naturally occurring bis-AAs include diaminopimelic acid [220,221] and dityrosine [222]. Furthermore, bis-AAs serve as a key structural unitin the design of antibiotics that disrupt microbial cell wall synthesis [223]. Due to their useful biological properties and bio structural functions, the synthesis of bis-AAs has received significant interest [224–231].

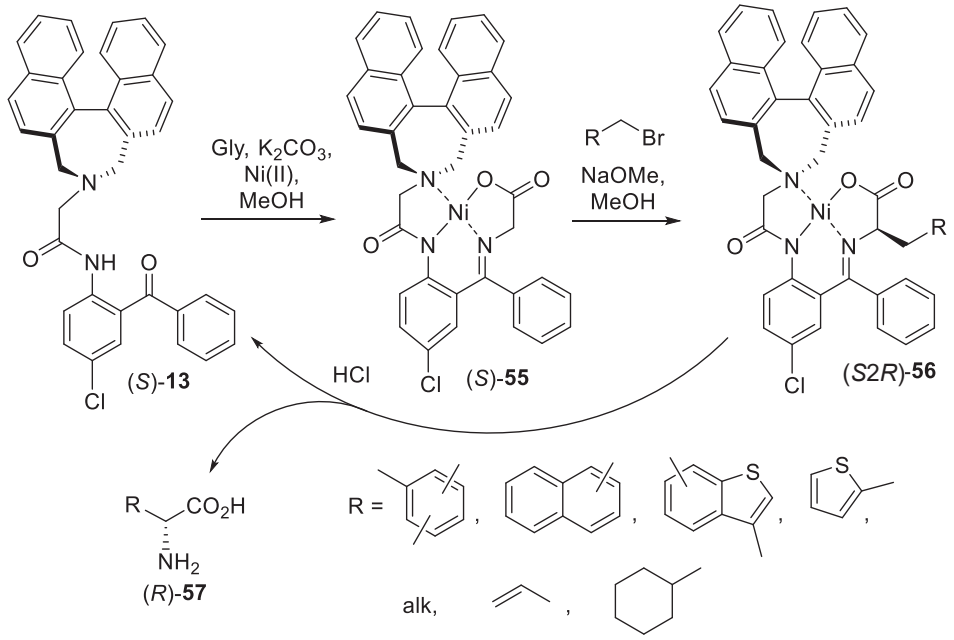

Scheme 14. Asymmetric synthesis of various tailor-made AAs via alkylation of glycine Ni(II) complex derived from Hamari ligand13.

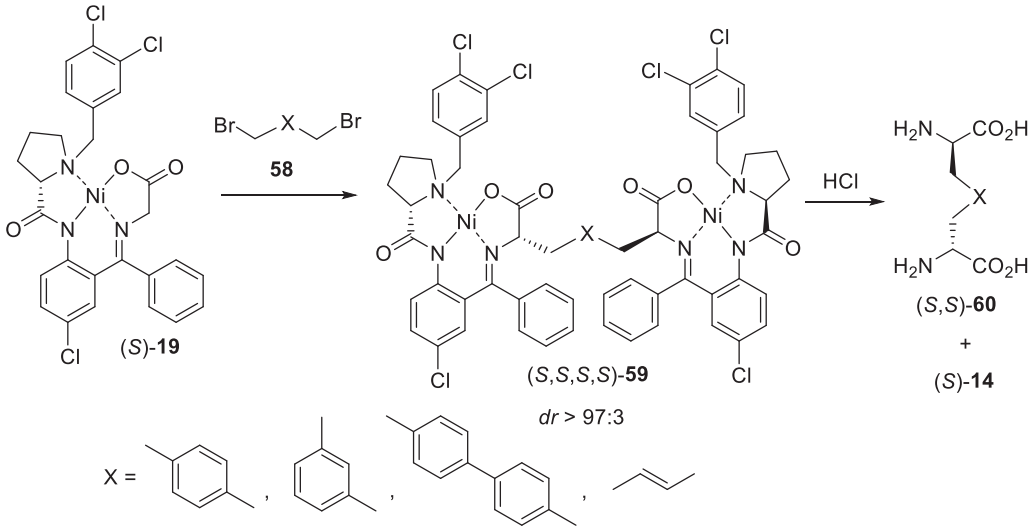

Scheme 15. Asymmetric synthesis of tailor-made bis-AAs via alkylation of a glycine Ni(II) complex.

As illustrated in Scheme 15, dibromides **58** can react with two equivalents of glycine–Ni(II) complex **19** to afford di-alkylated **59**. Despite some complexity of this process, the chemical yields of **59** are usually above 90% with diastereoselectivity >97:3. As expected, the reaction proceeds via intermediate monoalkylated derivatives which can be determined by TLC and,

if necessary, isolated. This approach, though, is limited to activated dibromides **58** such as benzyl or allyl derivatives [232]. Attempts to use inactivated alkyl halides require forcing conditions leading to significant decomposition and loss of stereochemical integrity. Disassembly of **59** under acidic conditions permits the isolation of the target bis-AAs **60** as well as the recovery of chiral ligand **14**.

Aldol addition reactions.

Aldol addition to glycine equivalents is the most convenient approach for the preparation of α-amino-β-hydroxy AAs [233–237]. For example, glycine Ni(II) complex **19** was shown to react with various aldehydes and activated ketones [238–240]. The aldol reactions of **19** can be conducted under either kinetic control using a weak base or under thermodynamic control using a strong base [241,242]. While the latter affords the corresponding aldol addition products with excellent levels of diastereoselectivity at the α- and β-positions (> 98:2), the former proceeds only sluggishly and with only a low degree of stereochemical preference(~60:40) at the β-stereogenic carbon. Considering these inherently challenging synthetic limitations, we were interested to know whether the stereochemical preference could be improved when the aldol addition is followed by transformation to irreversible products (Scheme 16) [243].

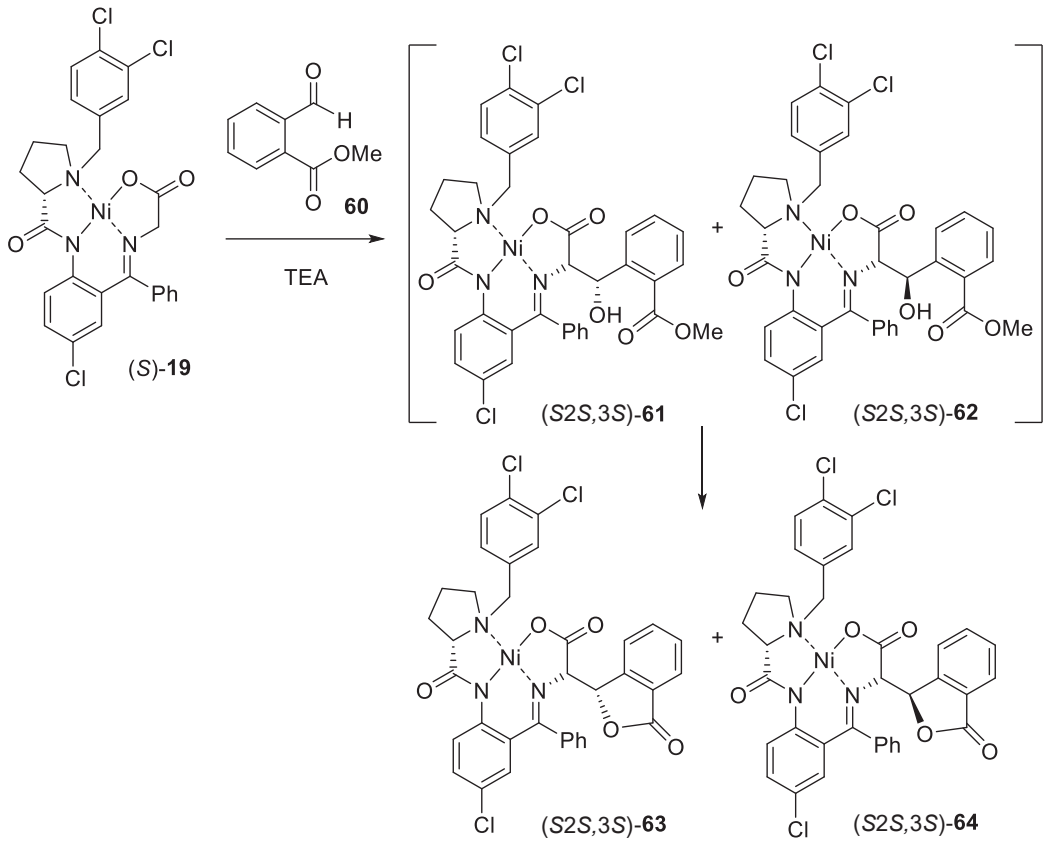

Scheme 16. Methodological study of the aldol addition–cyclization reaction cascade.

As presented in Scheme 16, using the chiral Ni(II) complex of glycine Schiff base **19** we designed an addition–cyclization reaction cascade to explore aspects of the kinetic triethylamine-catalyzed formation of the corresponding (*S*2*S*,3*S*)-**63** and (*S*)(2*S*,3*R*)-**64** diastereomers [243]. It was found that the final lactone products rather reflected thermodynamic stereocontrol due to much greater rates of the reversible aldol addition, products **61** and **62**, vs. a subsequent and irreversible cyclization step. The observed 80:20 diastereoselectivity for (*S*)(2*S*,3*S*)-**63** and (*S*)(2*S*,3*R*)-**64** in the reaction of Ni(II) complex **19** constitutes an improvement over the previously reported 60:40 ratio.

Mannich additions.

Mannich additions of chiral glycine equivalents represent the most direct approach for the preparation of *α*,*β*-bis-AAs [244–247]. In the chemistry of Ni(II) complexes of glycine Schiff bases, Mannich additions are one of the least studied reactions [248]. Nevertheless, *α*,*β*-bis-AAs constitute an important class of tailor-made AAs found in nature as structural motifs of biologically important molecules [249, 250].

As illustrated in Scheme 17, we designed a Mannich addition to investigate the case of matching vs. mismatching diastereomeric preferences between chiral complex **19** and chiral Mannich acceptor **65** [251].

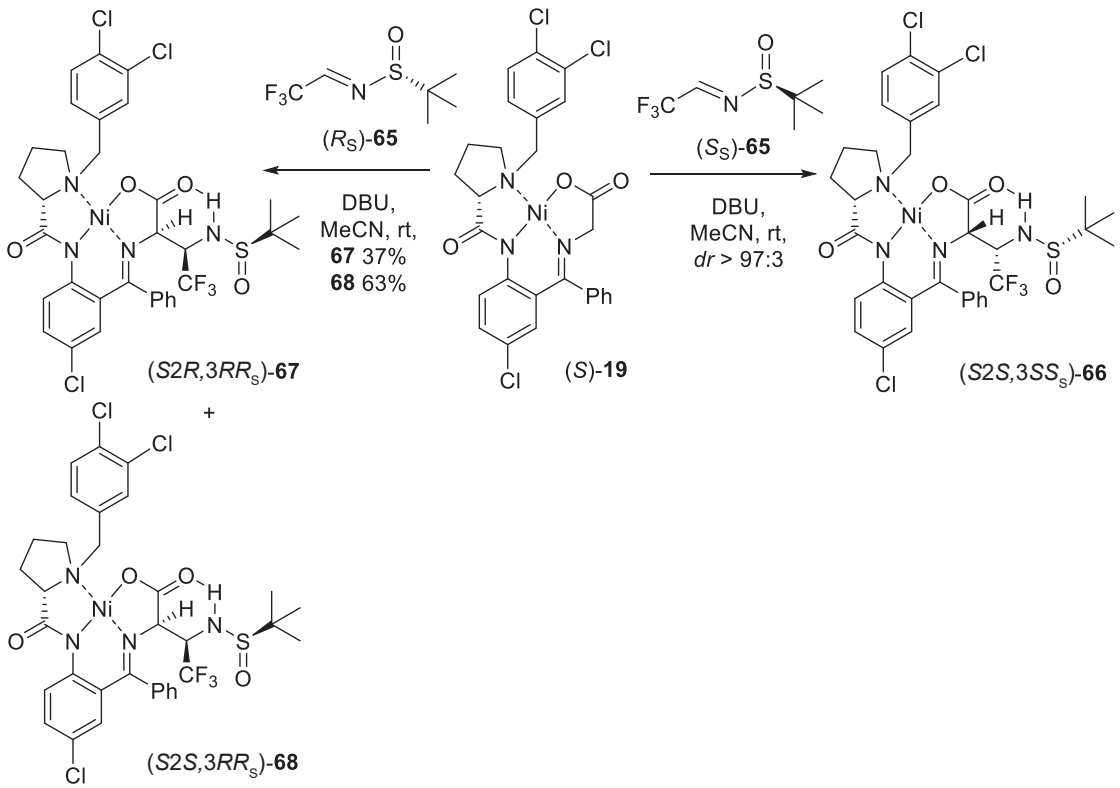

Scheme 17. Mannich additions of the chiral Ni(II) complex of glycine Schiff base **19** with a chiral Mannich acceptor **65**.

It was intriguing to find that *S*-configured Ni(II) complex **19** and *N-tert*-butylsulfinyl-3,3,3-trifluoroacetaldimine **65** with an (*S*) configuration have matching stereochemical preferences resulting in the formation of product **66** with virtually complete diastereoselectivity. The reaction of (*S*)-**19** with (*R*)-**65** is a case of mismatching stereochemical preferences and affords amixture of diastereomers **67** and **68** in a ratio of 37:63. These results suggest that the stereocontrol of the Ni(II) complex **19** prevails over the stereoselectivity provided by imine **65**. It is worth noting that *N-tert*-butylsulfiny l-3,3,3-trifluoroacetaldimine (**65**) is one of the most widely used and exceptionally high stereocontrolling chiral reagent for the asymmetric synthesis of amines and AAs [252–256].

Michael additions.

Michael additions are of great synthetic value for the preparation of various types of tailor-made AAs containing five carbon atoms in their skeleton. These include, but are not limited to, glutamic acid, glutamine, pyroglutamic acid, pyroglutamine, and proline [257–260]. The Michael addition of Ni(II)complexes with various *α*,*β*-unsaturated carboxylic acid derivatives has been one of the most prolific avenues of this research area [261–264]. We chose Michael addition for the synthesis of (2*S*,3*S*)-3-methylglutamine, one the key compounds used in the total synthesis of cytotoxic marine peptides callipeltin O and Q [265]. As presented in Scheme 18, glycine Ni(II) complex **19** was reacted with Michael acceptor **69** under specially designed conditions to keep intact the allyl ester moiety [266].

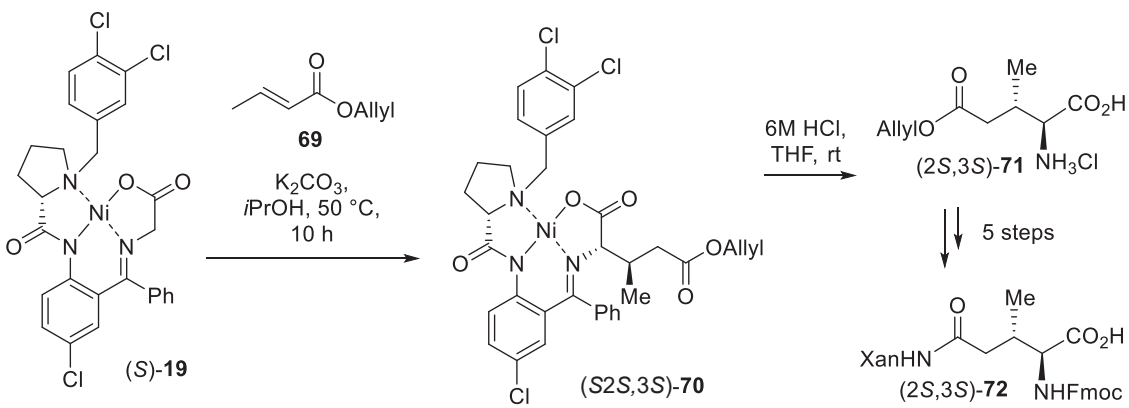

Scheme 18. Asymmetric synthesis of (2*S*,3*S*)-3-methylglutamine via Michael addition.

The acidic disassembly of the major diastereomeric product (*S*2*S*3*S*)-**70** was also performed under strictly controlled conditions using THF as a solvent. Allyl ester hydrochloride **71** was subsequently transformed into the target glutamine derivative **72** in five steps involving protection–deprotection procedures.

The substitution of phenylalanine (**73**, Figure 3) in endogenous peptides with a bulkier and more lipophilic *β*-phenylphenylalanine (diphenylalanine, DPA, **74**) usually leads to improved binding to the apolarsite of the targeted receptors. DPA-modified peptides were found to possess some encouraging biological pro-

files in the areas of thrombin inhibitors [267, 268], angiotensin-converting enzyme (ACE) inhibitors [269], HIV protease inhibitors [270], pain-related norepinephrine transporterinhibitors [271], μ and δ opioid receptors [272], and other types of peptidic substrate–receptor interactions [273–279].

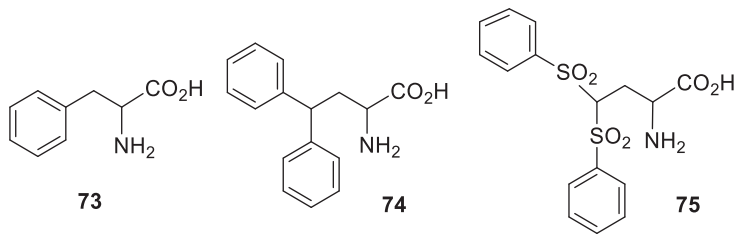

Fig. 3. Phenylalanine (**73**) and its more lipophilic analogs.

Numerous advanced in silico studies have generated structural profiles for hundreds of tailor-made AAs with rationally designed size control and vdW and electrostatic interactions that influence peptide ligand binding affinity with endogenous receptors [280–283]. 2-Amino-4,4-bis-(phenylsulfonyl)butanoic acid (**75**) is one of the promising structures featuring enhanced steric bulk and lipophilicity. We envisioned that this molecule could be assembled via Michael addition between glycine–Ni(II) complex **19** and the specially designed vinyl–disulfonyl Michael acceptor **76** (Scheme 19) [284–287].

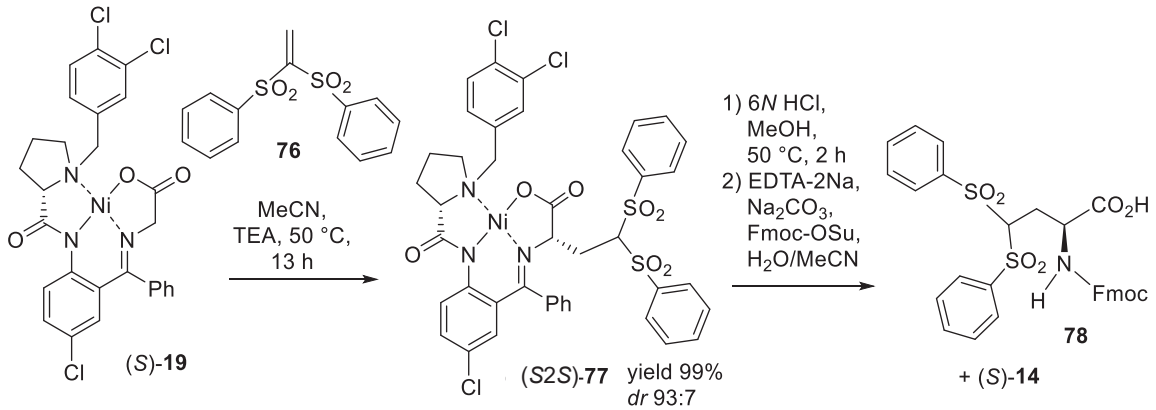

Scheme 19. Asymmetric synthesis of 2-amino-4,4-bis-(phenylsulfonyl)butanoic acid (**75**).

It was interesting to find that due to the high electrophilicity of acceptor **76**, the corresponding Michael addition with glycine complex **19** can be conveniently conducted using triethylamine as base. Optimization of the reaction conditions allowed for preparation of the diastereomeric products with an excellent yield of 99% and high diastereomeric ratio (*dr*) of 93:7. The major diastereomer **77** was transformed into the corresponding Fmoc derivative **78**

of 2-amino-4,4-bis-(phenylsulfonyl)butanoic acid (**75**) under standard conditions. As usual, chiral ligand (*S*)-**14** is able to be recovered and purified for future applications [288].

3-Methyleneglutamic acid (**79**, Figure 4) was reported as a racemic compound and tested as a potential suicide inhibitor of pig heart glutamate–aspartate transaminase [289,290]. Interestingly, (*S*)-4-methyleneglutamic acid (**80**) is a naturally occurring compound [291,292] and was prepared in enantiomerically pure form [293,294].

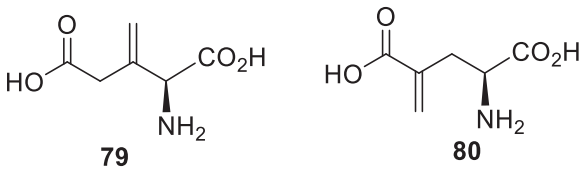

Fig. 4. Structures of (*S*)-3-methyleneglutamic acid (79) and (*S*)-4-methyleneglutamic acid (**80**).

We also examined the Michael addition between glycine Ni(II) complex **19** and Michael acceptor **81** bearing a tosylate leaving group (Scheme 20) [95]. Our goal was to prepare addition product **82** containing the corresponding *β*-methyl-unsaturated AA. Quite unexpectedly, we isolated compound **83** as the major product. This outcome was very welcome as it allowed for the asymmetric synthesis of (*S*)-3-methyleneglutamic acid (**79**) which was previously unknown in enantiomerically pure form.We reasoned that compound **82** underwent base-catalyzed isomerization to **83** via transition state **84**. This mechanistic rational is supported by the fact that using the same method we were able to prepare fluoro-AA **85** via the expected addition–elimination sequence [295].

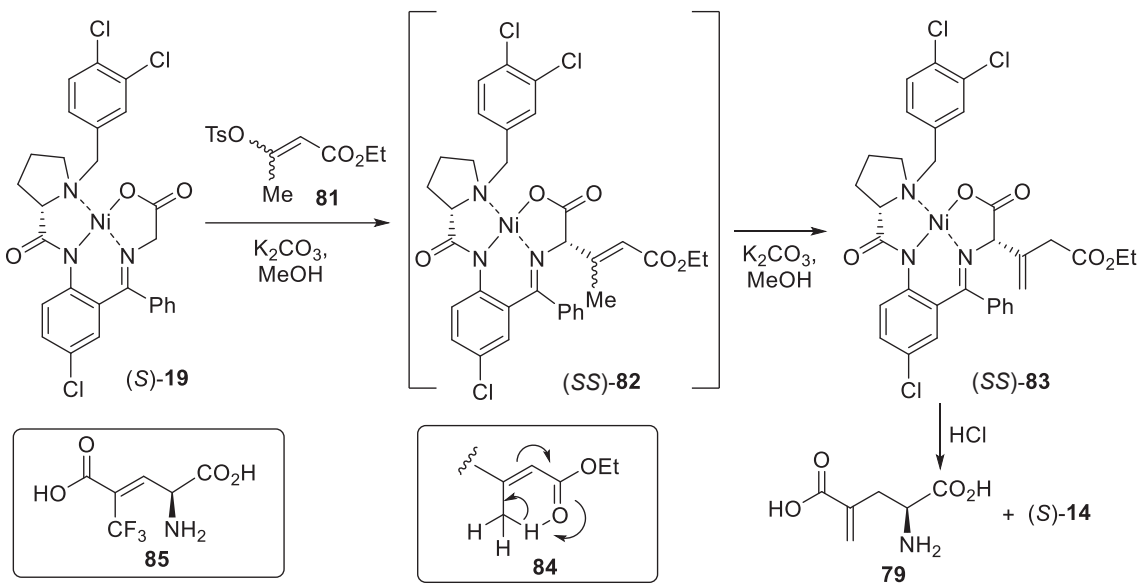

Scheme 20. Michael addition of glycine–Ni(II)complex with Michael acceptors containing tosylate leaving groups.

Organophosphorus derivatives are widely found in natural products, pharmaceuticals, chiral ligands, and functional materials [296–305]. Phosphorus-containing α-AAs are an important class of tailor-made AAs that have gained considerable attention in peptide design strategies as they enhance stability towards protease degradation and permit bioactivity to be modulated [306–314]. Previously, using Ni(II) complex chemistry, ω-phosphorus analogs of dicarboxylic AAs were prepared by alkylation of a glycine chiral Schiff base complex with the corresponding phosphorus alkyl halides [315]. We envisioned a different approach based on the Michael addition of dehydroalanine chiral Schiff base complex **86** (Scheme 21).

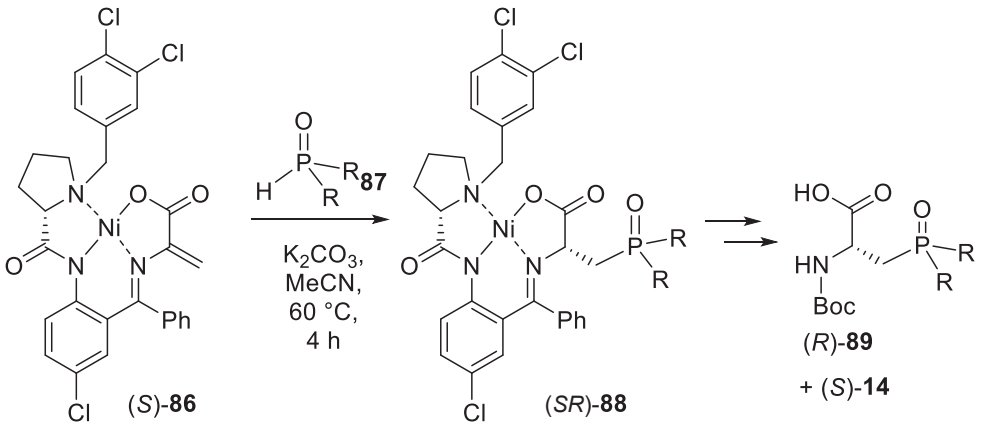

Scheme 21. Asymmetric synthesis of phosphorus analogs of AAs via Michael addition.

In sharp contrast to the previously discussed Ni(II) complexes representing nucleophilic glycine equivalents, dehydroalanine derivative **86** [316,317] represents an electrophilic alanine equivalent allowing homologation at the corresponding β position. The addition reactions of Ni(II)complex **86** with nucleophiles **87** were conducted under the usual nucleophilic conditions using methanol as a solvent and K_2CO_3 as base [318]. The Michael addition between dehydroalanine Ni(II) complex **86** and phosphorous nucleophiles **87**occurred very cleanly furnishing products **88** in good yields and with excellent diastereoselectivity. It should be noted that the α configuration of the addition products **88** appears to be of an unusual (*SR*) configuration, but this is simply due to the CIP priority rules favoring the phosphorus atom over the $-CO_2H$ group [319,320]. Complexes **88** were disassembled under the usual acidic conditions and the target AAs were in situ converted to the corresponding N–Boc derivatives **89** along with the recovery of the chiral ligand (*S*)-**14**.

Multistep procedures.

Described above are general methodological approaches requiring one key step before acquiring the target AA. In this section we provide examples of multiple synthetic transformations for the preparation of structurally complex tailor-made AAs as exemplified by the structures in Figure 5.

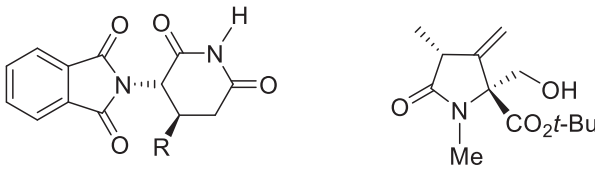

Fig. 5. Examples of products prepared using Ni(II) complex methodology.

Thalidomide is a notorious drug due to the monumental socio-scientific impact it had on-nearly every sector of the healthcare industry [321–324]. Nevertheless, in 1998 and 1999 the US Food and Drug Administration approved thalidomide for use in the treatment of erythema nodosum leprosum and multiple myeloma [325]. Moreover, the clinical success of thalidomide led to the development and marketing of several of its structural analogs [326–328]. The Michael addition of glycine–Ni(II) complexes were used as a key step in the asymmetric synthesis of novel 4-substituted enantiomerically stable analogs of thalidomide **90** [329,330]. Oxazolomycin A, isolated from the fermentation broth of *Streptomyces* sp., exhibits potent antibiotic properties against various Gram-positive bacteria and *Agrobacteriumtume faciens*, strong anticancer activity, as well as various other antiviralactivities [331–339]. It was envisioned that the pyroglutamate core unit, such as compound **91** which possesses appropriate functional groups at C-2 and C-3, can be viewed as a synthetic intermediate in the total synthesis of Oxazolomycin-type natural products.The first step in this process included the Michael addition of achiral glycine Schiff base with a chiral *α*,*β*-disubstituted acrylate derivative for the preparation of the enantiomerically pure *α*,*β*-disubstituted pyroglutamic acid core. A total of twelve reactions were utilized in the synthesis of **91** with an overall yield of 10% [340].

α, *β*-Methano-AAs, or methanologs of *α*-AAs, represent an extreme case of compounds containing a severely conformationally restricted cyclopropane ring [341, 342]. Remarkably, several cyclopropyl group-containing AAs, such as **92**–**94** (Figure 6), are naturally occurring compounds and have been isolated from various higher plants [343–351].

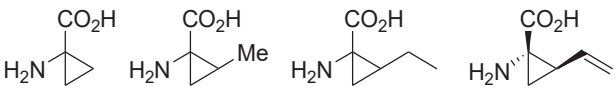

Fig. 6. Naturally occurring and tailor-made *α*,*β*-methano-*α*-AAs.

The interest in methanologs of AAs results from the discovery of a novel and very potent class of hepatitis C virus NS3/4A protease inhibitors [352] containing (1*R*,2*S*)-1-amino-2-vinylcyclopropanecarboxylic acid (**95**) as a key structural feature. Thus, at least sixdifferent drugs containing AA **95** are currently being developed for the treatment of hepatitis C. For example, Simeprevir [353], Danoprevir [354], Asunaprevir [355], Faldaprevir [356], Ciluprevir, and Grazoprevir [357] all have a fragment of acid **95** as a sulfonamide derivative.

Given this profound interest in the pharmaceutical applications of acid **95**, we examined Ni(II) complex chemistry for the asymmetric synthesis of this compound. The method developed by us is illustrated in Scheme 22 [358].

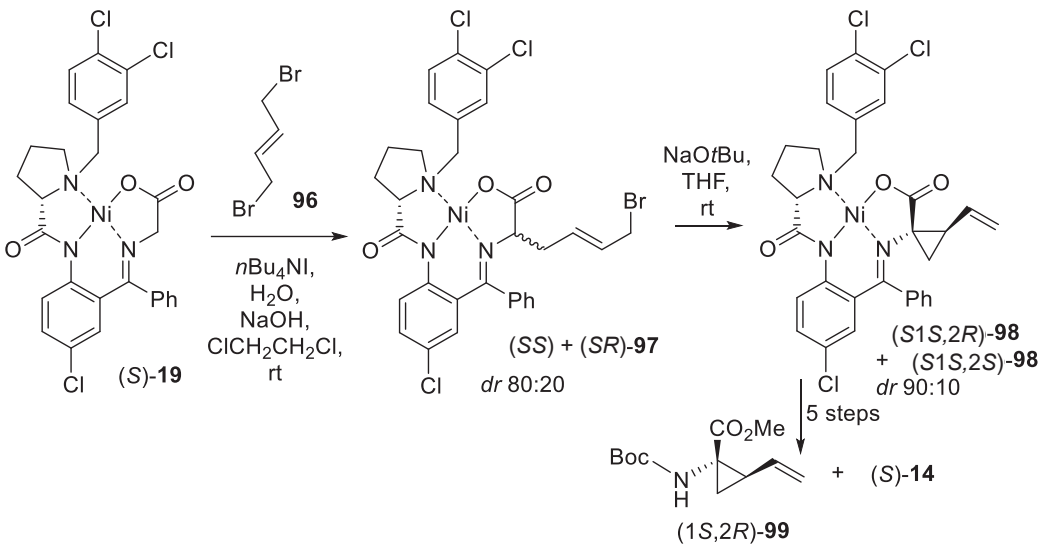

Scheme 22. Asymmetric synthesis of Boc-protected (1*S*,2*R*)-1-amino-2-vinylcyclopropanecarboxylic acid (**99**).

The synthetic sequence began with the selective alkylation of glycine complex **19** with dibromide **96**. We found that the first mono-alkylation reaction needed to be conducted under very mild phase-transfer conditions using dichloroethane as the solvent at ambient temperature. The diastereoselectivity of the first alkylation step is kinetically controlled and affords product **97** as a mixture of diastereomers in a ratio of 80:20, but unfortunately it is not high yielding. However, the ratio of diastereomers **97** is of no concern as the next alkylation step occurs via deprotonation of the α-stereogenic center. The second intramolecular, alkylation–cyclization requires very strong basic conditions giving rise to the targeted, highly sterically constrained, cyclic architecture. Product **98** was isolated in 75% yield as a mixture of diastereomers 90:10. The major compound with (1*S*,2*R*) configuration was obtained diastereomerically pure by column chromatography. Disassembly of compound **98** followed by four additional steps afforded the Boc-protected (1*S*,2*R*)-1-amino-2-vinylcyclopropanecarboxylic acid (**99**) [358]. A similar reaction sequence was used for the preparation of the (1*S*,2*R*) and (1*R*,2*S*) enantiomers of 1-amino-2-vinylcyclopropanecarboxylic acid starting from the glycine complex derived from the Hamari ligand **13** [359]. Both approaches provide for reliable access to this pharmacologically important tailor-made AA.

3-Amino-2-hydroxyoctadecanoic acid (Ahod **100**, Figure 7) is a common structural unit of naturally occurring peptides Ralstonin A and Ralstoamide A possessing chlamydospore-inducing activity in fungus and moderatephytotoxicity in plants [360]. The total synthesis of Ralstonin A and Ralstoamide A has not been reported and synthetic work on these molecules has been limited for a long time by the preparation of selected fragments, in particular the 3-hydroxy-tyrosine fragment with various stereochemistries and functional group protections [361–363]. Planning for the highly anticipated structural confirmation and a

structure–activity relationship study, we decided to focus on the preparation of Ahod AA **100** which is critically responsible for the lipophilic properties of these naturally occurring peptides.

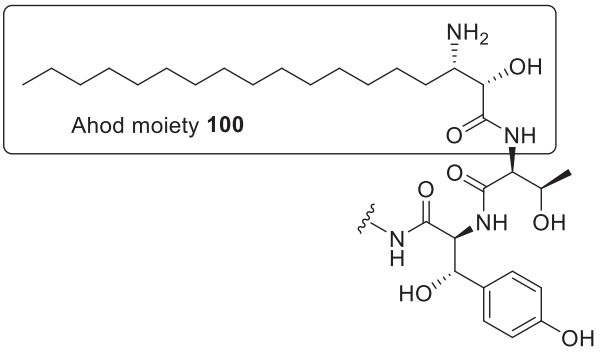

Fig. 7. The common structural fragment of Ralstonin A and Ralstoamide A.

As presented in Scheme 23 [364], the synthesis started with the alkylation of chiral glycine equivalent **19** with alkyl iodide **101**. The reaction was conducted under the usual strongly basic conditions at ambient temperature affording alkylation product **102** in high chemical yield and with high diastereoselectivity. Disassembly of diastereomerically pure **102** was followed by the esterification and protection of the amino group. The ester group in **103** was hydrolyzed using NaOH to yield **104**, which was reacted with reagent **105** to produce intermediate **106**. Compound **106** was treated with oxone in THF–methanol to provide keto–ester **107** in moderate yield. Finally, reduction of the keto group in **107** gave rise to two diastereomeric products, (2*S*,3*S*)-**108** and (2*R*,3*S*)-**108**, obtained in yields of 39% and 29%, respectively [120]. While the diastereoselectivity of this step was low, the preparation of both compounds fits well with the current research goals of confirming the stereochemistries of Ralstonin A and Ralstoamide A.

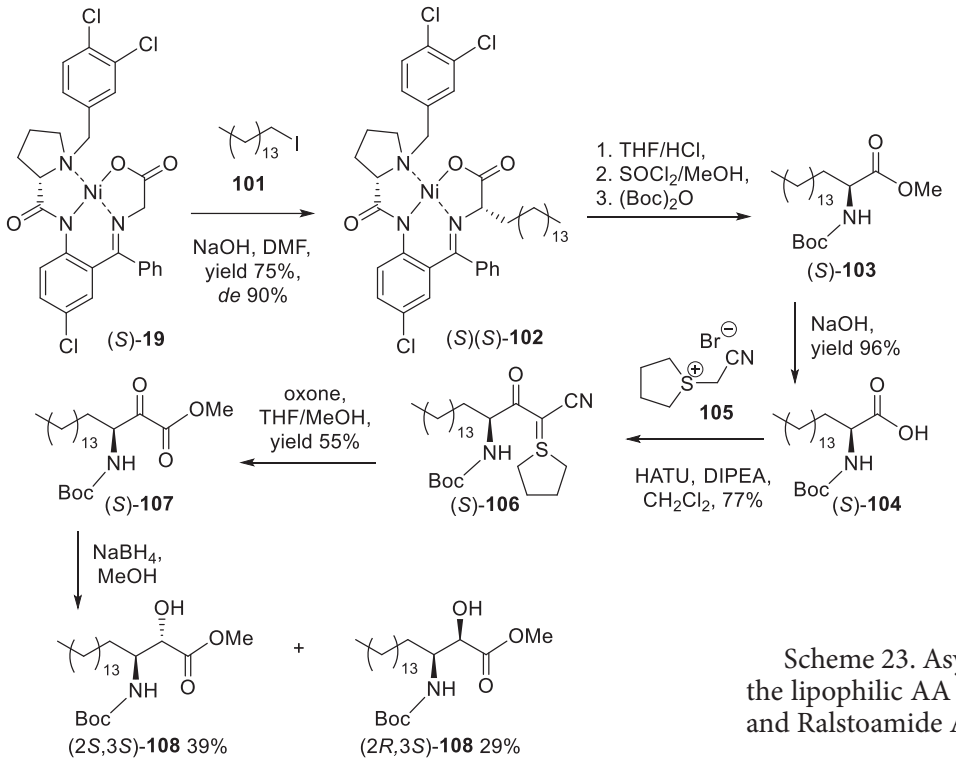

Scheme 23. Asymmetric synthesis of the lipophilic AA found in Ralstonin A and Ralstoamide A.

CONCLUSIONS. In the field of the asymmetric synthesis of AAs, only a few approaches possess the practical characteristics attractive to industry for large-scale pharmaceutical production. The chemistry of Ni(II) complexes is undoubtedly one of these promising methods. As emphasized in this review, the simplicity of the reaction conditions plays a crucial role in the overall cost structure and commercial success of chemical processes.

Depending on the structure of the target AA, one may choose either direct chiral modification of unprotected AAs or the elaboration of chiral glycine equivalents. Of particular commercial interest are the methods we have developed, which include SOAT, DKR, and inversion of chirality. In the homologation approach, construction of the desired AA architecture can be efficiently achieved through alkylation, aldol, Mannich, and Michael addition reactions.

We believe that Hamari's contributions to this field will be highly valued by practitioners in both industrial and academic laboratories and will be instrumental in future applications of our methods for the preparation of commercially marketed pharmaceuticals.

We gratefully acknowledge the financial support from the National Natural Science Foundation of China (No. 21761132021) and the Qing-Lan Project of Jiangsu Province (for Han) and IKERBASQUE, Basque Foundation for Science (for Soloshonok).

ВНЕСОК ХАМАРІ В АСИМЕТРИЧНИЙ СИНТЕЗ СПЕЦІАЛЬНО СТВОРЕНИХ АМІНОКИСЛОТ

Цзяньлінь Хань, Хонг Лю, Цзян Ван, Аліція Взорек, Олександр Е. Сорочинський, Карел Д. Кліка, Тайзо Оно, Хіроїкі Моріваkі, Тацунорі Сато, Кунісуке Ізава, Хіройукі Конно, Вадим А. Солошонок

[1] Цзянсу-Центр спільних інновацій для ефективного перероблення та використання лісових ресурсів, Коледж хімічної інженерії, Нанкінський лісотехнічний університет, Нанкін 210037, Китай;
[2] Державна Ключова лабораторія дослідження ліків, Шанхайський Інститут медичних матеріалів, Китайська Академія наук, Шанхай 201203, Китай;
[3] Інститут хімії, Університет Яна Кохановського у Кельце, Університетська 7, 25–406 Кельце, Польща;
[4] Інститут біоорганічної хімії та нафтохімії ім. В. П. Кухаря, Національна Академія наук України, Київ 02094, Україна;
[5] Німецький Центр дослідження раку (DKFZ), Нойенхаймер Фельд 280, 69120 Гейдельберг, Німеччина;
[6] Національний Інститут передових промислових наук і технологій, 463–8560, Нагоя, Японія;
[7] Хамарі Кемікал Лтд.., Осака, Японія;
[8] Департамент хімії та біологічної інженерії, Аспірантура наук та інженерії, Університет Ямагата, 992–8510 Йонедзава, Ямагата, Японія;
[9] Департамент органічної хімії, факультет хімії, Університет Країни Басків UPV/EHU, Пасео Мануель Лардизабал 3, 20018 Сан-Себастьян, Іспанія;
[10] ІКЕРБАСКЕ, Баскський Фонд науки, Марія Діас де Харо 3, плаза Бізкая, 48013 Більбао, Іспанія.
email: vadimsoloshonok@gmail.com

У цій статті розглянуто розвиток асиметричного синтезу спеціально створених амінокислот, проведений в компанії Hamari Chemicals за 10-річний період з 2013 по 2022 рік. Обговорення базується на стратегіях, таких як пряма хіральна модифікація незахищених амінокислот через проміжне утворення комплексів Ni(II) і розроблення хіральних нуклеофільних або електрофільних еквівалентів гліцину. Перший підхід включає, наприклад, асиметричну трансформацію другого порядку, динамічну кінетичну роздільність та інверсію хіральності, тоді як другий підхід включає побудову бажаної архітектури амінокислот за допомогою, наприклад, реакцій алкілування, альдольних, Манніха чи Міхаеля, а також багатоступінчастих процедур. Наголошується на зручності в експлуатації, масштабованості та практичності розроблених методів.

Ключові слова: спеціально створені амінокислоти; дизайн і розроблення ліків; асиметрична трансформація другого порядку; динамічна кінетична роздільність; інверсія хіральності.

REFERENCES

1. Vickery H.B., Schmidt C.L.A. The history of the discovery of the amino acids. *Chem. Rev*. 1931. **9**:169–318.
2. Fowden, L., Lea P.J., Bell E. A. *The non-protein amino acids of plants*. In *Advances in Enzymology*, Meister, A. Ed., John Wiley & Sons, New York, USA, 1979. Vol. 50. 117–175.
3. Lea P.J., Wallsgrove R.M., Miflin B.J. *The biosynthesis of amino acids in plants*. In *The Chemistry and Biochemistry of Amino Acids*, Barrett, G. C. Ed.; Chapman and Hall, London, UK, 1985. 197–226.
4. Bryan J.K. *Advances in the biochemistry of amino acid biosynthesis*. In *The Biochemistry of Plants*, Stump, P. K., Conn, E. E. Eds. In *Intermediary nitrogen metabolism*, Miflin B. J., Lea P. J. Eds.. 1990, Vol. 16. 169–195.
5. Bella A.E., Alison A., NashR. J. Non-Protein Amino Acids: A Review of the Biosynthesis and Taxonomic Significance. *Nat. Prod. Commun*. 2008. **3**: 93–110.
6. Frisch D.M., Dunnill P.M., Smith A., Fowden L. The specificity of amino acid biosynthesis in the Cucurbitaceae. *Phytochemistry.* 1967. **6**: 921–931.
7. Peterson P.J., Fowden L. The biosynthesis of γ-substituted glutamic acids in Gleditsia triacanthos. *Phytochemistry.* 1972. **11**: 663–673.
8. Murakoshi I., Kuramoto H., Haginiwa J., Fowden L. The enzymic synthesis of b-substituted alanines. *Phytochemistry.* 1972. **11**: 177–182.
9. Dunnill P.M., Fowden L. The biosynthesis of b-pyrazol-1-ylalanine.*J. Exp. Bot.*1963. **14**: 237–248.
10. Dunnill P.M., Fowden L. The amino acids of the genus Astragalus. *Phytochemistry.* 1967. **6**: 1659–1663.
11. Pilbeam D.J., Bell E.A. Free amino acids of *Crotalaria* seeds. *Phytochemistry.* 1979.**18**: 973–985.
12. Pilbeam D.J., Polhill R. M., Bell E.A. Free amino acids and alkaloids of South American, Asian and Australian Crotalaria species *Bot. J. Linn. Soc.*1979. **79**: 259–266.
13. Evans S.V., Fellows L.E., Bell E.A. Distribution and systematic significance of basic non-protein amino acids and amines in the Tephrosieae. *Biochem. Syst. Ecol.*1985. **13**: 271–302.
14. Watson R., Fowden L. Amino acids of Caesalpinia tinctoria and some allied species. *Phytochemistry.* 1973. **12**: 617–622.
15. Evans C.S., Bell E.A. Uncommon amino acids in the seeds of 64 species of Caesalpinieae. *Phytochemistry.* 1978. **17**: 1127–1129.
16. Soloshonok V. A., Kirilenko A. G., Kukhar

V. P., Resnati, G. Transamination of Fluorinated b-Keto Carboxylic Esters. A Biomimetic Approach to b-Polyfluoroalkyl-b-Amino Acids. *Tetrahedron Lett.*1993. **34**: 3621–3624.
17. Xue Y., Cao C., Zheng Y. Enzymatic asymmetric synthesis of chiral amino acids. *Chem. Soc. Rev*. 2018. **47**: 1516.
18. Roche S.P. In the Pursuit of (Ald) Imine Surrogates for the Direct Asymmetric Synthesis of Non-Proteinogenic a-Amino Acids. *Synthesis.* 2021. **53**: 2767–2776.
19. Soloshonok V. A., Sorochinsky A. E. Practical Methods for the Synthesis of Symmetrically a,a-Disubstituted-a-Amino Acids, *Synthesis.* 2010. **14**: 2319–2344.
20. Han J., Sorochinsky A. E., Ono T. *et al*. Biomimetic Transamination – a Metal-Free Alternative to the Reductive Amination. Application for Generalized Preparation of Fluorine-Containing Amines and Amino Acids. *Cur. Org. Synthesis.* 2011. **8**: 281–294.
21. Mikami K., Fustero S., Sánchez-Roselló M. *et al*. Synthesis of Fluorine Containing b-Amino Acids. *Synthesis.* 2011. **19**: 3045–3079.
22. Molinaro C., Scott J. P., Shevlin M. *et al*. Catalytic, Asymmetric, and Stereodivergent Synthesis of Non-Symmetric b,b-Diaryl-b-Amino Acids. *J. Am. Chem. Soc.* 2015. **137**: 999–1006.
23. Xue Y. P., Cao C. H., Zheng Y. G. Enzymatic asymmetric synthesis of chiral amino acids. *Chem. Soc. Rev.* 2018. **47**: 1516–1561.
24. Leonard D. J., Ward J. W., Clayden J. Asymmetric a-arylation of amino acids. *Nature.* 2018. **562**: 105–109.
25. He F. S., Jin J. H., Yang Z. T. *et al*. Direct Asymmetric Synthesis of b-bis-Aryl-a-Amino Acid Eesters via Enantioselective Copper-Catalyzed Addition of p-Quinone Methides. *ACS Catalysis.* 2016. **6**: 652–656.
26. Wei L., Zhu Q., Xu S. M. *et al*. Stereodivergent Synthesis of a,a-Disubstituted a-Amino Acids via Synergistic Cu/Ir Catalysis. *J. Am. Chem. Soc.* 2018. **140**: 1508–1513.
27. Metz A. E., Kozlowski M. C. Recent Advances in Asymmetric Catalytic Methods for the Formation of Acyclic a, a-Disubstituted a-Amino Acids. *J. Org. Chem.* 2015. **80**: 1–7.
28. He G., Wang B., Nack W. A., Chen, G. Syntheses and Transformations of a-Amino Acids via Palladium-Catalyzed Auxiliary-Directed sp3 C–H Functionalization. *Acc.Chem. Res.* 2016. **49**: 635–645.
29. Wei L., Xiao L., Hu Y. *et al*. Recent Advances in Metallated Azomethine Ylides for the Synthesis of Chiral Unnatural a-Amino Aacids. *Chin. J. Org. Chem.* 2019. **39**: 2119–2130.
30. Wzorek A., Han J., Lyutenko N. V. *et al*. Discovery of biomimetic transamination as a general synthetic method for preparation of fluorine-containing amines and amino acids.*Ukr. Bioorg. Acta.* 2023. **18**(2): 3–15. https://doi.org/10.15407/bioorganica2023.01.010
31. Lyutenko N. V., Sorochinsky A. E., Soloshonok V. A. Applications of chiral sulfinyl auxiliaries in the asymmetric synthesis of fluorinated amines and amino acids.*Ukr. Bioorg. Acta.* 2023. **18**(1): 10–21.
32. Soloshonok V. A., Ono T. The Effect of Substituents on the Feasibility of Azomethine-Azomethine Isomerization: New Synthetic Opportunities for Biomimetic Transamination. *Tetrahedron.* 1996. **52**: 14701–14712.
33. Ohkura H., Berbasov D. O., Soloshonok V. A. Chemo- and Regioselectivity in the Reactions between Highly Electrophilic Fluorine Containing Dicarbonyl Compounds and Amines. Improved Synthesis of the Corresponding Imines/Enamines. *Tetrahedron.* 2003. **59**: 1647–1656.
34. Wagner I., Musso H. New naturally occurring amino acids.*Angew. Chem., Int.Ed.* 1983. **22**: 816–828.
35. Soloshonok V. A., Cai C., Hruby V. J. *et al*. Stereochemically Defined *C*-Substituted Glutamic Acids and their Derivatives. 1. An Efficient

Asymmetric Synthesis of (2*S*,3*S*)-3-Methyl- and -3-Trifluoromethylpyroglutamic Acids. *Tetrahedron.* 1999. **55**: 12031–12044.
36. Hamley I. W. *Introduction to Peptide Science*. John Wiley & Sons, New York, USA. 2020. ISBN: 9781119698173.
37. Saladin K. *Anatomy and Physiology: The Unity of Form and Function*, sixth ed., McGraw-Hill, 2011.
38. *Asymmetric Synthesis and Application of α-Amino Acids. ACS Symposium Series #1009*; Soloshonok V. A., Izawa K., Eds., Oxford University Press, 2009.
39. Blaskovich M.A.T. Unusual amino acids in medicinal chemistry. *J. Med. Chem.* 2016. **59**: 10807–10836.
40. Hodgson D.R.W., Sanderson J.M. The synthesis of peptides andproteins containing non-natural amino acids. *Chem. Soc. Rev*. 2004. **33**: 422–430.
41. Henninot A., Collins J. C., Nuss J. M. The current state of peptidedrug discovery: Back to the future? *J. Med. Chem.* 2018. **61**:1382–1414.
42. Han J., Lyutenko N. V., Sorochinsky A. E. *et al.*Tailor-Made Amino Acids in Pharmaceutical Industry: Synthetic Approaches to Aza-Tryptophan Derivatives.*Chem.–Eur. J.* 2021. **27**: 17510–17528. doi.org/10.1002/chem.202102485.
43. Han J., Konno H., SatoT. *et al.* Peptidomimetics and Peptide-Based Blockbuster Drugs. *Curr. Org. Chem.* 2021. **25**: 1627–1658. DOI: 10.2174/1385272825666210610155047
44. Craik D.J., Fairlie D.P., Liras S., Price D. The future of peptidebased drugs. *Chem. Biol. Drug. Des.* 2013. **81**:136–147.
45. Bravo P., Guidetti M., Viani F. *et al.*Chiral Sulfoxide Controlled Asymmetric Additions to C,N Double Bond. An Efficient Approach to Stereochemically Defined a-Fluoroalkyl Amino Compounds. *Tetrahedron.* 1998. **54**: 12789–12806.
46. Han J.,Wzorek A., Dhawan G. *et al*. New drugs appearing on the market in 2023: molecules containing fluorine and fragments of tailor-made amino acids.*Ukr. Bioorg. Acta*. 2024. **19**(1): 3–20. https://doi.org/10.15407/bioorganica2024.01.003
47. Wang N., Mei H., Dhawan G. *et al*. New Approved Drugs Appearing in the Pharmaceutical Market in 2022, Featuring Fragments of Tailor-Made Amino Acids and Fluorine. *Molecules.* 2023. **28**: 3651. https://doi.org/10.3390/molecules28093651.
48. Wang Q., Han J., Sorochinsky A. E. *et al*. The Latest FDA-Approved Pharmaceuticals Containing Fragments of Tailor-Made Amino Acids and Fluorine. *Pharmaceuticals.* 2022. **15**: 999. https://doi.org/10.3390/ ph150809991847558.
49. Liu A., Han J., NakanoA. *et al.* New pharmaceuticals approved by FDA in 2020: Small-molecule drugs derived from amino acids and related compounds. *Chirality.* 2022. **34**: 86–103.
50. Han J., Konno H., Sato T. *et al*. Tailor-madeamino acids in the design of small-molecule blockbusterdrugs. *Eur. J. Med. Chem.* 2021. **220**:113448. doi.org/10.1016/j.ejmech.2021.113448.
51. Liu J., Han J., Izawa K. *et al*. Cyclic tailor-made amino acids inthe design of modern pharmaceuticals. *Eur. J. Med. Chem*. 2020. **208**:112736. Doi:10.1016/j.ejmech.2020.112736.
52. Mei H., Han J., White S. *et al*. Tailor-made amino acids andfluorinated motifs as prominent traits in modern pharmaceuticals. *Chem. – Eur. J.* 2020. **26**:11349–11390. https://doi.org/10.1002/chem.202000617.
53. Ma J.S. Unnatural amino acids in drug discovery. *Chim. Oggi–Chem. Today.* 2003. **21**: 65–68.
54. Yin Z., Hu W., Zhang W. *et al*. Tailor-made amino acid-derived pharmaceuticals approved by the FDA in 2019. *Amino Acids.* 2020. **52**: 1227–1261. DOI: 10.1007/s00726-020-02887-4.

55. Qiu W., Gu X., Soloshonok V. A. *et al*. Stereoselective synthesis of conformationally constrainedreverse turn dipeptide mimetics. *Tetrahedron Lett*. 2001. **42**:145–148.
56. Fosgerau K., Hoffmann T. Peptide therapeutics: Current statusand future directions. *Drug Discov. Today.* 2015. **20**: 122–128.
57. Mei H., Han J., Klika K. D. *et al*. Applications of fluorinecontainingamino acids for drug design. *Eur. J. Med. Chem.* 2020. **186**:111826. https://doi.org/10.1016/j.ejmech.2019.111826.
58. Cai M., Cai C., Mayorov A. V. *et al*. Biological and conformational study of b-substituted prolines in MT-II template: steric effects leading to human MC5 receptor selectivity. *J. Pept. Res.* 2004. 63: 116–131.
59. Stevenazzi A., Marchini M., Sandrone G. *et al*. Amino acidic scaffolds bearing unnatural sidechains: An old idea generates new and versatile tools for thelife sciences. *Bioorg. Med. Chem. Lett.* 2014. **24**: 5349–5356.
60. Soloshonok V. A., Kirilenko A. G., Galushko S. V., Kukhar V. P. Catalytic Asymmetric Synthesis of b-Fluoroalkyl-b-Amino Acids *via* Biomimetic [1,3]-Proton Shift Reaction.*Tetrahedron Lett.*1994. **35**: 5063–5064.
61. Zou Y., Han J., Saghyan A. S. *et al.* Asymmetric Synthesis of Tailor-Made Amino Acids Using Chiral Ni(II)-Complexes of Schiff Bases; An Update of the Recent Literature. *Molecules.* 2020. **25**: 2739. doi:10.3390/molecules25122739.
62. Wang Y., Song X.,Wang J. *et al.* Recent approaches for asymmetric synthesis of a-amino acids *via* homologation of Ni(II) complexes. *Amino Acids.* 2017. **49**: 1487–1520. DOI: 10.1007/s00726-017-2458-6.
63. Sorochinsky A. E., Aceña J. L., Moriwaki H. *et al*. Asymmetric synthesis of a-amino acids via homologation of Ni(II) complexes of glycine Schiff bases; Part 1: Alkyl halide alkylations. *Amino Acids.* 2013. **45**: 691–718. DOI: 10.1007/s00726-013-1539-4.
64. Sorochinsky A. E., Aceña J. L., Moriwaki H. *et al*. Asymmetric synthesis of a-amino acids via homologation of Ni(II) complexes of glycine Schiff bases. Part 2: Aldol, Mannich addition reactions, deracemization and (*S*) to (*R*) interconversion of a-amino acids. *mino Acids.* 2013. **45**: 1017–1033. DOI 10.1007/s00726-013-1580-3.
65. Aceña J. L., Sorochinsky A. E., Soloshonok V. A. Asymmetric synthesis of a-amino acids via homologation of Ni(II) complexes of glycine Schiff bases. Part 3: Michael addition reactions and miscellaneous transformations. *Amino Acids.* 2014. **46**: 2047–2073. DOI: 10.1007/s00726-014-1764-5.
66. Takahashi M., Moriwaki H., Miwa T. *et al*. Large scale synthesis of chiral (3*Z*, 5*Z*)-2,7-dihydro-1*H*-azepine-derived Hamari ligand for general asymmetric synthesis of tailor-made amino acids. *Org. Process Res. Dev*. 2019. **23**: 619–628. DOI: 10.1021/acs.oprd.8b00406.
67. Ellis T. K., Ueki H., Yamada T. *et al*. The Design, Synthesis and Evaluation of a New Generation ofModular Nucleophilic Glycine Equivalents for the Efficient Synthesisof Sterically Constrained a-Amino Acids. *J. Org. Chem*. 2006. **71**: 8572–8578.
68. Soloshonok V. A., Cai C., Hruby V. J. Toward Design of a Practical Methodology for Stereocontrolled Synthesis of c-Constrained Pyroglutamic Acids and Related Compounds. Virtually Complete Control of Simple Diastereoselectivity in the Michael Addition Reactions of Glycine Ni(II) Complexes with *N*-(Enoyl) oxazolidinones. *Tetrahedron Lett.* 2000. **41**: 135–139.
69. Soloshonok V. A., Ueki H., Ellis T. K. *et al*. Application of Modular Nucleophilic Glycine Equivalentsfor Truly Practical Asymmetric Synthesis of b-Substituted Pyroglutamic Acids. *Tetrahedron Lett*. 2005. **46**: 1107–1110.
70. Moore J. L., Taylor S. M., Soloshonok V. A.

An Efficient and Operationally Convenient General Synthesis of Tertiary Amines by Direct Alkylation of Secondary Amines with Alkyl Halides in the Presence of Hünig's Base. *Arkivoc.* 2005. **6**: 287–292.

71. Zhou S., Wang J., Chen X. *et al.* Chemical Kinetic Resolution of Unprotected b-Substituted-b-Amino Acids Using Recyclable Chiral Ligands. *Angew. Chem., Int. Ed*. 2014. **53**: 7883–7886. DOI: 10.1002/anie.201403556.
72. Soloshonok V. A., Kirilenko A. G., Fokina N. A. *et al.* Biocatalytic Resolution of b-Fluoroalkyl-b-Amino Acids. *Tetrahedron: Asymmetry.* 1994. **5**: 1119–1126.
73. Nian Y.,Wang J., Moriwaki H. *et al.* Analysis of crystallographic structures of Ni(II) complexes of a-amino acid Schiff bases; Elucidation of the substituents effect on stereochemical preferences. *Dalton Trans*. 2017. **46**: 4191–4198. DOI: 10.1039/C7DT00014F.
74. Romoff T. T., Palmer A. B., Mansour N. *et al.* Scale-up Synthesis of (*R*)- and (*S*)-*N*-(2-Benzoyl-4-chlorophenyl)-1-(3,4-dichlorobenzyl) pyrrolidine-2-carboxamide Hydrochloride, a Versatile Reagent for Preparation of Tailor-made a- and b-Amino Acids in Enantiomerically Pure Form. *Org. Process Res. Dev.* 2017. **21**: 732–739. DOI: 10.1021/acs.oprd.7b00055.
75. Ueki H., Ellis T. K., Martin C. H., Soloshonok V. A. Efficient Large-Scale Synthesis of Picolinic Acid Derived Ni(II)-Complexes of Glycine. *Eur. J. Org. Chem.* 2003. 1954–1957.
76. Ueki H., Ellis T. K., Martin C. H. *et al.* Improved Synthesis of Proline Derived Ni(II)-Complexes of Glycine, a Versatile Chiral Equivalents of Nucleophilic Glycine for General Asymmetric Synthesis of a-Amino Acids. *J. Org. Chem*. 2003. **68**: 7104–7107.
77. Romoff T. T., Goodman M. Urethane-protected *N*-carboxyanhydrides (UNCAs) as unique reactants for the study of intrinsic racemization tendencies in peptide synthesis. *J. Pept. Res*. 1997. **49**: 281–292.
78. Romoff T. T., Ignacio B. G., Mansour N. *et al.* Large-Scale Synthesis of the Glycine Schiff Base Ni(II) Complex Derived from (*S*)- and (*R*)-*N*-(2-Benzoyl-4-chlorophenyl)-1-[(3,4-dichlorophenyl)methyl]-2-pyrrolidinecarboxamide.*Org. Process Res. Dev*. 2020. **24**: 294–300. https://dx.doi.org/10.1021/acs.oprd.9b00399.
79. Zhang W., Eto Ekomo R., Roussel C. *et al.* Axially Chiral Ni(II) Complexes of a-Amino Acids; Separation of Enantiomers and Kinetics of Racemization. *Chirality*. 2018. **30**: 498–508. DOI: 10.1002/chir.22815.
80. Han J., Jean M., Roussel C. *et al.* Chromatographic Approach to Study the Configurational Stability of Ni(II) Complexes of Amino Acid Schiff Bases Possessing Stereogenic Nitrogen. *Chirality.* 2019. **31**: 328–335. https://doi.org/10.1002/chir.23059.
81. Mei H., Jean M., Albalat M. *et al.* Effect of Substituents on the Configurational Stability of the Stereogenic Nitrogen in Metal(II) Complexes of a-Amino Acid Schiff Bases. *Chirality.* 2019. **31**: 401–409. DOI:10.1002/chir.23066.
82. Bergagnini M., Fukushi K., Han J. *et al.* NH-type of chiral Ni(II) complexes of glycine Schiff base: design, structural evaluation, reactivity and synthetic applications. *Org. Biomol. Chem.* 2014. **12**:1278–1291. DOI:10.1039/C3OB41959B.
83. Jamison M. M., Turner E. E. The Inter-Relation ofFirst- and Second-Order Asymmetric Transformations. *J. Chem. Soc.*1942. 437–440.
84. Busch D. H. High Yield Resolution of Tris-(ethylenediamine)-cobalt(III) by a Second-order Asymmetric Process. *J. Am. Chem. Soc.*1955. **77**: 2747–2748.
85. Faigl F., Mátravölgyi B., Holczbauer T. *et al.*Resolution of 1-[2-Carboxy-6-(trifluoromethyl)phenyl]-1*H*-pyrrole-2-carboxylic Acid-

with Methyl (*R*)-2-Phenylglycinate, Reciprocal Resolution andSecond Order Asymmetric Transformation. *Tetrahedron: Asymmetry.* 2011. **22**: 1879–1884.

86. Tsubaki K., Miura M., Morikawa H. *et al*. Synthesis ofOptically Active Oligonaphthalenes via Second-Order AsymmetricTransformation. *J. Am. Chem. Soc*. 2003. **125**: 16200–16201.
87. Yamada K., Ishii R., Nakagawa H., Kawazura H. A. Second-Order Asymmetric Transformation of Racemic 2-Hydroxymethyl-[5]-thiaheterohelicene into a Single Enantiomer upon Uptake by Bovine Serum Albumin. *Tetrahedron: Asymmetry.* 1996. **7**: 737–746.
88. Donaldson W. A., Shang L., Rogers R. D. Reactivity ofTricarbonyl(pentadienyl)iron(1+) Cations: Preparation of an OpticallyPure Tricarbonyl(diene)iron Complex via Second-Order Asymmetric Transformation. *Organometallics.* 1994. **13**: 6–7.
89. Smrcina M., Lorenc M., Hanus V. *et al*. Synthesis of Enantiomerically Pure 2,2′-Dihydroxy-1,1′-binaphthyl,2,2′-Diamino-1,1′-binaphthyl, and 2-Amino-2′-hydroxy-1,1′-binaphthyl. Comparison of Processes Operating as Diastereoselective Crystallization and as Second Order Asymmetric Transformation. *J. Org. Chem*. 1992. **57**: 1917–1920.
90. Spilovska K., Zemek F., Korabecny J. *et al*. Adamantane – A Lead Structure for Drugs in Clinical Practice. *Curr. Med. Chem*. 2016. **23**: 3245–3266.
91. Ide K., Kawasaki Y., Kawakami K., Yamada H. Anti-influenza Virus Effects of Catechins: A Molecular and Clinical Review. *Curr. Med. Chem*. 2016. **23**: 4773–4783.
92. Das K. Antivirals targeting influenza A virus. *J. Med. Chem*. 2012. **55**: 6263–6277.
93. Kolocouris N., Kolocouris A., Foscolos G. B. *et al*. Synthesis and Antiviral Activity Evaluation of Some New Aminoadamantane Derivatives. *J. Med. Chem*.1996. **39**: 3307–3318.
94. Zoidis G., Kolocouris N., Kelly J. M. *et al*. New aminoadamantane derivatives with antiproliferative activity. *Eur. J. Med. Chem*. 2010. **45**: 5022–5030.
95. Han J., Takeda R., Sato T. H. *et al*. Optical Resolution of Rimantadine. *Molecules.* 2019. **24**: 1828.
doi: 10.3390/molecules24091828.
96. Soloshonok V. A., Ono T., Soloshonok I. V. Enantioselective Biomimetic Transamination of b-Keto Carboxylic Acid Derivatives. An Efficient Asymmetric Synthesis of b-Fluoroalkyl-b-Amino Acids. *J. Org. Chem.*1997. **62**: 7538–7539.
97. Wanka L., Iqbal K., Schreiner P. R. Discovery of innovative small molecule therapeutics. *Chem. Rev*. 2013. **113**: 3516–3604.
98. Soloshonok V. A., Ellis T. K. Design and Synthesis of a New Generation of "NH" Ni(II) Complexes of Glycine Schiff Bases and Their Unprecedented C-H vs. N-H Chemoselectivity in the Alkyl Halide Alkylations and Michael addition Reactions. *Synlett.* 2006. 533–538.
99. Soloshonok V. A., Ellis T. K., Ueki H., Ono T. Resolution/Deracemization of Chiral a-Amino Acids Using Resolving Reagents with Flexible Stereogenic Centers. *J. Am. Chem. Soc*. 2009. **131**: 7208–7209.
100. Takeda R., Kawamura A., Kawashima A. *et al*. Second-order asymmetric transformation and its application for the practical synthesis of α-amino acids. *Org. Biomol. Chem*. 2018. **16**: 4968–4972.
DOI: 10.1039/C8OB00963E.
101. Houck D., Aceña J. L., Soloshonok V. A. Alkylations of Chiral Nickel(II) Complexes of Glycine under Phase-Transfer Conditions. *Helv. Chim. Acta.* 2012. **95**: 2672–2679. DOI: 10.1002/hlca.201200536.
102. Takeda R., Kawashima A., Yamamoto J. *et al*. Tandem Alkylation–Second-Order Asymmetric Transformation Protocol for Preparation of Phenylalanine-Type Tailor-Made a-Amino

Acids. *ACS Omega* 2018. **3**: 9729–9737. DOI: 10.1021/acsomega.8b01424.
103. Pellissier H. Recent developments in dynamic kinetic resolution. *Tetrahedron.* 2011. **67**: 3769–3802.
104. Ward R.S. Dynamic kinetic resolution. *Tetrahedron: Asymmetry.* 1995. **6**: 1475–1490.
105. Zhang Y., Zhang Y., Ramström O. Dynamic covalent kinetic resolution. *Cataly. Rev.* 2020. **62**: 66–95.
106. Kamal A., Azhar M. A., Krishnaji T. *et al*. Approaches based on enzyme mediated kinetic to dynamic kinetic resolutions: A versatile route for chiral intermediates. *Coord. Chem. Rev*. 2008. **252**: 569–92.
107. Turner N.J. Enzyme catalysed deracemisation and dynamic kinetic resolution reactions. *Curr .Op. Chem. Biol*. 2004. **8**: 114–119.
108. De Risi C., Bortolini O., Di Carmine G. *et al*. Kinetic resolution, dynamic kinetic resolution and asymmetric desymmetrization by N-heterocyclic carbene catalysis. *Synthesis.* 2019. 1871–1891.
109. Ahn Y., Ko S. B., Kim M. J., Park J. Racemization catalysts for the dynamic kinetic resolution of alcohols and amines. *Coord. Chem. Rev*. 2008. **252**: 647–58.
110. Vedej E., Jure M. Efficiency in nonenzymatic kinetic resolution. *Angew. Chem., Int. Ed*. 2005. **44**: 3974–4001.
111. Huerta F.F., Minidis A.B., Bäckvall J.E. Racemisation in asymmetric synthesis. Dynamic kinetic resolution and related processes in enzyme and metal catalysis. *Chem. Soc. Rev.* 2001. **30**: 21–331.
112. Lee J.H., Han K., Kim M.J., Park J. Chemoenzymatic dynamic kinetic resolution of alcohols and amines. *Eur. J.Org. Chem*. 2010. 999–1015.
113. Liu W, Yang X. Recent advances in (dynamic) kinetic resolution and desymmetrization catalyzed by chiral phosphoric acids. *Asian J. Org. Chem*. 2021. **4**: 92–710.
114. Kim M.J., Ahn Y., Park J. Dynamic kinetic resolutions and asymmetric transformations by enzymes coupled with metal catalysis. *Curr Op. Biotech.* 2002. **13**: 578–87.
115. Bhat V., Welin E.R., Guo X., Stoltz B.M. Advances in stereoconvergent catalysis from 2005 to 2015: transition-metal-mediated stereoablative reactions, dynamic kinetic resolutions, and dynamic kinetic asymmetric transformations. *Chem. Rev*. 2017. **117**: 4528–4561.
116. Moriwaki H., Resch D., Li, H. *et al.* Synthesis and stereochemical assignments of diastereomeric Ni(II) complexes of glycine Schiff base with (*R*)-2-(*N*-{2-[*N*-alkyl-*N*-(1-phenylethyl) amino]acetyl}amino)benzophenone; a case of configurationally stable stereogenic nitrogen. *Beilstein J. Org. Chem.* 2014. **10**: 442–448. doi:10.3762/bjoc.10.41.
117. Moriwaki H., Resch D., Li, H. *et al*. Inexpensive chemical method for preparation of enantiomerically pure phenylalanine.*Amino Acids.* 2014. **46**: 945–952. DOI: 10.1007/s00726-013-1656-0.
118. Takeda R., Kawamura A., Kawashima A. *et al*. Design and synthesis of (*S*)- and (*R*)-a-(phenyl)-ethylamine-derived NH-type ligands and their application for the chemical resolution of a-amino acids.*Org. Biomol. Chem*. 2014. **12**: 6239–6249. DOI: 10.1039/c4ob00669k.
119. Sorochinsky A. E., Ueki H., Aceña J. L. *et al*. Chemical approach for interconversion of (*S*)- and (*R*)-a-amino acids. *Org. Biomol. Chem*. 2013. **11**: 4503–4507. DOI:10.1039/C3OB40541A.
120. Sorochinsky A. E., Ueki H., Aceña J. L. *et al*. Chemical deracemization and (*S*) to (*R*) interconversion of some fluorine-containing a-amino acids. *J. Fluor. Chem*. 2013. **152**: 114–118. DOI: 10.1016/j.jfluchem.2013.02.022.
121. Nian Y., Wang J., Zhou S. *et al*. Recyclable Ligands for the Non-Enzymatic Dynamic Kinetic Resolution of Challenging a-Amino Acids.

Angew. Chem., Int. Ed. 2015. **54**: 12918–12922. DOI: 10.1002/anie.201507273.

122. Nian Y., Wang J., Zhou S. *et al.* Purely Chemical Approach for Preparation o fD-alpha-amino Acidsvia(*S*)-to-(*R*)-interconversion of Unprotected Tailor-madealpha-aminoAcids. *J. Org. Chem*. 2016. **81**: 3501–3508. DOI: 10.1021/acs.joc.5b02707.
123. Mei H., Han J., Takeda R. *et al*. Practical Method for Preparation of (*S*)-2-Amino-5,5,5-trifluoropentanoic Acid via Dynamic Kinetic Resolution. *ACS Omega.* 2019. **4**: 11844–11851. DOI: 10.1021/acsomega.9b01537.
124. Nagaoka K., Nakano A., Han J. *et al*. Comparative Study of Different Chiral Ligands for Dynamic Kinetic Resolution of Amino Acids. *Chirality.* 2021. **33**: 685–702. DOI.10.1002/chir.23350.
125. Nakano A., Hayashi A., Nagaoka K. *et al*. Dynamic Thermodynamic Resolution of Unprotected Amino Acids Using Ni(II) Chiral Schiff Bases. *Eur. J. Org. Chem*. 2024. **27**: e202400417.
126. Takeda R., Kawamura A., Kawashima A. *et al*. Chemical Dynamic Kinetic Resolution and (*S*)/(*R*)-Interconversion of Unprotected a-Amino Acids.*Angew. Chem., Int. Ed.* 2014. **53**: 12214–12217. DOI: 10.1002/anie.201407944.
127. Wang S., Zhou S., Wang J. *et al*. Chemical Dynamic Thermodynamic Resolution and *S*/*R* Interconversion of Unprotected Unnatural Tailor-made a-Amino Acids. *J. Org. Chem*. 2015. **80**: 9817–9830. DOI: 10.1021/acs.joc.5b01292.
128. TakedaR., AbeH., Shibata N. *et al*. Asymmetric synthesis of a-deuterated a-amino acids. *Org. Biomol. Chem*. 2017. **15**: 6978–6983. DOI: 10.1039/C7OB01720K.
129. Anglister J., Srivastava G., Naider F. NMR Spectroscopy of Paramagnetic Molecules, *Prog. Nucl. Magn. Reson. Spectrosc*. 2016. **97**: 40–56.
130. Dubey A., Kadumuri R. V., Jaipuria G. *et al*. Crowding interactions perturb structure and stability by destabilizing the stable core of the a-subunit of tryptophan synthase. *Chem. BioChem*. 2016. **17**: 334–340.
131. Dayal P. V., Singh H., Busenlehner L. S.H., Ellis R. Exposing the Alkanesulfonate Monooxygenase Protein–Protein Interaction Sites. *Biochemistry.* 2015. **54**: 7531–7538.
132. Yu Y., Lv X., Li J. *et al*. De Novo Design of Chemical Stability Near-Infrared Molecular Probes for High-Fidelity Hepatotoxicity Evaluation In Vivo. *J. Am. Chem. Soc*. 2015. **137**: 4594–4597.
133. Wei L., Shen Y., Xu F. *et al*. I maging complex protein metabolism in live organisms by stimulated Raman scattering microscopy with isotope labeling. *ACS Chem. Biol*. 2015. **10**: 901–908.
134. Pantoja-Uceda D., Santoro J. Amino-acid-type identification for deuterated proteins with a beta-carbon-edited HNCOCACB experiment. *J. Biomol. NMR*2012. **54**: 145–153.
135. Tonelli M., Singarapu K. K., Makino S. *et al*. Ligand-specific structural changes in the vitamin D receptor in solution. *J. Biomol. NMR*2011. **51**: 467–476.
136. Miyanoiri Y.,Takeda M., Jee J.G. *et al*. Stereo-array isotope labeling method for studying protein structure and dynamics. *J. Biomol. NMR*2011. **51**: 425–435.
137. Torizawa T., Ono A. M., Terauchi T., Kainosho M. NMR Assignment Methods for the Aromatic Ring Resonances of Phenylalanine and Tyrosine Residues in Proteins.*J. Am. Chem. Soc*. 2005. **127**: 12620–12626.
138. Yokoyama J., Matsuda T., Koshiba S .*et al*. Cell-free protein synthesis system from Escherichia coli cells cultured at decreased temperatures improves productivity by decreasing DNA template degradation. *Anal. Biochem*. 2011. **411**: 223–229.
139. Bornoe A., van Hall G. Quantitative amino acid profiling and stable isotopically labeled

amino acid tracer enrichment used for in vivo human systemic and tissue kinetics measurements. *J. Chromatogr. B.* 2014. **951–952**: 69–77.
140. Claydon A. J., Thom M. D., Hurst J. L., Beynon R. J. Protein turnover methods in single-celled organisms: dynamic SILAC. *Proteomics.* 2012. **12**: 1194–1206.
141. Chatterjee B., Krishnakumar V., Gunanathan C. Ruthenium Catalyzed Selective Hydroboration of Carbonyl Compounds. *Org. Lett*. 2016. **18**: 5892–5895.
142. Hutchby M., Sedgwick A. C., Bull S. D. Orthogonally Protected Schöllkopf's Bis-lactim Ethers for the Asymmetric Synthesis of a-Amino Acid Derivatives and Dipeptide Esters. *Synthesis.* 2016. 2036–2049.
143. Oh J.-S., Kim K. I., Song C. E. Enantioselective synthesis of a-deuterium labelled chiral a-amino acids via dynamic kinetic resolution of racemic azlactones.*Org. Biomol. Chem*. 2011. **9**: 7983–7985.
144. Zlatopolskiy B. D., Loscha K., Alvermann P. *et al*. Final elucidation of the absolute configuration of the signal metabolite hormaomycin. *Chem.–Eur. J*. 2004. **10**: 4708–4717.
145. Winnicka E., Pająk M., Pałka *et al*. Enzymatic Synthesis of Halogen Derivatives of Aromatic Amino Acids Labeled with Hydrogen Isotopes. *J. Chem. Chem. Eng*. 2014. **8**: 54–60.
146. Mosin O. V., Shvets V. I., Skladnev D. A. Ignatov I. Microbiological synthesis of [^{2}H]-inosine with a high degree of isotopic enrichment by the gram-positive chemoheterotrophic bacterium Bacillus subtilis.*Appl. Biochem. Microbiol.*1998. **62**: 233–243.
147. Raap J., Nieuwenhuis S., Creemers A. *et al*. Synthesis of Isotopically Labelled L-Phenylalanine and L-Tyrosine. *Eur. J. Org. Chem*. 1999. 2609–2621.
148. Lygo B., Humphreys L. D. Enantioselective synthesis of a-carbon deuterium-labelled l-a-amino acids. *Tetrahedron Lett.* 2002. **43**: 6677–6679.
149. Taylor P. J. M., Bull S. D. An improved synthesis of deuterated Schöllkopf's bis-lactim ether and its use for the asymmetric synthesis of (*R*)-[a-2H]-phenylalanine methyl esters. *Tetrahedron: Asymmetry.* 2006. **17**: 1170–1178.
150. Kendall J. T., Preliminary Research of Radiolabeled Atezolizumab for the Noninvasive Evaluation of TNBC PD-L1 Expression In Vivo. *J. Labelled Comp. Radiopharm.* 2000. **43**: 917–924.
151. Moozeh K., So S. M., ChinJ. Catalytic Stereoinversion of L-Alanine to Deuterated D-Alanine. *Angew. Chem., Int. Ed*. 2015. **54**: 9381–9385.
152. Ellis T. K., Martin C. H., Tsai G. M. *et al*. Efficient Synthesis of Sterically Constrained Symmetrically a, a-Disubstituted a-Amino Acids under Operationally Convenient Conditions.*J. Org. Chem*. 2003. **68**: 6208–6214.
153. Soloshonok V. A., Tang X., Hruby V. J., Meervelt L. V. Asymmetric Synthesis of a,b-Dialkyl-a-Phenylalanines via Direct Alkylation of Chiral Alanine Derivative with Racemic a-Alkylbenzylbromides. A Case of High Enantiomer Differentiation at Room Temperature. *Org. Lett.* 2001. **3**: 341–343.
154. Tang X., Soloshonok V. A., Hruby V. J. Convenient Asymmetric Synthesis of Enantiomerically Pure 2',6'-Dimethyltyrosine (DMT) via Alkylation of Chiral Nucleophilic Glycine Equivalent. *Tetrahedron: Asymmetry.* 2000. **11**: 2917–2925.
155. Bott F., Field L.D., Sternhell S. Steric efects. A study of a rationally designed system. *J. Am. Chem. Soc*. 1980. **102**: 5618–5626.
156. Lunazzi L., Mancinelli M., Mazzanti A. *et al*. Rotational barriers of biphenyls having heavy heteroatoms as ortho substituents: Experimental and theoretical determination of steric effects. *Org. Biomol. Chem*. 2012. **10**: 1847–1855.
157. de Riggi I., Virgili A., de Moragas M., Jaime C.

Restricted rotation and NOE transfer: A conformationalof some substituted (9-anthry1)carbinol derivatives. *J. Org. Chem.*1995. **60**: 27–31.
158. Belot V., Farran D., Jean M. *et al*. Steric Scale of Common Substituentsfrom Rotational Barriers of *N*-(o-Substituted aryl)thiazoline-2-thione Atropisomers. *J. Org. Chem*. 2017. **82**: 10188–10200.
159. Bravo P., Capelli S., Meille S. V. *et al*. Synthesis of Optically Pure (*R*)- and (*S*)-a-Trifluoromethyl-Alanine. *Tetrahedron: Asymmetry.* 1994. **5**: 2009–2018.
160. Jagodzinska M., Huguenot F., Candiani G., Zanda M. Assessing the bioisosterism of the trifluoromethyl group with a protease probe. *Chem. Med. Chem.* 2009. **4**: 49–51.
161. Walborsky H. M., Baum M. E. Chemical Effects of the Trifluoromethyl Group: III. Synthesis of 2-Amino-4,4,4-trifluorobutyric Acid. *J. Org. Chem*. 1956. **21**: 538–539.
162. Steglich W., Heininger H. U., Dworschak H., Weygand F. A General Method for the Preparation of Perfluoroalkylalanines. *Angew. Chem., Int. Ed*. 1967. **6**: 807–808.
163. Tsushima T., Kawada K., Ishihara S., *et al*. Fluorine containing amino acids and their derivatives. 7. Synthesis and antitumor activity of a-substituted methotrexate analogs. *Tetrahedron* 1988. **44**: 5375–5387.
164. Seebach D., Buerger H. M., Schickli C. P. Stereoselektive Umsetzungen von rac-, (R), oder (S)-5-Alkyliden-2-tbutyl-3-methyl-4-oxo-1-imidazolidincarbonsäure-t-butylestern (chirale 2,3-Dehydroaminosäure-Derivate) und Herstellung einiger nichtproteinogener Aminosäuren. *Ann. Chem*. 1991. **7**: 669–684.
165. Kondratov I. S., Logvinenko I. G., Tolmachova N. A., *et al*. Synthesis and physical chemical properties of 2-amino-4-(trifluoromethoxy) butanoic acid–CF3O-containing analogue of natural lipophilic amino acids. *Org. Biomol. Chem*. 2017. **15**: 672–679.
166. Xin B. T., Huber E. M., de Bruin G., *et al*. Structure-Based Design of Inhibitors Selective for Human Proteasome b2c or b2i Subunits. *J. Med. Chem*. 2019. **62**: 1626–1642.
167. Franko N., Grammatoglou K., Campanini B., et al. Inhibition of O-acetylserine sulfhydrylase by fluoroalanine derivatives. J. Enzyme Inhib. *Med. Chem*. 2018. **33**: 1343–1351.
168. Gambini L., Salem A. F., Udompholkul P., *et al*. Structure-Based Design of Novel EphA2 Agonistic Agents with Nanomolar Affinity in Vitro and in Cell. *ACS Chem. Biol*. 2018. **13**: 2633–2644.
169. Soloshonok V. A., Kukhar V. P. Biomimetic Transamination of a-Keto Perfluorocarboxylic Esters. An Efficient Preparative Synthesis of b,b,b-Trifluoroalanine. *Tetrahedron* 1997. **53**: 8307–8314.
170. Soloshonok V. A., Ohkura H., Yasumoto M. Operationally Convenient Asymmetric Synthesis of (S)- and (R)-3-Amino-4,4,4-trifluorobutanoic Acid. Part II: Enantioselective Biomimetic Transamination of 4,4,4-Trifluoro-3-oxo-N-(R)-1-phenylethyl)butanamide. *J. Fluor. Chem*. 2006. **127**: 930–935.
171. Soloshonok V. A., Kukhar V. P. Biomimetic Base-Catalyzed [1,3]-Proton Shift Reaction. A Practical Synthesis of b-Fluoroalkyl-b-Amino Acids. *Tetrahedron* 1996. **52**: 6953–6964.
172. Han J., Takeda R., Liu X. *et al*. Preparative Method for Asymmetric Synthesis of (S)-2-Amino-4,4,4-trifluorobutanoic Acid. *Molecules* 2019. **24**: 4521. doi:10.3390/molecules24244521.
173. Mei H., Hiramatsu T., Takeda R. *et al*. Expedient Asymmetric Synthesis of (S)-2-Amino-4,4,4-trifluorobutanoic Acid via Alkylation of Chiral Nucleophilic Glycine Equivalent. *Org. Process Res. Dev.* 2019. **23**: 629–634. DOI: 10.1021/acs.oprd.8b00404.
174. Soloshonok V. A., Tang X., Hruby V. J. Large-Scale Asymmetric Synthesis of Novel Sterically Constrained 2',6'-Dimethyl- and a,2',6'-Trimethyltyrosine and –phenylalanine Derivatives

via Alkylation of Chiral Equivalents of Nucleophilic Glycine and Alanine. *Tetrahedron.* 2001. **57**: 6375–6382.
175. Qiu W., Soloshonok V. A., Cai C. *et al*. Convenient, Large-Scale Asymmetric Synthesis of Enantiomerically Pure trans-Cinnamylglycine and -a-Alanine. *Tetrahedron* 2000. **56**: 2577–2582.
176. Ellis T. K., Hochla V. M., Soloshonok V. A. Efficient Synthesis of 2-Aminoindane-2-Carboxylic Acid via Dialkylation of Nucleophilic Glycine Equivalent. *J. Org. Chem*. 2003. **68**: 4973–4976.
177. Wang J., Lin D., Zhou S. *et al.*Asymmetric Synthesis of Sterically Constrained Linear Trifluoromethyl Containing Amino Acids via Alkylation of Chiral Equivalents of Nucleophilic Glycine and Alanine. *J. Org. Chem*. 2011.**76**: 684–687.
178. Mei H., Yin Z., Miwa T., *et al*. Convenient Asymmetric Synthesis of Fmoc-(S)-6,6,6-trifluoro-Norleucine. *Symmetry.* 2019. **11**: 578. doi:10.3390/sym11040578.
179. Yin Z., Moriwaki H., Abe H., *et al*. Large-Scale Asymmetric Synthesis of Fmoc-(S)-2-Amino-6,6,6-Trifluorohexanoic Acid. *ChemistryOpen* 2019. **8**: 701–704. DOI: 10.1002/open.201900131.
180. Fu B., Takeda R., Zou Y., *et al*. Asymmetric Synthesis of (S)-a-(octyl)Glycine via Alkylation of Ni(II)-Complex of Chiral Glycine Schiff Base. *Chirality* 2020. **32**: 1354–1360. DOI https://doi.org/10.1002/chir.23281.
181. Soloshonok V. A., Ono T., Ueki H., *et al*. Ridge-tile-like chiral topology: Synthesis, Resolution and Complete Chiroptical Characterization of Enantiomers of Edge-Sharing Binuclear Square Planar Complexes of Ni(II) Bearing Achiral Ligands. *J. Am. Chem. Soc*. 2010. **132**: 10477–10483.
182. Soloshonok V. A., Ueki H., Moore J. L., Ellis T. K. Design and Synthesis of Molecules with Switchable Chirality via Formation and Cleavage of Metal-Ligand Coordination Bonds. *J. Am. Chem. Soc*. 2007. **129**: 3512–3513.
183. Gibson S. E., Guillo N., Tozer M. J. Towards control of c-space: Conformationally constrained analogues of Phe, Tyr, Trp and His. *Tetrahedron* 1999. **55**: 585–615.
184. Soloshonok V. A. Highly Diastereoselective Michael Addition Reactions between Nucleophilic Glycine Equivalents and b-substituted-a,b-Unsaturated Carboxylic acid Derivatives a General Approach to the Stereochemically Defined and Sterically c-Constrained a-Amino Acids. *Curr. Org. Chem*. 2002. **6**: 341–364.
185. Urman S., Gaus K., Yang Y., *et al*. The Constrained Amino Acid b-Acc Confers Potency and Selectivity to Integrin Ligands. *Angew. Chem., Int. Ed*. 2007. **46**: 3976–3978.
186. Mikhailiuk P. K., Afonin S., Chernega A. N., *et al*. Conformationally Rigid Trifluoromethyl-Substituted a-Amino Acid Designed for Peptide Structure Analysis by Solid-State 19F NMR Spectroscopy. *Angew. Chem., Int. Ed*. 2006. **45**: 5659–5661.
187. Ma J. S. Unnatural amino acids in drug discovery. *Chim. Oggi–Chem. Today.* 2003. **21**: 65–68.
188. Kukhar V. P., Sorochinsky A. E., Soloshonok V. A. Practical synthesis of fluorine-containing a- and b-amino acids: recipes from Kiev, Ukraine. *Future Med. Chem*. 2009. **1**. 793–819. doi.org/10.4155/fmc.09.70.
189. Soloshonok V. A., Kirilenko A. G., Fokina N. A. *et al*. Chemo-Enzymatic Approach to the Synthesis of Each of the Four Isomers of a-Alkyl-b-Fluoroalkyl-Substituted b-Amino Acids.*Tetrahedron: Asymmetry.* 1994. **5**: 1225–1228.
190. Soloshonok V. A., Soloshonok I. V., Kukhar V. P., Svedas V. K. Biomimetic Transamination of a-Alkyl-b-keto Carboxylic Esters. Chemo-Enzymatic Approach to the Stereochemically Defined a-Alkyl-b-Fluoroalkyl-b-Amino Acids. *J.*

*Org. Chem.*1998. **63**: 1878–1884.
191. Aceña J. L., Sorochinsky A. E., Soloshonok V. A. Recent advances in asymmetric synthesis of a-(trifluoromethyl)-containing a-amino acids. *Synthesis*. 2012. **44**: 1591–1602. DOI: 10.1055/s-0031-1289756.
192. Ellis T. K., Martin C. H., Ueki H., Soloshonok V. A. Efficient, Practical Synthesis of Symmetrically a,a-Disubstituted a-Amino Acids. *Tetrahedron Lett.* 2003. **44**: 1063–1066.
193. Jansen R., Kunze B., Reichenbach H. *et al*. Antibiotics from Gliding Bacteria. Part 43. Phenoxan: A Novel Inhibitor of HIV1 Infection in Cell Cultures from *Polyangium* sp., Strain Pl VO19 (Myxobacteria). *Liebigs Ann. Chem.*1992. 357–359.
194. Wipf P., Venkatraman S. Total Synthesis of (–)-Thiangazole and Structurally Related Polyazoles. *Synlett* 1997. 1–10.
195. Parsons R. L., Heathcock C. H. Revision of the stereostructure of mirabazole C. *Tetrahedron Lett*. 1994. **35**: 1379–1382.
196. Parsons R. L., Heathcock C. H. Total synthesis of mirabazole B. *Tetrahedron Lett*. 1994. **35**: 1383–1384.
197. Carmeli S., Paik S., Moore R. E., *et al*. Revised structures and biosynthetic studies of tantazoles A and B. *Tetrahedron Lett*. 1993. **34**: 6680–6684.
198. Parsons R. L., Heathcock C. H. Total synthesis of mirabazole B. *J. Org. Chem.* 1994. **59**: 4733–4734.
199. Boyce R. L., Mulqueen G. C., Pattenden G. Total synthesis of thiangazole. a novel inhibitor of HIV-1 from Polyangium sp. *Tetrahedron Lett*. 1994. **35**: 5705–5708.
200. Yamamoto J., Kawashima A., Kawamura A., *et al.* Operationally Convenient and Scalable Asymmetric Synthesis of (2S)- and (2R)-a-(Methyl)cysteine Derivatives through Alkylation of Chiral Alanine Schiff Base Ni II Complexes. *Eur. J. Org. Chem*. 2017. 1931–1939. DOI: 10.1002/ejoc.201700018.
201. Filippis V. D., Boni S. D., Dea D. E., *et al*. Protein engineering by chemical methods: Incorporation of nonnatural amino acids as a tool for studying protein folding, stability, and function. *Protein Sci*. 2004. **13**: 1489–1502.
202. Chao W. C., Chiang T. H., Chaudhari P. D., *et al*. Highly sensitive metal-insulator-metal plasmonic refractive index sensor with a centrally coupled nanoring containing defects. *Bioorg. Chem*. 2018. **81**: 504–511.
203. Newton L. D., Pascu S. I., Tyrrell R. M., Eggleston I. M. Development of a peptide-based fluorescent probe for biological heme monitoring. *Org. Biomol. Chem*. 2019. **17**: 467–471.
204. Hoesl M. G., Larregola M., Cui H., Budisa N. Azatryptophans as tools to study polarity requirements for folding of green fluorescent protein. *J. Pept. Sci.* 2010. **16**: 589–595.
205. Beghyn T. B., Charton J., Leroux F., *et al*. Drug to Genome to Drug: Discovery of New Antiplasmodial Compounds. *J. Med. Chem*. 2011. **54**: 3222–3240.
206. Gazzard L., Appleton B., Chapman K., *et al*. Antagonists of inhibitor of apoptosis proteins based on thiazole amide isosteres. *Bioorg. Med. Chem. Lett*. 2014. **24**: 5704–5709.
207. Katragadda M., Lambris J. D. Expression of compstatin in Escherichia coli: incorporation of unnatural amino acids enhances its activity. *Protein Expres. Purif*. 2006. **47**: 289–295.
208. Broos J., Gabellieri E., Beimans-Oldehinkel E., Strambini G. B. Efficient biosynthetic incorporation of tryptophan and indole analogs in an integral membrane protein. *Protein Sci.* 2003. **12**: 1991–2000.
209. Crestey F., Collot V., Stiebing S., Rault S. New practical access to 2-azatryptophans and dehydro derivatives via the Wittig-Horner reaction. *Tetrahedron* 2006. **62**: 7772–7775.
210. Cretey F., Collot V., Stiebing S., *et al*. Design and synthesis of a new indazole library: direct conversion of N-methoxy-N-methylamides (Weinreb amides) to 3-keto and 3-formylindazoles.

Tetrahedron Lett. 2007. **48**: 2457–2460.
211. Jeanty M., Suzenet F., Guillaumet G. Synthesis of C3-Substituted 4-Azaindoles: An Easy Access to 4-Azamelatonin and Protected 4-Azatryptophan. *J. Org. Chem*. 2008. **73**: 7390–7393.
212. Sanchez-Obregon R., Fallis A. G. Syntheses of a potential fluorescence probe, (–)-(R)-7-azatryptophan, via alkylation of the (1R, 4R)-camphor imine of tert-butylglycinate. *Can. J. Chem.* 1992. **70**: 1531–1536.
213. Lecointe L., Rolland-Fulcrand V., Roumestant M. L., *et al*. Chemoenzymatic synthesis of the two enantiomers of 7-azatryptophan. *Tetrahedron: Asymmetry* 1998. **9**: 173–1758.
214. Nakano S., Minamino Y., Hasebe F., Ito S. Deracemization and Stereoinversion to Aromatic D-Amino Acid Derivatives with Ancestral l-Amino Acid Oxidase. *ACS Catal*. 2019. **9**: 10152–10158.
215. Winn M., Francis D., Micklefield J. De novo Biosynthesis of "Non-Natural" Thaxtomin Phytotoxins. *Angew. Chem., Int. Ed*. 2018. **57**: 6830–6833.
216. Zou Y., Takeda R., Han J., *et al*. Asymmetric Synthesis of N-Fmoc-(S)-7-azatryptophan via Alkylation of Chiral Nucleophilic Glycine Equivalent. *Eur. J. Org. Chem*. 2021. 2962–2965. DOI: 10.1002/ejoc.202100485.
217. Li J., Zhou S., Wang J., *et al*. Asymmetric Synthesis of Aromatic and Hetero-Aromatic a-Amino Acids Using Recyclable Axially Chiral Ligand. *Eur. J. Org. Chem*. 2016. 999–1006. DOI: 10.1002/ejoc.201501442.
218. Soloshonok V. A., Yamada T., Ueki H., *et al*. Operationally Convenient, Efficient Asymmetric Synthesis of Enantiomerically Pure 4-Aminoglutamic Acids via Direct Methylenedimerization of Chiral Glycine Equivalents with Dichloromethane. *Tetrahedron*. 2006. **62**: 6412–6419.
219. Taylor S. M., Yamada T., Ueki H., Soloshonok V. A. Asymmetric Synthesis of Enantiomerically Pure 4-Aminoglutamic Acids via Methylenedimerization of Chiral Glycine Equivalents with Dichloromethane under Operationally Convenient Conditions. *Tetrahedron Lett*. 2004. **45**: 9159–9162.
220. Cox R. J. The DAP pathway to lysine as a target for antimicrobial agents.*Nat. Prod.Rep.* 1996. **13**: 29–43.
221. Cox R. J., Sutherland A., Vederas J. C. Synthesis and Testing of Heterocyclic Analogs of Diaminopimelic Acid (DAP) as Inhibitors of DAP Dehydrogenase and DAP Epimerase. *Bioorg. Med. Chem*. 2000. **8**: 843–871.
222. Andersen S. O. The cross-links in resilin identified as dityrosine and trityrosine. *Biochim. Biophys. Acta*. 1964. **93**: 213–215.
223. Hubbard B. K., Walsh C. T. Vancomycin assembly: nature's way.*Angew. Chem., Int. Ed.* 2003. **42**: 730–765.
224. Schafmeister C. E., Po J., Verdine G. L. An All-Hydrocarbon Cross-Linking System for Enhancing the Helicity and Metabolic Stability of Peptides. *J. Am. Chem. Soc*. 2000. **122**: 5891–5892.
225. Feliu L., Planas M. Solid-phase synthesis of biaryl bicyclic peptides containing a 3-arylytyrosine or a 4-arylphenylalanine moiety. *Int. J. Pept. Res. Ther*. 2005. **11**: 53–97.
226. Del Valle J. R., Goodman M. Stereoselective Synthesis of Boc-Protected cis and trans-4-Trifluoromethylprolines by Asymmetric Hydrogenation Reactions. *J. Org. Chem*. 2004. **69**: 5946–5948.
227. Skaff O., Jollife K. A., Hutton C. A. Synthesis of the side chain cross-linked tyrosine oligomers dityrosine, trityrosine, and pulcherosine. *J. Org. Chem*. 2005. **70**: 7353–7363.
228. Tadd A. C., Meinander K., Luthman K., Wallén E. A. A. Pseudopeptides with a centrally positioned alkene-based disulphide bridge mimetic stimulate kallikrein-related peptidase 3 activity. *J. Org. Chem*. 2011. **76**: 673–675.
229. Kastrinsky D. B., Kumar P., Marriner G. A.,

Barry III C. E. A Convergent Synthesis of Chiral Diaminopimelic Acid Derived Substrates for Mycobacterial l,d-Transpeptidases. *Synthesis* 2012. 3043–3048.

230. Ritzén A., Basu B., Chattopadhyay S. K., *et al*. Phenyltrisalanine: a new, C3-symmetric, trifunctional amino acid. *Tetrahedron*: *Asymmetry*. 1998. **9**: 503–512.
231. Wang W., Xiong C., Yang J., Hruby V. J. Synthesis of specifically deuterated S-benzylcysteines and of oxytocin and related diastereomers deuterated in the half-cystine positions. *Synthesis*. 2002. 94–98.
232. Wang J., Liu H., Aceña J. L., *et al*. Synthesis of bis-a,a-amino acids through diastereoselective bis-alkylations of chiral Ni(II)-complexes of glycine. *Org. Biomol. Chem*. 2013. **11**: 4508–4515.
DOI: 10.1039/C3OB40594J.
233. Soloshonok V. A., Hayashi T. Gold(I)-Catalyzed Asymmetric Aldol Reaction of Fluorinated Benzaldehydes with a-Isocyanoacetamide. *Tetrahedron*: *Asymmetry* 1994. **5**: 1091–1094.
234. Soloshonok V. A., Hayashi T. Gold(I)-Catalyzed Asymmetric Aldol Reaction of Methyl Isocyanoacetate with Fluorinated Benzaldehydes. *Tetrahedron Lett*. 1994. **35**: 2713–2716.
235. Soloshonok V. A., Hayashi T., Ishikawa K., Nagashima N. Highly Diastereoselective Aldol Reaction of Fluoroalkyl Aryl Ketones with Methyl Isocyanoacetate Catalyzed by Silver(I)/Triethylamine. *Tetrahedron Lett*. 1994. **35**: 1055–1058.
236. Soloshonok V. A., Kacharov A. D., Hayashi T. Gold(I)-Catalyzed Asymmetric Aldol Reactions of Isocyanoacetic Acid Derivatives with Fluoroaryl Aldehydes. *Tetrahedron* 1996. **52**: 245–254.
237. Soloshonok V. A., Kacharov A. D., Avilov D. V., *et al*. Transition Metal/Base-Catalyzed Aldol Reactions of Methyl a-Isocyanoacetate with Prochiral Ketones, a Straightforward Approach to Stereochemically Defined b,b-Disubstituted-b-Hydroxy-a-Amino Acids. Scope and Limitations. *J. Org. Chem*. 1997. **62**: 3470–3479.
238. Soloshonok V. A., Avilov D. V., Kukhar V. P. Highly Diastereoselective Asymmetric Aldol Reactions of Chiral Ni(II)-Complex of Glycine with Trifluoromethyl Ketones. *Tetrahedron*: *Asymmetry*. 1996. **7**: 1547–1550.
239. Soloshonok V. A., Kukhar V. P., Galushko S. V., *et al*. General method for the synthesis of enantiomerically pure b-hydroxy-a-amino acids, containing fluorine atoms in the side chains. Case of stereochemical distinction between methyl and trifluoromethyl groups. X-ray crystal and molecular structure of the Nickel(II) complex of (2S,3S)-2-(trifluoromethyl)threonine. *J. Chem. Soc., Perkin Trans. 1*, 1993. 3143–3155.
240. Soloshonok V. A., Avilov D. V., Kukhar V. P. Asymmetric Aldol Reactions of Trifluoromethyl Ketones with a Chiral Ni(II) Complex of Glycine: Stereocontrolling Effect of the Trifluoromethyl Group. *Tetrahedron* 1996. **52**: 12433–12442.
241. Li T., Zhou S., Wang J., *et al*. Asymmetric synthesis of (2S,3S)-a-(1-oxoisoindolin-3-yl) glycines under low-basicity "kinetic" control. *J. Org. Chem*. 2015. **80**: 11275–11280. DOI: 10.1021/acs.joc.5b01730.
242. Li T., Zhou S., Wang J., *et al*. Asymmetric synthesis of a-(1-oxoisoindolin-3-yl)glycine: synthetic and mechanistic challenges. *Chem. Commun*. 2015. **51**: 1624–1626. DOI: 10.1039/C4CC05659K.
243. Zou Y., Yin Z., Mei H., *et al*. Aldol Addition-Cyclization Reaction Cascade on a Platform of Chiral Ni(II) Complex of Glycine Schiff Base. *Ukr. Bioorg. Acta* 2021. **16**(1): 3–9.
244. Duthaler R. O. Recent developments in the stereoselective synthesis of a-aminoacids. *Tetrahedron*, 1994. **50**: 1539–1560.
245. Maruoka K., Ooi T. Enantioselective Amino Acid Synthesis by Chiral Phase-Transfer

Catalysis.*Chem. Rev*. 2003. **103**: 3013–3028.
246. Ma J.-A. Recent Developments in the Catalytic Asymmetric Synthesis of a- andb-Amino Acids.*Angew. Chem., Int. Ed*. 2003. **42**: 4290–4299.
247. Nájera C., Sansano J. M. Catalytic asymmetric synthesis of alpha-amino acids.*Chem. Rev*. 2007, **107**, 4584–4671.
248. Soloshonok V. A., Avilov D. V., Kukhar V. P., *et al*. Highly Diastereoselective aza-Aldol Reactions of a Chiral Ni(II) Complex of Glycine with Imines. An Efficient Asymmetric Approach to 3-Perfluoroalkyl-2,3-Diamino Acids. *Tetrahedron Lett*. 1997. **38**: 4671–4674.
249. Gómez Arrayás R., Carretero J. C. Catalytic asymmetric direct Mannich reaction: a powerful tool for the synthesis of a,b-diamino acids. *Chem. Soc. Rev*. 2009. **38**: 1940–1948.
250. Viso A., Fernández de la Pradilla R., Tortosa M., García A., Flores A. Update 1 of: a,b-Diamino Acids: Biological Significance and Synthetic Approaches. *Chem. Rev*. 2011. **111**: PR1–PR42.
251. Kawamura A., Moriwaki H., Röschenthaler G.-V., *et al*. Synthesis of (2S,3S)-b-(trifluoromethyl)-a,b-diamino acid by Mannich addition of glycine Schiff base Ni(II) complexes to N-tert-butylsulfinyl-3,3,3-trifluoroacetaldimine. *J. Fluor. Chem*. 2015. **171**: 67–72. DOI: 10.1016/j.jfluchem.2014.09.013.
252. Mimura H., Kawada K., Yamashita T., *et al*. Trifluoroacetaldehyde: A useful industrial bulk material for the synthesis of trifluoromethylated amino compounds. *J. Fluor. Chem*. 2010. **131**: 477–486.
253. Robak M. T., Herbage M. A., Ellman J. A. Synthesis and Applications of tert-Butanesulfinamide. *Chem. Rev*. 2010. **110**: 3600–3740.
254. Xie C., Wu L., Mei H., *et al.* Generalized access to fluorinated b-keto amino compounds through asymmetric additions of a,a-difluoroenolates to CF3-sulfinylimine. *Org. Biomol. Chem*. 2014. **12**: 7836–7843. DOI: 10.1039/C4OB01575D.
255. Mei H., Xie C., Wu L., *et al*. Asymmetric Mannich reactions of imidazo-[2,1-b]-thiazole-derived nucleophiles with (SS)-N-tert-butanesulfinyl-(3,3,3)-trifluoroacetaldimine. *Org. Biomol. Chem*. 2013. **11**: 8018–8021. DOI: 10.1039/c3ob41785a.
256. Shibata N., Nishimine T., Shibata N., *et al*. Organic base-catalyzed stereodivergent synthesis of (R)- and (S)-3-amino-4,4,4-trifluorobutanoic acids. *Chem. Commun*. 2012. **48**: 4124–4126. DOI: 10.1039/C2CC30627A.
257. Cai C., Soloshonok V. A., Hruby V. J. Michael Addition Reactions Between Chiral Ni(II) Complex of Glycine and 3-(trans-enoyl)oxazolidin-2-ones. A Case of Electron Donor-Acceptor Attractive Interactions-Controlled Face Diastereoselectivity. *J. Org. Chem*. 2001. **66**: 1339–1350.
258. Soloshonok V. A., Ueki H., Tiwari R., *et al*. Virtually Complete Control of Simple and Face Diastereoselectivity in the Michael Addition Reactions between Achiral Equivalents of a Nucleophilic Glycine and (S)- or (R)-3-(E-Enoyl)-4-phenyl-1,3-oxazolidin-2-ones: Practical Method for Preparation of β-Substituted Pyroglutamic Acids and Prolines. *J. Org. Chem*. 2004. **69**: 4984–4990.
259. Soloshonok V. A., Avilov D. V., Kukhar V. P., *et al*. An Efficient Asymmetric Synthesis of (2S, 3S)-3-Trifluoromethylpyroglutamic Acid. *Tetrahedron Lett*. 1997. **38**: 4903–4904.
260. Soloshonok V. A., Cai C., Hruby V. J. Asymmetric Michael Addition Reactions of Chiral Ni(II) Complex of Glycine with N-(Enoyl) oxazolidinones: Improved Reactivity and Stereochemical Outcome. *Tetrahedron*: *Asymmetry.* 1999. **10**: 4265–4269.
261. Soloshonok V. A., Cai C., Hruby V. J. A Unique Case of Face Diastereoselectivity in the Michael Addition Reactions Between Ni(II)-Complexes of Glycine and Chiral 3-(E-enoyl)-1,3-oxa-

zolidin-2-ones. *Tetrahedron Lett*. 2000. **41**: 9645–9649.
262. Soloshonok V. A., Cai C., Hruby V. J. A Practical Asymmetric Synthesis of Enantiomerically Pure 3-Substituted Pyroglutamic Acids and Related Compounds. *Angew. Chem., Int. Ed*. 2000. **39**: 2172–2175.
263. Soloshonok V. A., Cai C., Hruby V. J. (S)- or (R)-N-(E-enoyl)-4-phenyl-1,3-oxazolidin-2-ones: Ideal Michael Acceptors to Afford a Virtually Complete Control of Simple and Face Diastereoselectivity in Addition Reactions with Glycine Derivatives. *Org. Lett*. 2000. **2**: 747–750.
264. Soloshonok V. A., Cai C., Yamada T., *et al*. Michael Addition Reactions Between Chiral Equivalents of a Nucleophilic Glycine and (S)- or (R)-3-(E-Enoyl)-4-phenyl-1,3-oxazolidin-2-ones as a General Method for Efficient Preparation of β-Substituted Pyroglutamic Acids. Case of Topographically Controlled Stereoselectivity. *J. Am. Chem. Soc*. 2005. **127**: 15296–15303.
265. Stierhof M., Hansen K. Ø., Sharma M., *et al*. New cytotoxic callipeltins from the Solomon Island marine sponge Asteropus sp. *Tetrahedron* 2016. **72**: 6929–6934.
266. Tokairin Y., Soloshonok V. A., Moriwaki H., Konno H. Asymmetric synthesis of (2S,3S)-3-Me-glutamine and (R)-allo-threonine derivatives proper for solid phase peptide coupling. *Amino Acids* 2019. **51**: 419–432. https://doi.org/10.1007/s00726-018-2677-5.
267. Tucker T. J., Lumma W. C., Mulichak A. M., *et al*. Potent noncovalent thrombin inhibitors that utilize the unique amino acid D-dicyclohexylalanine in the P3 position. Implications on oral bioavailability and antithrombotic efficacy. *J. Med. Chem*. 1997. **40**: 1565–1569.
268. Cheng L., Goodwin C. A., Schully M. F., *et al*. Synthesis and biological activity of ketomethylene pseudopeptide analogs as thrombin inhibitors. *J. Med. Chem*. 1992. **35**: 3364–3369.
269. Pavar M. C., Hanif K., Azam A., *et al*. Structure–activity relationship study between ornithyl-proline and lysyl-proline based tripeptidomimics as angiotensinconverting enzyme inhibitors. *Bioorg. Med. Chem. Lett*. 2006. **16**: 2117–2121.
270. Stranix B. R., Lavallée J.-F., Sévigny G., *et al*. Lysine sulfonamides as novel HIV-protease inhibitors: Nε-acyl aromatic a-amino acids. *Bioorg. Med. Chem. Lett*. 2006. **16**: 3459–3462.
271. Brust A., Palant E., Croker D. E., *et al*. x-Conopeptide pharmacophore development: toward a novel class of norepinephrine transporter inhibitor (Xen2174) for pain. *J. Med. Chem*. 2009. **52**: 6991–7002.
272. Lee Y. S., Nyberg J., Moye S., *et al*. Understanding the structural requirements of 4-anilidopiperidine analogues for biological activities at m and s opioid receptors. *Bioorg. Med.Chem. Lett*. 2007. **17**: 2161–2165.
273. Müller J., Feifel S. C., Schmiederer T., *et al*. In vitro Synthesis of New Cyclodepsipeptides of the PF1022-Type: Probing the a-D-Hydroxy Acid Tolerance of PF1022 Synthetase. *Chem Bio Chem*. 2009. **10**: 323–328.
274. Jørgensen M. R., Olsen C. A., Mellor I. R., *et al*. The Effects of Conformational Constraints and Steric Bulk in the Amino Acid Moiety of Philanthotoxins on AMPAR Antagonism. *J. Med. Chem*. 2005. **48**: 56–70.
275. Li X., Taylor J. S. General strategy for the preparation of membrane permeable fluorogenic peptide ester conjugates for in vivo studies of ester prodrug stability. *Bioorg. Med. Chem*. 2004. **12**: 545–552.
276. Haug B. E., Skar M. L., Svenden J. S. Bulky aromatic amino acids increase the antibacterial activity of 15-residue bovine lactoferricin derivatives. *J. Pept. Sci*. 2001. **7**: 425–432.
277. Gomez-Catalan J., Perez J. J., Jimenez A. I., Cativiela C. Study of the conformational profile of selected unnatural amino acid residues derived from L-phenylalanine. *J. Pept. Sci.*

1999. **5**: 251–262.
278. Alvarez R., Valazquez S., San-Felix A., *et al*. 1,2,3-Triazole–[2',5'-Bis-O-(tert-butyldimethylsilyl)-β-D-ribofuranosyl]-3'-spiro-5''-(4''-amino-1'',2''-oxathiole 2'',2''-dioxide) (TSAO) Analogues: Synthesis and Anti-HIV-1 Activity. *J. Med. Chem*. 1994. **37**: 4185–4194.
279. Sharp R. E., Palmitessa A., Gibney B. R., *et al*. Ubiquinone Binding Capacity of the Rhodobacter capsulatus Cytochrome bc1 Complex: Effect of Diphenylamine, a Weak Binding QO Site Inhibitor. *Biochemistry.* 1999. **38**: 3440–3446.
280. Khoury G. A., Smadbeck J., Tamamis P., *et al*. Forced_NCAA: ab initio charge parameters to aid in the discovery and design of therapeutic proteins and peptides with unnatural amino acids and their application to complement inhibitors of the compstatin family. *ACS Synth. Biol*. 2014. **3**: 855–869.
281. Mao S., Rui Y., Yunru Z., *et al*. Predicting the activity of antimicrobial peptides with amino acid topological information. *Med. Chem*. 2013. **9**: 32–44.
282. Gfeller D., Michielin O., Zoete V. Expanding molecular modeling and design tools to non-natural sidechains. *J. Comput. Chem*. 2012. **33**: 1525–1535.
283. Tian F., Zhou P., Li Z. T-scale as a novel vector of topological descriptors for amino acids and its application in QSARs of peptides. *J. Mol. Struct*. 2007. **830**: 106–115.
284. Zhu Q., Cheng L., Lu Y. Asymmetric organocatalytic Michael addition of ketones to vinylsulfone. *Chem. Commun*. 2008. **47**: 6315–6317.
285. Dou X., Lu Y. Enantioselective conjugate addition of 3-fluoro-oxindoles to vinyl sulfone: an organocatalytic access to chiral 3-fluoro-3-substituted oxindoles. *Org. Biomol. Chem*. 2013. **11**: 5217–5221.
286. Zhu Y., Ni Y. F., Soloshonok V. A., *et al*. Catalytic enantioselective Michael addition reactions between in situ detrifluoroacetylatively generated 3-fluorooxindole-derived enolates and 1-(1-(phenylsulfonyl) vinylsulfonyl)benzene. *J. Fluor. Chem*. 2019. **219**: 32–38. https://doi.org/10.1016/j.jfluchem.2018.12.009.
287. Zhu Y., Zhang W., Mei H., *et al*. Catalytic enantioselective Michael addition reactions of tertiary enolates generated by detrifluoroacetylation. *Chem. –Eur. J*. 2017. **23**: 11221–11225. DOI: 10.1002/chem.201702091.
288. Nagaoka K., Mei H., Guo Y., *et al*. Michael addition reactions of chiral glycine Schiff base Ni (II)-complex with 1-(1-phenylsulfonyl)benzene. *Chirality* 2020. **32**: 885–893. https://doi.org/10.1002/chir.23203.
289. Cooper A. J. L., Haber M. T., Ginos J. Z., *et al*. Interaction of soluble pig heart glutamate-aspartate transaminase with various b,g-unsaturated amino acids. *Biochem. Biophys. Res. Commun*. 1985. **129**: 193–199.
290. Paik Y. H., Dowd P. b-Methyleneglutamic acid and b-methyleneglutamine. *J. Org. Chem*. 1986. **51**: 2910–2913.
291. Winter H. C., Powel G. K., Dekker E. E. 4-Methyleneglutamic acid and 4-methyleneglutamine: isolation from extracts of peanut seedlings and determination by high-performance liquid chromatography. *Prep. Biochem*. 1988. **18**: 121–136.
292. Receveur J. M., Roumestant M. L., Viallefont P. Neuroexcitatory amino acids: 4-methylene glutamic acid derivative. *Amino Acids.* 1995. **9**: 391–395.
293. Kang S., Shi Q., Ha M. W., *et al*. Enantioselective synthesis of (S)-4-methyleneglutamic acid via tandem conjugate addition–elimination under phase-transfer catalytic conditions. *Tetrahedron.* 2010. **66**: 4326–4329.
294. Eacquerra J., Pedregal C., Micó I., Nájera C. Efficient synthesis of 4-methylene-L-glutamic acid and its cyclopropyl analogue. *Tetrahedron: Asymmetry*.1994. **5**: 921–926.
295. Shigeno Y., Han J., Soloshonok V. A., *et al*.

Asymmetric synthesis of (S)-3-methyleneglutamic acid and its N-Fmoc derivative via Michael addition of chiral glycine Schiff base Ni(II) complex with enol tosylates. *Chirality* 2021. **33**: 115–123.

296. Babine R. E., Bender S. L. Molecular Recognition of Protein–Ligand Complexes: Applications to Drug Design. *Chem. Rev*. 1997. **97**: 1359–1472.
297. Tang W., Zhang X. New Chiral Phosphorus Ligands for Enantioselective Hydrogenation. *Chem. Rev*. 2003. **103**: 3029–3070.
298. Feng Y., Coward J. K. Prodrug Forms of N-[(4-Deoxy-4-amino-10-methyl)pteroyl]glutamate-γ-[wP(O)(OH)]-glutarate, a Potent Inhibitor of Folylpoly-g-glutamate Synthetase: Synthesis and Hydrolytic Stability. *J. Med. Chem*. 2006. **49**: 770–788.
299. Baumgartner T., Réau R. Organophosphorus π-Conjugated Materials. *Chem. Rev*. 2006. **106**: 4681–4727.
300. Yang Y., Coward J. K. Synthesis of p-Aminophenyl Aryl H-Phosphinic Acids and Esters via Cross-Coupling Reactions: Elaboration to Phosphinic Acid Pseudopeptide Analogues of Pteroyl Glutamic Acid and Related Antifolates. *J. Org. Chem*. 2007. **72**: 5748–5758.
301. Boëdec A., Sicard H., Dessolin J. G., *et al*. Synthesis and Biological Activity of Phosphonate Analogues and Geometric Isomers of the Highly Potent Phosphoantigen (E)-1-Hydroxy-2-methylbut-2-enyl 4-Diphosphate. *J. Med. Chem*. 2008. **51**: 1747–1754.
302. Allen D. W. Phosphines and related C–P bonded compounds. *Organophos. Chem*. 2016. **45**: 1–50.
303. Kukhar V. P., Soloshonok V. A., Solodenko V. A. Asymmetric Synthesis of Phosphorus Analogs of Amino Acids. *Phosphorus, Sulfur, and Silicon and the Related Elements.* 1994. **92**. 239–264.
DOI: 10.1080/10426509408021478.
304. Turcheniuk K. V., Kukhar V. P., Röschenthaler G.-V., *et al*. Recent advances in the synthesis of fluorinated aminophosphonates and aminophosphonic acids. *RSCAdv*. 2013. **3**: 6693–6716. DOI: 10.1039/c3ra22891f.
305. Wzorek A., Han J., Lyutenko N. V., *et al*. Enzymatic approaches for preparation of α-aminophosphonic acids and fluorine-containing β-amino acids. *Ukr. Bioorg. Acta*. 2024. **19**(1): 21–32.
306. Turski L., Klockgether T., Turski W. A., *et al*. Blockade of excitatory neurotransmission in the globus pallidus induces rigidity and akinesia in the rat: implications for excitatory neurotransmission in pathogenesis of Parkinson's diseases. *Brain Res*. 1990. **512**: 125–131.
307. Yoneda Y., Ogita K. Current topics on glutamate receptors. *Yakugaku Zasshi* 1991. **111**: 329–344.
308. Nadlewska A., Car H., Wiśniewska R., *et al*. Behavioral effects of D-AP7 in rats subjected to experimental hypoxia. *Pol. J. Pharmacol*. 2003. **55**: 337–344.
309. Zhang H.-M., Chen S.-R., Pan H.-L. Effects of activation of group III metabotropic glutamate receptors on spinal synaptic transmission in a rat model of neuropathic pain. *Neuroscience*. 2009. **158**: 875–884.
310. Morris R. G. M. NMDA receptors and memory encoding.*Neuropharmacology*. 2013, **74**: 32.
311. Lopez S., Turle N., Lorenzo F., *et al*. Targeting Group III Metabotropic Glutamate Receptors Produces Complex Behavioral Effects in Rodent Models of Parkinson's Disease. *J. Neurosci*. 2007. **27**: 6701–6711.
312. Turcheniuk K. V., Poliashko K. O., Kukhar V. P., *et al*. Efficient asymmetric synthesis of trifluoromethylated b-aminophosphonates and their incorporation into dipeptides. *Chem. Commun*. 2012. **48**: 11519–11521.
DOI: 10.1039/c2cc36702e.
313. Röschenthaler G.-V., Kukhar V. P., Kulik I. B., *et al*. Asymmetric synthesis of phosphonotrifluoroalanine and its derivatives using

N-tert-butanesulfinyl imine derived from fluoral. *Tetrahedron Lett*. 2012. **53**: 539–542. doi:10.1016/j.tetlet.2011.11.096.
314. Röschenthaler G.-V., Kukhar V. P., Kulik I. B., *et al*. Convenient Synthesis of Fluoroalkyl a- and b-Aminophosphonates. *J. Fluor. Chem*. 2011. **132**: 834–837.
315. Soloshonok V. A., Belokon Y. N., Kuzmina N. A., *et al*. Asymmetric Synthesis of Phosphorus Analogs of Dicarboxylic a-Amino Acids. *J. Chem. Soc., Perkin Trans. 1*. 1992. 1525–1529.
316. Tokairin Y., Soloshonok V. A., Konno H., *et al*. Convenient synthesis of racemic 4,4-difluoro glutamic acid derivatives via Michael-type additions of Ni(II)-complex of dehydroalanine Schiff bases. *J. Fluor. Chem*. 2019. **227**: 109376. doi.org/10.1016/j.jfluchem.2019.109376.
317. Tokairin Y., Shigeno Y., Han J. G., *et al*. Asymmetric Synthesis of 4,4-(Difluoro)glutamic Acid via Chiral Ni(II)-Complexes of Dehydroalanine Schiff Bases. Effect of the Chiral Ligands Structure on the Stereochemical Outcome. *Chemistry Open*. 2020. **9**: 93–96. DOI: 10.1002/open.201900343.
318. Tokairin Y., Konno H., Noireau, A. *et al*. Asymmetric synthesis of the two enantiomers of b-phosphorus-containing a-amino acids via hydrophosphinylation and hydrophosphonylation of chiral Ni(II)-complexes.*Org. Chem. Front*. 2021. **8**: 2190–2195. https://doi10.1039/D1QO00159K.
319. Cahn R. S., Ingold C. K., Prelog V. Specification of Molecular Chirality. *Angew. Chem., Int. Ed*. 1966. **5**: 385–415.
320. Prelog V., Helmchen G. Basic Principles of the CIP-System and Proposals for a Revision. *Angew. Chem., Int. Ed*. 1982. **21**: 567–58.
321. Diggle G. E. Thalidomide: 40 years on. *Int. J. Clin. Pract*. 2001. **55**: 627–631.
322. Thomas F. X. C. History and Evolution of Reproductive and Developmental Toxicology Guidelines. *Curr. Pharm. Des*. 2006. **12**: 1449–65.
323. Miller M. T., Stromland K. K. What can we learn from the thalidomide experience: an ophthalmologic perspective. *Curr. Opin. Ophthalmol*. 2011. **22**: 356–364.
324. Hendrickx A. G., Binkerd P. E. Nonhuman primates and teratological research. *J. Med. Primatol*. 1990. **19**: 81–108.
325. Powell R. J. Thalidomide: current uses. *BioDrugs*. 1999. **11**: 409–416.
326. Guirguis, A. A., Ebert B. L. Lenalidomide: deciphering mechanisms of action in myeloma, myelodysplastic syndrome and beyond. *Curr. Opin. Cell. Biol*. 2015. **37**: 61–67.
327. Engelhardt M., Wasch R., Reinhardt H., Kleber M. Pomalidomide. Recent Results. *Cancer Res*. 2014. **201**: 359–372.
328. Tokunaga E., Akiyama H., Soloshonok V. A., *et al*. Biological evaluation of both enantiomers of fluoro-thalidomide using human myeloma cell line H929 and others. *PLoS ONE* 2017. **12**: e0182152. DOI 10.1371/journal.pone.0182152.
329. Soloshonok V. A., Yamada T., Sakaguchi K., Ohfune Y. Concise Asymmetric Synthesis of Configurationally Stable 4-trifluoromethyl Thalidomide. *Future Med. Chem*. 2009. **1**: 897–908. doi.org/10.4155/fmc.09.63.
330. Yamada T., Okada T., Sakaguchi K., *et al*. Efficient Asymmetric Synthesis of Novel 4-Substituted and Configurationally Stable Analogs of Thalidomide. *Org. Lett*. 2006. **8**: 5625–5628.
331. Mori T., Takahashi K., Kashiwabara M., Uemura D. Structure of oxazolomycin, a novel b-lactone antibiotic. *Tetrahedron Lett*. 1985. **26**: 1073–1076.
332. Kanzaki H., Wada K., Nitoda T., Kawazu K. Novel bioactive oxazolomycin isomers produced by Streptomyces albus JA3453. *Biosci. Biotechnol. Biochem*. 1998. **62**: 438–442.
333. Kawazu K., Kanzaki H., Kawabata G., *et al*. Oxazolomycin Esters, Specific Inhibitors of Plant Transformation. *Biosci. Biotechnol. Biochem*. 1992. **56**: 1382–1385.

334. Tonew E., Tonew M., Gräfe U., Zöpel P. Griseochelin methyl ester, a new polyether derivative with antiviral activity. *Acta Virol*. 1992. **36**: 166–172.
335. Grigorjev P. A., Schegel R., Gräfe U. Formation of membrane pores by aurantimycins A and B, new lipopeptide antibiotics from Streptomyces aurantiacus. *Pharmazie*. 1992. **47**: 707–709.
336. Bullough P. A., Hughson F. M., Skehel J. J., Wiley D. C. Structure and topology of the influenza virus fusion peptide in lipid bilayers. *Nature*. 1994. **371**: 37–43.
337. Carr C. M., Kim P. S. A spring-loaded mechanism for the conformational change of influenza hemagglutinin. *Cell*. 1993. **73**: 823–832.
338. Kawai S., Kawabata G., Kobayashi A., Kawazu K. Inhibitory Effect of Oxazolomycin on Crown Gall Formation. *Agric. Biol. Chem*. 1989. **53**: 1127–1133.
339. Takahashi K., Kawabata M., Uemura D. *et al*. Structure of neooxazolomycin, an antitumor antibiotic. *Tetrahedron Lett*. 1985. **26**: 1077–1078.
340. Yamada T., Sakaguchi K., Shinada T., *et al*. Efficient asymmetric synthesis of the functionalized pyroglutamate core unit common to oxazolomycin and neooxazolomycin using Michael reaction of nucleophilic glycine Schiff base with a,b-disubstituted acrylate. *Tetrahedron: Asymmetry* 2008. **19**: 2789–2795. doi.org/10.1016/S0040-4020(98)00779-0.
341. Cativiela C., Ordóñez M. Recent progress on the stereoselective synthesis of cyclic quaternary α-amino acids. *Tetrahedron: Asymmetry*. 2009. **20**: 1–63.
342. Brackmann F., de Meijere A. Natural occurrence, syntheses, and applications of cyclopropyl-group-containing alpha-amino acids. 1. 1-aminocyclopropanecarboxylic acid and other 2,3-methanoamino acids. *Chem. Rev*. 2007. **107**: 4493–4537.
343. Burroughs L. F. I-Aminocyclopropane-I-Carboxylic Acid: A New Amino-Acid in Perry Pears and Cider Apples. *Nature* 1957. **179**: 360–361.
344. Adams D. O., Yang S. F. Ethylene biosynthesis: Identification of 1-aminocyclopropane-1-carboxylic acid as an intermediate in the conversion of methionine to ethylene. *Proc. Natl. Acad.Sci. U. S. A* 1979. **76**: 170–174.
345. Stammer C. H. Cyclopropane amino acids: 2,3- and 3,4-methanoamino acids. *Tetrahedron* 1990. **46**: 2231–2254.
346. Alami A., Calmes M., Daunis J., Jacquier R. Synthesis of Enantiomerically Pure (1S,2S)-1-Aminocyclopropanephosphonic Acids from (2S)-Methylcyclopropanone Acetal. *Bull. Soc. Chim. Fr.* 1993. **130**: 5–24.
347. Burgess K., Ho K.-K., Moye-Sherman D. Asymmetric Syntheses of 2,3-Methanoamino Acids. *Synlett* 1994. 575–583.
348. Ichichara A., Shiraishi K., Sato H., *et al*. The structure of coronatine. *J. Am. Chem. Soc.* 1977. **99**: 636–637.
349. Mitchell R. E. Norcoronatine and N-coronafacoyl-L-valine, phytotoxic analogues of coronatine produced by a strain of Pseudomonas syringae pv. glycinea. *Phytochemistry* 1985. **24**: 1485–1487.
350. Hoffman N. E., Yang S. F., Ichihara A., Sakamura S. Stereospecific conversion of 1-aminocyclopropanecarboxylic acid to ethylene by plant tissues: conversion of stereoisomers of 1-amino-2-ethylcyclopropanecarboxylic acid to 1-butene. *Plant Physiol*. 1982. **70**: 195–199.
351. Pirrung M. C., McGeehan G. M. Asymmetric Synthesis of cis and trans 2-Methyl and 2-Ethyl 1-Amino Cyclopropanecarboxylic acids. *J. Org. Chem*. 1986. **51**: 2103–2106.
352. Tsantrizos Y. S. A practical and scalable system for heteroaryl amino acid synthesis. *Acc. Chem. Res*. 2008. **41**: 1252–1263.
353. Rosenquist A., Samuelsson B., Johansson P.-O., *et al*. New treatments for genotype 1 chronic hepatitis C – focus on simeprevir. *J. Med. Chem*. 2014. **57**: 1673–1693.

354. Jiang Y., Andrews S. W., Condroski K. R., *et al*. Discovery of a New Class of Macrocyclic Antagonists to the Human Motilin Receptor. *J. Med. Chem*. 2014. **57**: 1753–1769.
355. Scola P. M., Sun L.-Q., Wang A. X., *et al*. Discovery of Hepatitis C Virus NS3-4A Protease Inhibitors with Improved Barrier to Resistance and Favorable Liver Distribution. *J. Med. Chem*. 2014. **57**: 1730–1752.
356. Llinàs-Brunet M., Bailey M. D., Goudreau N. P., *et al*. Discovery of a Potent and Selective Noncovalent Linear Inhibitor of the Hepatitis C Virus NS3 Protease (BI 201335). *J. Med. Chem*. 2010. **53**: 6466–6476.
357. Llinàs-Brunet M., Bailey M. D., Bolger G., *et al*. Structure–Activity Study on a Novel Series of Macrocyclic Inhibitors of the Hepatitis C Virus NS3 Protease Leading to the Discovery of BILN 2061. *J. Med. Chem*. 2004. **47**: 1605–1608.
358. Kawashima A., Xie C., Mei H., *et al*. Asymmetric synthesis of (1R,2S)-1-amino-2-vinylcyclopropanecarboxylic acid by sequential SN2–SN2' dialkylation of (R)-N-(benzyl)proline-derived glycine Schiff base Ni(II) complex. *RSC Adv*. 2015. **5**: 1051–1058. DOI: 10.1039/C4RA12658K.
359. Kawashima A., Shu S., Takeda R., *et al*. Advanced asymmetric synthesis of (1R,2S)-1-amino-2-vinylcyclopropanecarboxylic acid by alkylation/cyclization of newly designed axially chiral Ni(II) complex of glycine Schiff base. *Amino Acids* 2016. **48**: 973–986. DOI: 10.1007/s00726-015-2138-3.
360. Murai Y., Mori S., Konno H., *et al.* Ralstonins A and B, Lipopeptides with Chlamydospore-Inducing and Phytotoxic Activities from the Plant Pathogen Ralstonia solanacearum. *Org. Lett*. 2017. **19**: 4175–4178.
361. Konno H., Sasaki Y., Sato R., *et al*. Synthesis of b-Hydroxytyrosine, A Component of Burkholdines. *Nat. Prod. Commun*. 2016. **11**: 213–218.
362. Kato S., Sasaki M., Yano S., Konno H. Synthesis of burkholdine analogue containing the b-hydroxytyrosine. *Biosci. Biotechnol. Biochem*. 2019. **83**: 1216–1219.
363. Boyle P. H., Davis A. P., Dempsey K. J., Hosken G. L. Synthesis of (S)-2-Amino-1,1-diphenylbutan-4-ol; conversion of an a-amino acid into an a-(diphenylmethyl)amino without loss of optical purity. *Tetrahedron: Asymmetry* 1995. **6**: 2819–2828.
364. Oyama K., Han J., Moriwaki H., *et al*. Synthesis of Ahod moiety of ralstonin A using amino acid Schiff base Ni(II)-complex chemistry. *Helv. Chim. Acta*. 2020. **103**: e2000077. https://doi.org/10.1002/hlca.202000077.

Стаття надійшла 05.10.2024.